

Identification and characterization of Sgo2 interactions

**Insights into dynamic chromosomal localization, mechanism of
cohesin protection and putative checkpoint function**

DISSERTATION

zur Erlangung des Grades

- Doktor der Naturwissenschaften -

der Fakultät für Biologie, Chemie und Geowissenschaften

der Universität Bayreuth

vorgelegt von

Bernd Mayer

aus Memmingen

Bayreuth 2010

Die Untersuchungen zur vorliegenden Arbeit wurden zwischen September 2005 und Dezember 2009 unter Anleitung von Prof. Dr. Olaf Stemmann in der Abteilung Molekulare Zellbiologie am Max-Planck-Institut für Biochemie in Martinsried sowie am Lehrstuhl für Genetik der Universität Bayreuth durchgeführt.

Vollständiger Abdruck der von der Fakultät für Biologie, Chemie und Geowissenschaften der Universität Bayreuth genehmigten Dissertation zur Erlangung des akademischen Grades eines Doktors der Naturwissenschaften (Dr. rer. nat.)

Promotionsgesuch eingereicht am:	13.01.2010
Tag des wissenschaftlichen Kolloquiums:	12.03.2010

Erstgutachter:	Prof. Dr. Olaf Stemmann
Zweitgutachter:	Prof. Dr. Benedikt Westermann
Vorsitzender:	Prof. Dr. Stephan Clemens

Table of contents

1. Zusammenfassung.....	6
2. Summary.....	8
3. Introduction.....	10
3.1. The cell cycle and mitosis.....	10
3.2. Spindle assembly and error correction by Aurora B.....	11
3.3. Sister chromatid cohesion.....	14
3.4. Cohesin.....	15
3.4.1. Components of the cohesin complex.....	15
3.4.2. The cohesin ring model.....	15
3.4.3. Loading of cohesin and establishment of cohesion.....	16
3.4.4. Resolving cohesin in mitosis.....	17
3.4.5. Regulation of separase.....	18
3.5. The anaphase promoting complex or cyclosome (APC/C).....	19
3.6. Specific properties of meiosis.....	21
3.7. Cohesin removal during meiosis.....	22
3.8. Shugoshin proteins protect centromeric cohesin.....	23
3.8.1. Cohesin protection by human Sgo1 in mitosis.....	23
3.8.2. Cohesin protection by Sgo2 during meiosis.....	24
3.8.3. Localization of shugoshin.....	25
3.9. The spindle assembly checkpoint (SAC).....	25
3.9.1. Attachment and tension.....	26
3.9.2. Kinetochores as signaling hubs of the SAC.....	27
3.9.3. The molecular components of the SAC.....	28
3.10. Implications of yeast shugoshin homologs in the SAC.....	30
3.11. Clinical relevance of human shugoshin homologs.....	30
3.12. Aim of this work.....	31

4. Results	33
4.1. Identification of new shugoshin interaction partners	33
4.1.1. Interaction partners of hSgo1 identified by mass spectrometry	33
4.1.2. Conserved binding mode of PP2A between Sgo1 and Sgo2.....	36
4.1.3. Sgo2 regulates PP2A.....	38
4.1.4. Human Sgo1 but not Sgo2 is required to protect centromeric cohesin in mitosis	39
4.1.5. Cohesin protects DNA catenations until the metaphase-anaphase transition	41
4.1.6. Candidate binding screen - Mad2 interacts with <i>X. laevis</i> Sgo1.....	43
4.1.7. Human Sgo2 but not Sgo1 interacts with Mad2.....	44
4.2. Sgo2 is dispensable for mitosis	46
4.2.1. Sgo2 does not cause an override of a short-term SAC arrest	46
4.2.2. Sgo2 is not required for maintenance of a prolonged mitotic SAC arrest.....	47
4.2.3. Sgo2 does not regulate mitotic checkpoint complex composition.....	48
4.2.4. Cdc20 is the only known Mad2 binding partner that becomes destabilized in mitosis	49
4.2.5. Sgo2 is not required for normal mitotic progression	51
4.3. The Sgo2-Mad2 complex resembles the SAC complexes Mad1-Mad2 and Cdc20-Mad2	53
4.3.1. The Sgo2-Mad2 complex can be isolated from living cells	53
4.3.2. The Mad2 binding site is located between amino acid residues 101 and 200 of xSgo1....	55
4.3.3. Only Mad2 in its closed conformation can bind to Sgo2.....	57
4.3.4. Mad2 phosphorylation is incompatible with Sgo2 binding	57
4.3.5. xSgo1 and Cdc20 compete for Mad2 binding	59
4.3.6. A conserved putative Mad2 binding motif in xSgo1 and hSgo2	60
4.3.7. The MIM is required for Mad2 binding to hSgo2.....	61
4.3.8. Sgo2 binding induces a global conformational change of Mad2	63
4.3.9. p31 binding to Sgo2 is modulated by Mad2 levels.....	64
4.3.10. xSgo1 forms a trimeric complex with Mad2 and PP2A <i>in vitro</i>	66
4.3.11. Sgo2 can form multimers	67
4.4. Regulation of the Sgo2 subcellular localization	68
4.4.1. Localization pattern of Sgo2 during mitosis.....	68
4.4.2. Microtubule attachment promotes Sgo2 relocalization	69
4.4.3. Sgo2 mutants localize correctly in mitotic human cells	69
4.4.4. The C-terminus of Sgo2 is required for localization.....	72
4.4.5. Sgo2 is a predominantly chromatin associated protein	73
4.4.6. Sgo2 is a mitotic phosphoprotein.....	74
4.4.7. Aurora B catalytic activity is required for proper Sgo2 localization.....	75

5. Discussion.....	77
5.1. The shugoshin-Mad2 interaction resembles the known SAC interactions Mad1-Mad2 and Cdc20-Mad2	77
5.2. The shugoshin recruitment cascade in human cells.....	79
5.3. Evolutionary conservation of the PP2A binding motif.....	80
5.4. Sgo2 stimulates PP2A activity	81
5.5. A three-step model for the removal of cohesive elements in mitosis	82
5.6. The roles of Sgo1 and Sgo2 in mitotic cohesin protection	83
5.7. Potential implications of the Sgo2-Mad2 complex in meiosis	84
5.7.1. A role of Mad2 in meiotic cohesion is unlikely	84
5.7.2. Shugoshin 2 as a Mad1-like activator of the meiotic SAC?	85
5.8. The role of Aurora B in Sgo2 localization	86
5.9. Downstream factors of Aurora B in the tension SAC.....	87
5.10. Sgo2 inactivation in meiosis	90
6. Materials and methods	92
6.1. Materials	92
6.1.1. Hard- and software	92
6.1.2. Protocols.....	92
6.1.3. Chemicals and reagents	92
6.1.4. Antibodies.....	93
6.1.5. DNA oligonucleotides.....	93
6.1.6. Target sequences for dsRNA oligonucleotides	94
6.1.7. Plasmids.....	94
6.2. Microbiological techniques	95
6.2.1. <i>E. coli</i> strains	95
6.2.2. <i>E.coli</i> vectors	96
6.2.3. <i>E. coli</i> media.....	96
6.2.4. Cultivation and storage of <i>E. coli</i>	96
6.2.5. Preparation of chemically competent <i>E. coli</i>	96
6.2.6. Transformation of plasmid DNA into chemically competent <i>E. coli</i>	97
6.2.7. Expression of proteins in <i>E. coli</i>	97

6.2.8.	<i>S. cerevisiae</i> strain.....	97
6.2.9.	Yeast media	98
6.2.10.	Yeast vectors	98
6.2.11.	Preparation of chemically competent <i>S. cerevisiae</i>	98
6.2.12.	Plasmid transformation in <i>S. cerevisiae</i>	99
6.2.13.	Yeast-2-Hybrid assay.....	99
6.2.14.	Preparation of denatured cell extracts from <i>S. cerevisiae</i>	100
6.3.	Molecular biological methods	100
6.3.1.	Isolation of plasmid DNA from <i>E. coli</i>	100
6.3.2.	Determination of DNA/RNA concentration in solution	100
6.3.3.	Restriction digestion of DNA	101
6.3.4.	Dephosphorylation of DNA fragments	101
6.3.5.	Separation of DNA fragments by gel electrophoresis.....	101
6.3.6.	Isolation of DNA from agarose gels.....	101
6.3.7.	Ligation of DNA fragments	102
6.3.8.	Sequencing of DNA.....	102
6.3.9.	Site-directed mutagenesis of DNA.....	102
6.3.10.	Polymerase chain reaction (PCR)	103
6.3.11.	Reverse transcription (RT)-PCRs.....	103
6.4.	Protein methods.....	103
6.4.1.	SDS-polyacrylamide gel electrophoresis (SDS-PAGE).....	103
6.4.2.	Immunoblotting	104
6.4.3.	Coomassie staining	105
6.4.4.	Purification of proteins - common buffers and steps.....	105
6.4.5.	Amylose affinity purification of maltose binding protein (MBP)-tagged proteins.....	106
6.4.6.	Ni ²⁺ -NTA affinity purification of 6x-Histidine-tagged proteins	106
6.4.7.	Coupled <i>in vitro</i> transcription/translation.....	107
6.4.8.	<i>In vitro</i> pulldown assay	107
6.4.9.	Phosphatase activity assay	107
6.4.10.	Lambda phosphatase treatment.....	107
6.5.	Cell biological methods.....	108
6.5.1.	Mammalian cell lines.....	108
6.5.2.	Vectors for cell culture	108
6.5.3.	Cultivation of mammalian cells	108
6.5.4.	Storage of mammalian cells	108
6.5.5.	Transfection of 293T cells.....	109
6.5.6.	Transfection of HeLa cells.....	109
6.5.7.	Synchronization of mammalian cells	110

6.5.8.	Co-Immuno-Precipitation (Co-I.P.) experiments from transfected 293T cells.....	110
6.5.9.	Co-I.P. experiments of endogenous proteins.....	111
6.5.10.	Competitive elution.....	111
6.5.11.	Elution by TEV protease cleavage.....	111
6.5.12.	Plasmid transfection of HeLa cells.....	112
6.5.13.	siRNA transfection of HeLa cells	112
6.5.14.	siRNA rescue experiment	112
6.5.15.	Immunofluorescence staining and microscopy.....	113
6.5.16.	Determination of the mitotic index by flow cytometry	113
6.5.17.	Live cell imaging.....	114
6.5.18.	Chromosome spreads.....	114
6.5.19.	Preparation of <i>Xenopus laevis</i> egg extract.....	115
6.5.20.	Purification of active recombinant human separase.....	116
6.5.21.	Isolation of Metaphase Chromosomes.....	116
6.5.22.	Metaphase chromosome separation assay	117
7.	Abbreviations	119
8.	References	121
9.	Supplementary figures.....	136
10.	Publikationsliste.....	142
11.	Danksagung.....	144

1. Zusammenfassung

DNA-Replikation in S-Phase und Chromosomensegregation in Mitose sind im Zellzyklus getrennte Ereignisse. Die Identität der jeweiligen Schwesterchromatiden wird durch den ringförmigen Kohäsion-Multiproteinkomplex sichergestellt, der die beiden DNA-Stränge umschließt. Shugoshin-Proteine verhindern die vorzeitige Dissoziation von Kohäsion und tragen somit entscheidend zur genomischen Integrität bei.

In dieser Arbeit konnte gezeigt werden, dass hSgo2, eines der beiden humanen Shugoshin-Homologe, in der Prophase erst an Kinetochore rekrutiert wird, danach während Prometaphase an Zentromere bindet, um schließlich in Metaphase wieder an die Kinetochore zurückzukehren. Des Weiteren wurde nachgewiesen, dass (1) die Chromatin-Bindung von hSgo2 durch seinen C-Terminus vermittelt wird, dass (2) die katalytische Aktivität der Kinase Aurora B benötigt wird, um hSgo2 am Zentromer anzureichern und dass (3) die Bindung von Mikrotubuli an Kinetochore ausreichend ist für die Relokalisierung von hSgo2 in Metaphase; durch Mikrotubuli ausgeübte Zugkräfte sind hierfür nicht zwingend notwendig. Durch diese neu identifizierten Regulationsmechanismen ist es möglich, ein Modell für die subzelluläre Lokalisierung von Shugoshin aufzustellen.

Gegenwärtig gibt es in der Literatur widersprüchliche Angaben darüber, ob und in wiefern hSgo1 und hSgo2 in der Mitose benötigt werden. Detaillierte zellbiologische Untersuchungen im Rahmen dieser Arbeit zeigen, dass hSgo2 entgegen früherer Annahmen an mehreren Prozessen während der Mitose nicht beteiligt ist. Insofern kann darauf geschlossen werden, dass die Funktionsbereiche der Shugoshin-Homologe weitestgehend getrennt sind: Sgo1 fungiert in Mitose während Sgo2 in der Meiose benötigt wird.

Zu Beginn dieser Arbeit war es noch nicht klar, wie Shugoshin-Proteine auf molekularer Ebene positiv auf die Schwesterchromatid-Kohäsion wirken können. Es konnte hier mittels eines biochemischen Ansatzes die Proteinphosphatase 2A (PP2A) als neuer Interaktionspartner von hSgo1 identifiziert werden. Obwohl in der Zwischenzeit bekannt wurde, dass Shugoshin-gebundene PP2A Kohäsion durch direkte Dephosphorylierung schützt, konnte hier erstmals gezeigt werden, dass hSgo2 mittels seines N-Terminus an PP2A bindet. Außerdem bewirkt hSgo2-Bindung eine deutliche Stimulierung der katalytischen Aktivität von PP2A. Deshalb ist die Schlussfolgerung möglich, dass die

Funktion von Shugoshin über eine bloße Verbindung zwischen Kohäsin und PP2A hinausgeht.

Der Spindelaufbau-Kontrollpunkt (SAC) verzögert als essentieller Regulator von Mitose und Meiose den Beginn der Anaphase so lange, bis alle Chromosomen korrekt an der mitotischen Spindel angebracht sind. Der Signaltransduktionsweg des SAC beinhaltet einen Kinetochor-gebundenen Mad1-Mad2-Komplex, der eine Konformationsänderung von löslichem Mad2 katalysiert, das hierdurch die Fähigkeit erlangt, das Cdc20-Protein durch Bindung zu inhibieren. Die durch den SAC bewirkte Verhinderung von Anaphase überlappt mit dem Zeitraum, in dem Shugoshin benötigt wird. In dieser Arbeit konnte Mad2 als ein weiterer neuer Interaktor von hSgo2 gefunden werden. Die exakte Kartierung der Mad2-Bindestelle führte zur Entdeckung eines konservierten Mad2-Interaktionsmotivs (MIM) im N-terminalen Bereich von hSgo2, wie es auch in den schon bekannten Mad2-Bindepartnern Mad1 und Cdc20 vorkommt. Durch eine eingehende Charakterisierung des Sgo2-Mad2-Komplexes konnte gezeigt werden, dass dieser in seiner Struktur den Mad1-Mad2- und Cdc20-Mad2-Komplexen sehr ähnlich ist. Die hier durchgeführten biochemischen Analysen stellen die bisherige Überzeugung in Frage, nach der der SAC lediglich einen Signalgeber (Mad1 am Kinetochor) und ein Zielobjekt (Cdc20) hat. Die Mad2-Bindung ist für das einzige Shugoshin-Homolog in *Xenopus laevis*, xSgo1, konserviert. Dies legt eine wichtige Funktion dieser Interaktion in der Meiose nahe.

2. Summary

Sister chromatids are embraced and held together by a ring-shaped multiprotein complex called cohesin, from the time of their generation in S-phase until their separation in M-phase. Shugoshins protect centromeric cohesin from premature dissociation and, hence, are important regulators of genome stability.

This work demonstrates that hSgo2, one of the two shugoshins in humans, first binds to kinetochores in prophase, then localizes to centromeres in prometaphase before finally traveling back to kinetochores in metaphase. It is further shown that (1) chromatin binding requires the C-terminus of hSgo2, (2) the catalytic activity of the aurora B kinase is essential to focus hSgo2 at centromeres, and (3) attachment of microtubules to kinetochores is not only necessary for the metaphase-specific re-localization of hSgo2 but also sufficient; pulling forces are not required. These newly discovered regulations allow to formulate a mechanistic model that explains shugoshin's dynamic subcellular localization.

An existing conflict in the literature concerns the relative importance of mammalian Sgo1 and Sgo2 in mitosis. Cell biological analyses now demonstrate unambiguously that, contrary to earlier claims, hSgo2 is dispensable for several aspects of mitotic cell divisions. Thus, shugoshin functions are strictly separated, being fulfilled by hSgo1 in mitosis and by hSgo2 in meiosis.

Initially, it was unclear how shugoshins exert their cohesin protective function at the molecular level. Using a biochemical approach, protein phosphatase 2A (PP2A) was identified as a prominent interactor of shugoshins in this thesis. Shortly thereafter, it was reported that shugoshins protect cohesin by mediating PP2A-dependent dephosphorylation. Nevertheless, it is shown here for the first time that hSgo2 binds PP2A via its N-terminus. A Sgo2 point mutant deficient in PP2A binding is created and characterized by cell biological experiments. Importantly, biochemical assays demonstrate that hSgo2 greatly stimulates PP2A's enzymatic activity. Shugoshin function therefore extends beyond simple provision of a linkage between cohesin and PP2A.

Mitosis and meiosis are chiefly controlled by the spindle assembly checkpoint (SAC), which allows anaphase to take place only after all chromosomes have become properly attached to the mitotic spindle. Central to SAC signaling, kinetochore bound Mad1-Mad2 complex catalyzes a conformational switch of soluble Mad2, thereby allowing its

inhibitory binding to the downstream effector protein Cdc20. SAC-dependent inhibition of anaphase correlates well in timing with shugoshin-dependent protection of cohesin. Here, Mad2 is identified as another novel interactor of hSgo2. Precise mapping reveal a conserved Mad2 interaction motif (MIM) in hSgo2, which is shared by the known Mad2 interactors Mad1 and Cdc20. In fact, several lines of evidence show that the Sgo2-Mad2 complex is structurally very similar to the Mad1-Mad2 and the Cdc20-Mad2 complexes. These biochemical studies challenge the current “one source (kinetochore bound Mad1) – one target (Cdc20)” dogma in the field of SAC research. Mad2 binding is conserved in the only *Xenopus laevis* shugoshin, xSgo1, indicating an important function of this interaction during vertebrate meiosis.

3. Introduction

3.1. The cell cycle and mitosis

Proliferation of tissues relies on the amplification of cell number by means of cell growth and cell division (Alberts et al., 2008). Cell cycle regulation involves several basic principles: among them is the cyclic synthesis of key regulatory proteins, e.g. the cyclin family proteins. Furthermore, reversible post-translational modifications like protein phosphorylation or acetylation play an important role. The cell cycle has a clear directionality that relies on irreversible, switch-like protein degradation events. Two main functions of the cell cycle are the replication of the genome and the actual cell division. Separated in time, replication and division are executed in S-phase (for synthesis) and M-phase (for mitosis, from greek mitos, thread), respectively. The two other cell cycle phases are the "gap" phases G1 (between M and S) and G2 (between S and M). The gap phases provide time for growth of the cell, synthesis of components required for the next phase and control points for cell cycle regulation. G1, S and G2 phase are collectively referred to as interphase. Mitosis in mammalian cells can again be subdivided into distinct phases. During prophase, DNA condenses into densely packed chromosomes. Cell-cell contacts are reduced and cells detach from their substrate. Also in prophase, assembly of the mitotic spindle is initiated (see chapter 3.2). Prometaphase in mammalian cells starts with the breakdown of the nuclear envelope. Chromosomes are aligned on the mitotic spindle until they all gather in the equatorial plane of the cell at metaphase, an arrangement called "metaphase plate". Finally, the two copies of each chromosome are separated and pulled to opposite poles of the cell by the mitotic spindle in anaphase. During telophase and cytokinesis, the cell elongates and a contractile actin-myosin ring in collaboration with the secretory pathway mediates cleavage and abscission of the two daughter cells.

The key regulator of mitosis is cyclin-dependent kinase 1 (Cdk1). During S-phase and G2-phase, B-type cyclins slowly accumulate and bind to Cdk1. Cyclin B1 binding is necessary but not sufficient for Cdk1 activation. Cdk1 has to be additionally activated by Cdk activating kinase (CAK) dependent phosphorylation of T161. Furthermore, inhibitory phosphorylations at T14 and Y15, imposed by the kinases Wee1 and Myt1, have to be removed by the dual specificity phosphatase Cdc25. Mitotic entry is a switch like event due to positive feedback loops. Once Cdk1 is activated, it contributes to activation of Cdc25 and inhibition of Wee1.

Active Cdk1-cyclin B1 complex phosphorylates a series of cellular targets leading to the morphological changes characteristic of mitotic cells. For example, the disassembly of the nuclear envelope is facilitated by direct phosphorylation of nuclear lamins, leading to their depolymerization (Heald and McKeon, 1990). In cell free extracts of *Xenopus* eggs, DNA compaction into highly condensed mitotic chromosomes is influenced by the 5-subunit condensin protein complex. *In vitro*, the ATP dependent introduction of positive writhe into DNA ("knotting activity") by condensin requires Cdk1-cyclin B1 (Kimura and Hirano, 1997). Furthermore, formation of the mitotic spindle (see below) depends on the phosphorylation of microtubule associated proteins (MAPs) by Cdk1-cyclin B1.

3.2. Spindle assembly and error correction by Aurora B

One of the hallmarks of mitosis is the formation of the mitotic spindle. Spindle formation involves a global rearrangement of the microtubule cytoskeleton. In G2 phase, microtubules (MTs) emanate from the cellular microtubule organizing center (MTOC) composed of two centrosomes and a series of accessory proteins, the pericentriolar material (PCM). Microtubules are an inherently polar structure with a plus end distal of the MTOC and a minus end proximal to the MTOC. Plus ends of microtubules are defined by a higher growth rate than minus ends.

In early prophase, centrosome separation and migration of the two centrosomes to opposite sides of the nucleus set the stage for the formation of a bipolar structure, the mitotic spindle (Fig. 1A). The mitotic spindle comprises mainly three different types of microtubule (MT) arrangements. (1) Polar MTs from the two opposing spindle poles overlap in an antiparallel fashion in the spindle midzone, where they are linked by bi- or multivalent MAPs or motor proteins (Blangy et al., 1995). They define the overall spindle geometry. (2) Astral MTs point from the centrosomes towards the cell cortex and serve to position the mitotic spindle within the cell. (3) The third type of spindle microtubules are the kinetochore-fibers (K-fibers), that link MTOCs and chromosomes.

The site of MT attachment at chromosomes is the kinetochore, a huge multi-subunit protein complex that assembles at the centromeric heterochromatin region of the chromosomes (Cleveland et al., 2003; Santaguida and Musacchio, 2009) (Fig. 1B). Especially in anaphase, maintenance of stable kinetochore-microtubule attachment is challenging since kinetochores are pulled towards the spindle poles by following the ends of depolymerizing microtubules.

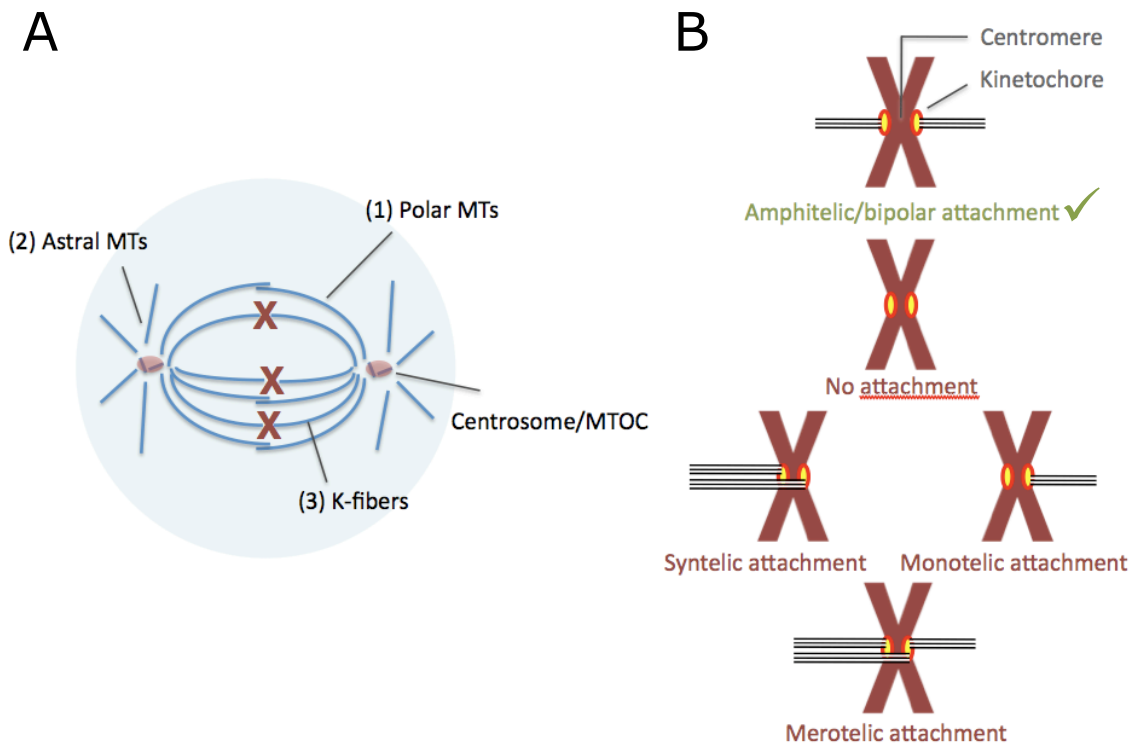


Fig. 1: The mitotic spindle and chromosome attachment. (A) The three main types of spindle microtubules (MTs). *Polar microtubules* (1) range from centrosomes to the spindle midzone. There they overlap in an antiparallel fashion. *Astral MTs* (2) link the centrosomes with the cell cortex. *K-fibers* (3) are microtubule bundles that link the kinetochores of chromosomes with the spindle poles. (B) Types of kinetochore-spindle attachments. *Amphitelic attachment*: correct bipolar attachment with both kinetochores linked to opposite spindle poles. *Syntelic attachment*: both kinetochores are bound to microtubules emanating from the same spindle pole. *Monotelic attachment*: only one kinetochore is attached to K-fibers. *Merotelic attachment*: one kinetochore is attached to K-fibers from the two spindle poles.

Different components of the kinetochore have been implicated in microtubule binding. A large molecular complex named the KMN network (KNL-Mis12-Ndc80) is both associated with kinetochore subunits as well as with microtubules (Cheeseman et al., 2006; Ciferri et al., 2008). The motor protein CENP-E is able to bind to microtubules (Neumann et al., 2006) and on the other hand to Nuf2 (Liu et al., 2007), a component of the Ndc80 complex. CENP-E deficient cells have problems capturing their chromosomes with the mitotic spindle (McEwen et al., 2001). In yeast, Bir1 and Sli15, both components of the chromosomal passenger complex (Vagnarelli and Earnshaw, 2004) have been shown to build an accessory connection between kinetochores and microtubules that might possess regulatory functions (Sandall et al., 2006).

Although MTs can be nucleated at kinetochores, the most common mechanism of K-fiber formation is based on "search and capture" of MTs emanating from centrosomes (Kirschner and Mitchison, 1986). A characteristic property of microtubules is their dynamic instability, i.e. they undergo alternating growth and shrinkage at their plus ends.

As cells enter mitosis, the dynamic instability of MTs increases (Verde et al., 1990). Dynamically unstable microtubules probe the cellular space and eventually get captured by kinetochores via their plus ends. Ideally, the two kinetochores of a chromosome should be attached to opposing poles of the spindle, an arrangement referred to as bipolar or amphitelic. Although there is an inherent bias towards this bipolar configuration (Indjeian and Murray, 2007; Sakuno et al., 2009), the stochastic nature of the search and capture mechanism also leads to a series of unproductive chromosome attachments (Cimini and Degrossi, 2005). In the case of monotelic attachment, only one kinetochore is attached to K-fibers. Syntelic attachment refers to a chromosome having both kinetochores attached to the same spindle pole. A merotelic attachment denotes a situation where one kinetochore is attached to K-fibers emanating from both spindle poles. Any chromosome orientation apart from the amphitelic case would result in breakage or missegregation of chromosomes in anaphase, if uncorrected. This is avoided in living cells due to activation of the spindle assembly checkpoint (SAC) allowing time to resolve erroneous attachments by a repair mechanism. In yeast as well as in higher eukaryotes the kinase Ipl1/Aurora B is instrumental in this error correction (Tanaka et al., 2002). Ipl1/Aurora B together with Sli15 and Bir1 (INCENP and survivin in higher eukaryotes) form the chromosomal passenger complex (CPC) (Vagnarelli and Earnshaw, 2004). The CPC concentrates specifically at centromeres of those chromosomes that do not display amphitelic attachment (Knowlton et al., 2006). Interestingly, Aurora B kinase activity is able to disrupt interactions of microtubules with the KMN network *in vitro*. This activity is, at least in part, mediated by direct phosphorylation of the Ndc80 N-terminal MT interaction domain (Cheeseman et al., 2006; Ciferri et al., 2008). In vertebrates, another important downstream factor of Aurora B is the mitotic centromere-associated kinesin (MCAK). This microtubule depolymerase is recruited by Aurora B to incorrect microtubule-kinetochore contacts (Knowlton et al., 2006). Since MCAK has an *in vitro* microtubule depolymerizing activity (Hunter et al., 2003), it is thought to destabilize K-fibers that do not lead to bipolar attachments. The now free kinetochores can undergo a new round of search and capture based attachment. When all chromosomes have achieved stable bipolar attachment, they are aligned in one plane at the center of the mitotic spindle, the metaphase plate.

Aurora B activity has to be lowered once correct attachments are forming. On the one hand, this can happen by reducing centromeric Aurora B to basal levels (Knowlton et al., 2006). On the other hand, productive kinetochore-MT attachments generate

intrakinetochores tension (Maresca and Salmon, 2009) which pulls outer kinetochores components like Ndc80 further away from centromeric Aurora B, resulting in dephosphorylation of Aurora B substrates by competing phosphatases (Liu et al., 2009). As a consequence, tension generating bipolar attachments within the mitotic spindle, are preferentially stabilized.

3.3. *Sister chromatid cohesion*

Species that organize their genomes in multiple chromosomes are facing the problem of how to identify the respective sister chromatids when it comes to distribution of the previously replicated genomes in a subsequent mitosis. An elegant mechanism preventing this problem is cohesion, i.e. the fact that the two copies of a chromosome stay together from the time of replication until the onset of anaphase. Two distinct properties of chromosomes contribute to cohesion. The first is DNA concatenation which naturally occurs during S-phase when two replication forks encounter each other (Sundin and Varshavsky, 1980). In theory, catenation could account for keeping sister chromatids together (Murray and Szostak, 1985). However, most catenations are resolved already prior to anaphase and cohesion is maintained even in the absence of catenation (Koshland and Hartwell, 1987). Nevertheless, a small fraction of catenations persists at centromeres until the onset of anaphase in human cells. They can be visualized as thin DNA threads labeled by the marker protein Plk1 interacting checkpoint helicase (PICH) (Baumann et al., 2007). PICH positive threads connect the separating chromatin masses until the catenations are resolved, presumably by Topoisomerase II (TOPO II) (Porter and Farr, 2004). The second source for sister chromatid cohesion is the cohesin protein complex (Nasmyth and Haering, 2005). Cohesin is the more crucial factor compared to catenation since the latter cannot sustain sister chromatid pairing in the absence of cohesin (Sonoda et al., 2001). How centromeric DNA catenation is maintained until anaphase and what purpose – if any – it might serve in chromosome segregation, is still an open question.

3.4. *Cohesin*

3.4.1. Components of the cohesin complex

Factors required for sister chromatid cohesion have initially been discovered in yeast genetic screens (Guacci et al., 1997; Michaelis et al., 1997). The respective protein products are specifically required for cohesion before the onset of anaphase. Among

them are two large coiled-coil proteins, structural maintenance of chromosomes 1 and 3 (Smc1 and Smc3). Smc proteins are characterized by their highly elongated shape. They fold back onto themselves at a globular hinge domain in the middle of the molecule which allows the formation of a very long antiparallel intramolecular coiled-coil (Melby et al., 1998). The very N- and C-termini of Smc proteins come in close proximity and together adopt a globular fold, the head domain which is associated with ATPase activity (Arumugam et al., 2003). Additional components of the cohesin complex involve Pds5 (Panizza et al., 2000), Scc1 and Scc3 (Michaelis et al., 1997). While Pds5 is a substoichiometric cohesin component (Sumara et al., 2000), Scc1 and Scc3 are integral subunits of the cohesin complex. Scc1 interacts with the head domains of Smc1 and Smc3 via its C- and N-terminus, respectively (Gruber et al., 2003). Scc3, which in higher eukaryotes comes in the two mutually exclusive "flavors" SA1 and SA2, is a binding partner of Scc1.

3.4.2. The cohesin ring model

How does cohesin hold sister chromatids together? Smc1 and Smc3 form heterodimers mediated by interaction via their hinge domains (Melby et al., 1998). In electron micrographs, Smc dimers appear either as V-shaped structures, linked at the hinge domain or as closed circles with an additional contact involving the head domains. The circular structure of the cohesin complex and the appropriate molecular dimensions inspired the hypothesis that DNA strands might be entrapped within the cohesin ring (Fig. 2). The linkage between sister chromatids in this model is hence topological rather than mediated by direct protein-DNA contacts. Although the Smc1 and Smc3 head domains can interact directly (Mc Intyre et al., 2007; Melby et al., 1998), integrity of Scc1 is clearly required for cohesin function (Uhlmann et al., 1999) and for stable closure of the three-partite ring (Gruber et al., 2003).

Substantial proof for this model has been contributed by a series of elegant studies from the Nasmyth lab. Proteolytic cleavage of one of the three members of the cohesin ring does not cause dissociation of the cleavage fragments from each other because they remain linked by the other cohesin subunits. Yet, artificial cleavage of engineered Scc1 or Smc3 leads to sister chromatid separation *in vivo* and to dissociation of cohesin from circular plasmid DNA *in vitro* (Gruber et al., 2003; Uhlmann et al., 2000). The topological nature of the cohesin-DNA interaction was further underscored by the finding that cleavage of circular plasmid DNA by a restriction endonuclease also leads to

its dissociation from associated cohesin (Haering et al., 2008; Ivanov and Nasmyth, 2005, 2007). Consistent with the model, cohesin is able to slide along DNA. This is reflected by the accumulation of cohesin at sites of convergent transcription (Lengronne et al., 2004). Cohesin complexes are highly conserved from yeast to mammals (Darwiche et al., 1999).

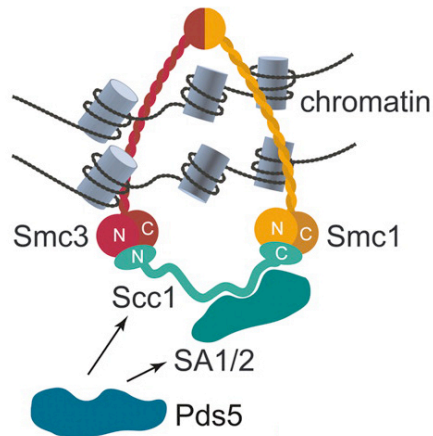


Fig. 2: The cohesin ring complex. The two large anti-parallel coiled coil proteins Smc1 and Smc3 form a V-shaped structure connected via their hinge domains. The N- and C-termini of Smc1/3 form a globular head domain that has ATPase activity. The Smc1/3 head domains are linked by Scc1. SA1/2 is associated with Scc1 while Pds5 shows binding to both Scc1 and SA1/2. Two chromosomal DNA strands can be accommodated within the cohesin ring. Image with modifications from Peters et al. (2008).

3.4.3. Loading of cohesin and establishment of cohesion

In genetic screens for sister chromatid cohesion factors were picked up that are not direct members of the cohesin complex but rather required for the establishment of cohesion. Two main steps can be distinguished: loading of cohesin onto DNA and the subsequent establishment of the physical linkage between sister chromatids. Cohesin loading onto DNA requires a complex of Scc2 and Scc4 and occurs in late mitosis (vertebrates) or late G1 phase (yeast). While the Scc2/Scc4 complex becomes dispensable after cohesin loading (Ciosk et al., 2000), other factors including Ctf4, Ctf18 and the acetyl transferase Eco1 mediate the proper cohesin dependent pairing of the emerging sister chromatids during the subsequent S-phase (Toth et al., 1999) and consistently co-localize with DNA replication forks (Lengronne et al., 2006). Surprisingly, entering the two sister chromatids into the cohesin ring seems to involve transient opening of the otherwise extremely stable Smc1/3 interaction at the hinge region (Gruber et al., 2006). Mutations in the gene sequence of the human Eco1 homolog Esco2 are found in patients suffering from Robert's syndrome, an autosomal recessive genetic disorder, characterized by defects in sister chromatid cohesion (Vega et al., 2005).

3.4.4. Resolving cohesion in mitosis

To allow equal segregation of the two genome copies to the newly arising daughter cells, physical linkages between sister chromatids have to be removed in mitosis. In cells of

higher eukaryotes, this is ensured by two different pathways (Waizenegger et al., 2000) (Fig. 3A). Most cohesin is displaced from chromatin early in mitosis by action of the so-called "prophase pathway" (Sumara et al., 2000). It requires the cohesin associated factor Wapl (Gandhi et al., 2006; Kueng et al., 2006), the polo like kinase 1 (Plk1) (Sumara et al., 2002) and phosphorylation of several serine and threonine residues within the C-terminal part of the cohesin subunit SA1/2 (Hauf et al., 2005).

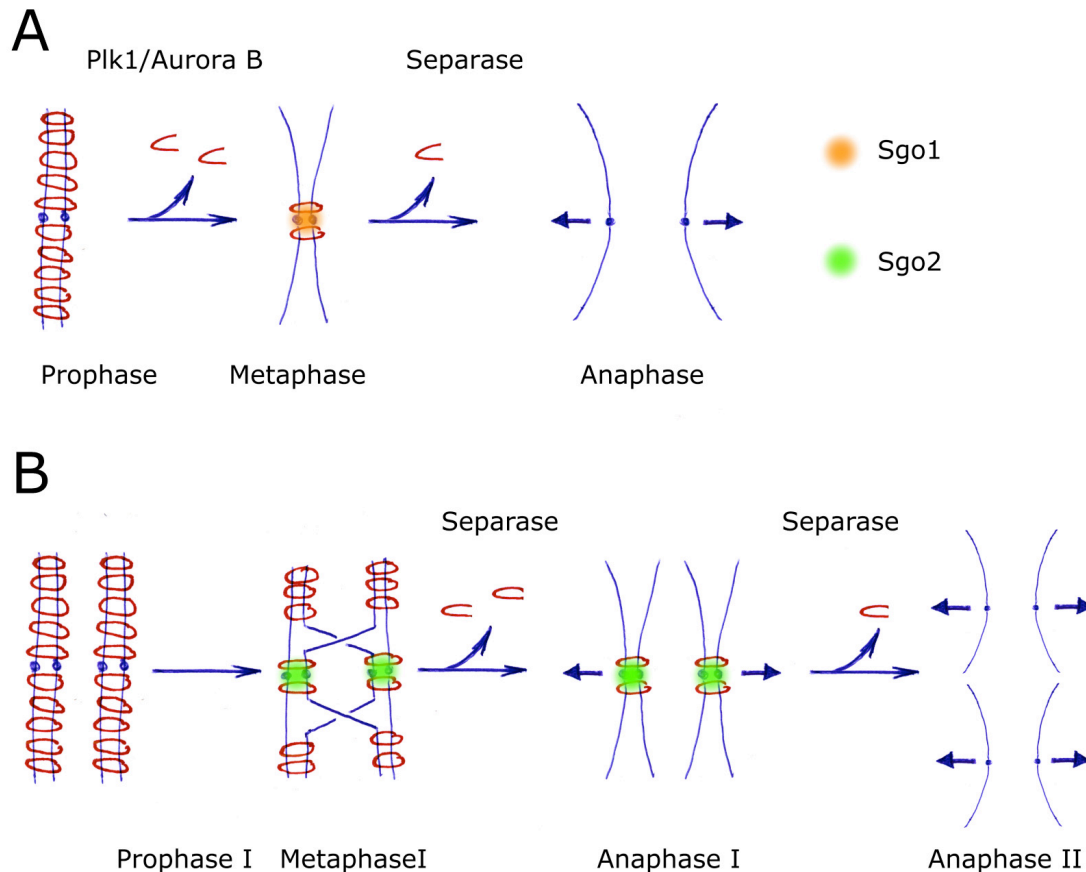


Fig. 3: Resolution of sister chromatid cohesion in mitosis and meiosis. (A) Cohesin removal in mitosis is a two-step process. The majority of cohesin complexes is removed from chromosome arms in prophase and prometaphase of mitosis. Opening of the cohesin ring complex requires Wapl, Plk1 and phosphorylation of SA1/2. Centromeric cohesin is not targeted by the prophase pathway due to presence of the cohesin protector shugoshin 1 (Sgo1). Sgo1 is associated with protein phosphatase 2A (PP2A), which supposedly keeps SA1/2 dephosphorylated. At the metaphase-anaphase transition, separase becomes active and cleaves Scc1 thereby removing residual cohesin complexes from centromeres. (B) Cohesin removal in meiosis. Crossing-over formation in prophase of meiosis I results in chiasmata. As a consequence, homologous chromosome pairs are held together by arm cohesion. At the transition from metaphase to anaphase of meiosis I, arm cohesin is removed by separase. This leads to segregation of homologs and reductional division. Rec8, the meiotic counterpart of Scc1 needs to be phosphorylated to become a separase substrate. Centromeric cohesin is protected in meiosis I by a complex of Sgo2 and PP2A which keeps Rec8 dephosphorylated and hence shielded from cleavage by separase. In meiosis II, Sgo2 is somehow inactivated which is why in anaphase II separase can remove the remaining centromeric cohesin. Sister chromatid separation and cytokinesis lead to the formation of haploid germ cell precursors.

Although Plk1 is able to phosphorylate cohesin, it has not been formally shown that direct phosphorylation of SA1/2 by Plk1 is required for prophase cohesin removal.

A small fraction of cohesin at the centromere is spared from the prophase pathway and persists until the metaphase-anaphase transition (Fig. 3A). In *S. cerevisiae*, removal of cohesin complexes requires the proteolytic cleavage of its Scc1 subunit (Uhlmann et al., 1999) mediated by the giant cysteine protease separase (Uhlmann et al., 2000). This process is conserved in higher eukaryotes (Hauf et al., 2001). At the onset of anaphase, cohesin cleavage initiates K-fiber mediated movement of chromosomes towards the spindle poles.

3.4.5. Regulation of separase

Premature or delayed activation of separase would be detrimental to cells. Therefore, it comes at no surprise that the protease is highly regulated (Fig. 4). Inhibition of separase is mediated by the binding of the stoichiometric proteinaceous factor Pds1/securin (Yamamoto et al., 1996). The facts that *securin*^{-/-} mice are viable (Wang et al., 2003) and that human cells can maintain their genomic integrity in the absence of securin (Pfleghaar et al., 2005) suggested alternative regulatory mechanisms. One such mechanism is the phosphorylation of separase by Cdk1-cyclin B1 and the subsequent phosphorylation dependent binding of Cdk1-cyclin B1 to separase (Gorr et al., 2005; Stemmann et al., 2001). The most critical inhibitory Cdk1 phosphorylation site within human separase is the residue serine 1126 (serine 1121 in murine separase). Homozygous *securin* knockout mice that in addition carry at the endogenous locus one *separase* allele that can no longer be phosphorylated at a serine 1121 (*securin*^{-/-} *separase*^{+S1121A}) have been created (Huang et al., 2005). Comparison of the phenotypes of various combination of alleles shows that securin and separase phosphorylation collaborate to ensure proper separase regulation.

3.5. *The anaphase promoting complex or cyclosome (APC/C)*

In order to exit mitosis, cells have to revert properties that define the mitotic state. The two main inhibitors of late mitotic events are the Cdk1-cyclin B1 complex and Pds1/securin (Thornton and Toczyski, 2003). Their downregulation leads to the dephosphorylation of Cdk1-cyclin B1 targets by counteracting phosphatases and to the activation of separase, thereby initiating anaphase. Securin as well as the cyclin B1 subunit of the Cdk1-cyclin B1 complex are inactivated by means of proteolytic destruction via the 20S proteasome (Cohen-Fix et al., 1996; Glotzer et al., 1991). This

multi-subunit ATP-dependent degradation machinery specifically recognizes and degrades proteins which are labeled by chains of covalently coupled monomers of the 76 amino acid polypeptide ubiquitin (Pickart, 1997). Ubiquitin attachment to target proteins is a three step process catalyzed by the enzymes E1 (ubiquitin activating enzyme), E2 (ubiquitin carrier protein or ubiquitin conjugating enzyme) and E3 (ubiquitin protein ligase). Ubiquitin is activated for covalent coupling to substrates by the hydrolysis of ATP to AMP + PP_i. The free energy of this reaction is conserved in a relay system involving a thioester bond between ubiquitin's C-terminal glycine residue and a cysteine residue of the E1 or later the E2. E3 enzymes come in two flavors. E3s of the HECT type also form a thioester intermediate with ubiquitin while RING type E3s catalyze the direct transfer from the E2 to substrates by optimally aligning both reaction partners. At the substrate level, the first ubiquitin becomes attached via an isopeptide bond of its C-terminal glycine residue and the ε-amino group of a substrate lysine side chain. If a substrate is to be labeled for proteasomal destruction, additional ubiquitin moieties are coupled to lysine 48 or pre-conjugated ubiquitin (Hershko and Ciechanover, 1992).

Substrate specificity is achieved at the level of E3 enzymes. There are many specific enzymes of the E3 class, compared to only one E1 and few E2 enzymes. The RING type E3 enzyme responsible for cyclin B1 and securin ubiquitylation is the anaphase promoting complex or cyclosome (APC/C) (Irniger et al., 1995; King et al., 1995; Sudakin et al., 1995). Important subunits of this large complex are summarized briefly below. Apc1 is the largest APC/C subunit and acts as a scaffold. Apc11, the subunit with the E3 enzyme activity, is linked to this scaffold by Apc2, which shares a cullin fold with other ubiquitin ligases. The subunits Apc3, and Apc6-Apc8 comprise tetratricopeptide repeats (TPR) important for protein-protein interactions (Vodermaier, 2004).

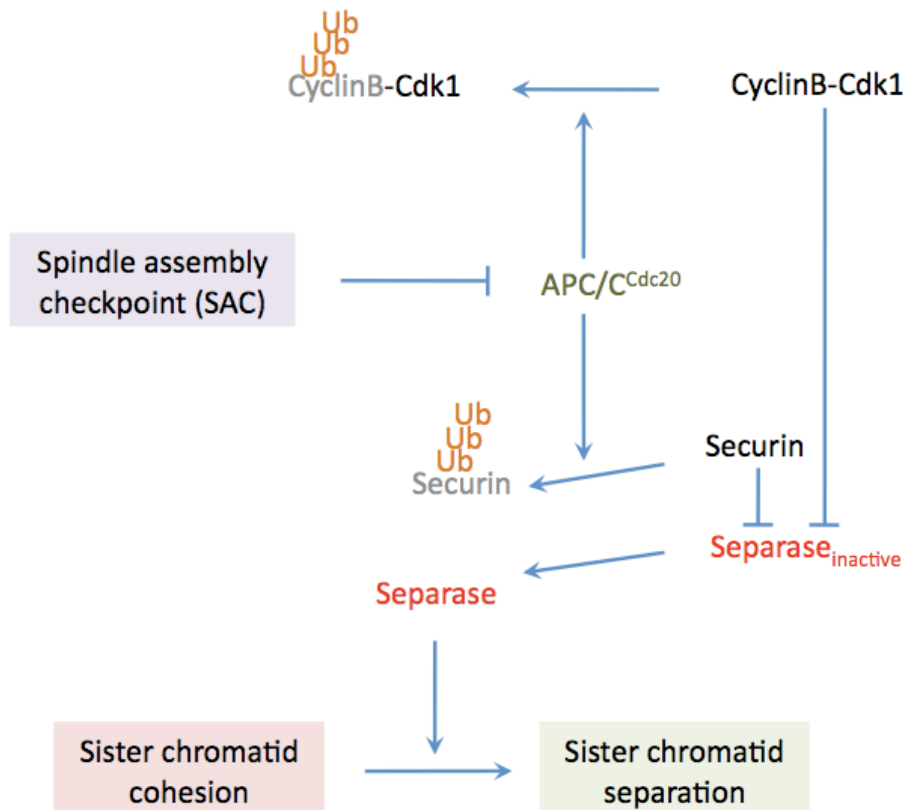


Fig. 4: Regulatory network of mitotic sister chromatid separation. Separase triggers an important aspect of anaphase. Via its protease activity, it mediates the resolution of sister chromatid separation. In early mitosis, separase is inhibited by securin and cyclin B1. At anaphase onset, the two separase inhibitors are ubiquitylated by the APC/C^{Cdc20} and subsequently degraded. The APC/C^{Cdc20} is kept inactive by the SAC until all chromosomes have achieved correct bipolar attachment to the mitotic spindle.

For full functionality, the APC/C requires either of the substrate recruiting factors Cdc20 and Cdh1 (Sigrist et al., 1995; Sigrist and Lehner, 1997; Visintin et al., 1997). Both factors bind to the APC/C via their C-terminal isoleucine-arginine (IR) motif, which interacts with the TPR containing APC subunits (Vodermaier et al., 2003). Cdc20 and Cdh1 recognize their substrates via an extended C-terminal WD40 repeat domain (Kraft et al., 2005). Short sequence motifs (degrons), predominantly close to the N- and C-termini, qualify APC/C substrates. The destruction box (D-box, Arg-X-X-Leu) is common to APC/C^{Cdc20} substrates while substrates harboring either a D-box or a KEN-box (Lys-Glu-Asn) become recruited to APC/C^{Cdh1}. In addition to substrate recruitment, Cdc20 also stimulates the ubiquitin ligase activity of the APC/C. This function requires a motif called the C-box located within the N-terminal part of Cdc20 (Kimata et al., 2008). The APC/C^{Cdc20} is tightly controlled by the spindle assembly checkpoint (SAC, see chapter 3.9) and only becomes active when the metaphase plate has properly formed. Cdh1 is kept inactive until anaphase due to inhibitory phosphorylations mainly imposed

by cyclin B1/Cdk1 (Jaspersen et al., 1999; Zachariae et al., 1998). As Cdh1 becomes gradually dephosphorylated, APC/C^{Cdh1} starts to ubiquitylate its substrates in late anaphase. Among them are mitotic regulators like Plk1 but also Cdc20 (Charles et al., 1998). As APC/C^{Cdc20} activity diminishes, APC/C^{Cdh1} takes over as an important regulator of G1 phase that prevents premature entry into the next S-phase (Irniger et al., 1995).

3.6. *Specific properties of meiosis*

Meiosis is a modified type of cell division with several deviations from mitosis, all aimed at producing haploid gametes from diploid precursor cells. One such difference is the functional incorporation of different subunits into the cohesin complex and the use of these complexes for cohesion establishment during the pre-meiotic S-phase. In *S. cerevisiae* as well as in higher eukaryotes, Rec8 is the meiotic counterpart of Scc1 (Michaelis et al., 1997; Watanabe et al., 2001). In addition, Smc1 is replaced by Smc1 β and SA1/2 by Stag3 in mammalian meiosis.

In the first meiotic division (meiosis I), homologous chromosomes are segregated to the two daughter cells. This requires a series of deviations from the mitotic program. The two sister kinetochores of a chromosome behave as one unit and become attached to one pole of the meiotic spindle. Meiosis specific proteins, such as Moa1 in *S. pombe* (Martin-Castellanos et al., 2005; Yokobayashi and Watanabe, 2005) or the monopolin complex in *S. cerevisiae* (Toth et al., 2000), as well as cohesin bound to the core centromere (Sakuno and Watanabe, 2009) are responsible for kinetochore fusion and monopolar attachment. In order to build tension and thus to allow stable formation of K-fibers, homologous chromosomes need a physical linkage. This is achieved by recombination events in prophase of meiosis I. A meiosis specific nuclease induces double strand break (DSB) formation (Keeney et al., 1997). For DSB repair by means of homologous recombination, mainly the homologous chromosome and not the corresponding sister chromatid is used. Resolution of the intermediate Holliday junction structures will sometimes result in crossing-overs between homologous chromosomes, which later manifest as visible chiasmata. The arm cohesin complexes distal of these crossing-overs/chiasmata are what keeps homologous chromosomes paired (Fig. 3B).

The reductional character of the first meiotic division is due to the lack of DNA replication between meiosis I and II. This is achieved by only partial but not full downregulation of Cdk1 activity after meiosis I enabling spindle disassembly but not formation of prereplicative complexes required for DNA replication. Meiosis II largely

resembles a normal mitotic division with bipolar attachment of chromosomes and segregation of sister chromatids.

In mammalian males, four haploid spermatids are the result of meiosis. In females, only one oocyte is produced due to extremely asymmetric cell divisions leading to the extrusion of a so-called polar body both in meiosis I and in meiosis II. While male germ cells progress through meiosis to the post-meiotic G1 phase, female vertebrate oocytes will arrest in metaphase of meiosis II until fertilization. This arrest is due to APC/C^{Cdc20} inhibition by a signaling cascade collectively referred to as "cytostatic factor" (CSF) (Haccard et al., 1993; Masui and Markert, 1971). The most downstream component of the CSF pathway is xErp1 in *X. laevis* or Emi2 in *H. sapiens*. It acts as a direct and stoichiometric inhibitor of APC/C^{Cdc20}. Upon fertilization, an influx of Ca²⁺ ions triggers the proteolytic degradation of xErp1, leading to APC/C^{Cdc20} activation and rapid exit from meiosis II (Rauh et al., 2005; Schmidt et al., 2005). Following the fusion of female and male pronuclei, the zygote can now progress into G1 phase of the first embryonic cell cycle.

3.7. Cohesin removal during meiosis

Once cohesin has fulfilled its role as a molecular glue between homologous chromosomes, it has to be removed from chromosome arms. This happens at the metaphase-anaphase transition of meiosis I. The cohesin ring is opened by separase mediated proteolytic cleavage of the subunit Rec8 (Buonomo et al., 2000) and the meiotic spindle can now pull homologs towards the spindle poles (Fig. 3B). Centromeric cohesin is left intact and keeps sister chromatids paired until anaphase of meiosis II. Then, the remaining cohesin fraction is removed, again by separase cleavage of Rec8. The two step process with a resistant centromeric cohesin population is faintly reminiscent of the mitotic situation. However, in meiosis both steps involve proteolysis and spread over two rounds of cell division.

Mitotic (Scc1) and meiotic (Rec8) cohesin become phosphorylated in the vicinity of their separase cleavage sites by Cdc5/Plk1 and possibly other kinases in *S. cerevisiae* (Alexandru et al., 2001) and human cells (Hauf et al., 2005; Hornig and Uhlmann, 2004). Phosphorylation merely ameliorates the separase dependent cleavage of Scc1, while it is an essential precondition for the proteolysis of Rec8 by separase *in vitro* (Hauf et al., 2005; Kudo et al., 2009). Accordingly, Scc1 phosphorylation of cohesin is largely dispensable *in vivo* (Hauf et al., 2005), while Rec8 phosphorylation is a crucial aspect of meiosis (Brar et al., 2006).

The full dependence on phosphorylation is a shared characteristic of meiotic Rec8 cleavage and of proteolysis independent opening of cohesin in the mitotic prophase. As outlined below, it is the key to understanding how resolution of meiotic cohesin is solely dependent on separase activity, yet occurs in two, temporally well separated steps.

3.8. *Shugoshin proteins protect centromeric cohesin*

Centromeric cohesin resists its removal in prophase of mitosis as well as in anaphase of meiosis I. The molecular basis of centromeric cohesin protection remained elusive until the *Drosophila* meiosis mutant *mei-S332* (Sandler et al., 1968) was found to be defective in centromeric cohesion during meiosis (Kerrebrock et al., 1992). The MEI-S332 protein localizes to meiotic centromeres. While not containing any conserved domains, an N-terminal coiled-coil region was predicted, that is required for oligomerization. Furthermore, the C-terminal end of MEI-S332 is rich in basic amino acid residues (Kerrebrock et al., 1995; Tang et al., 1998).

The identification of MEI-S332 homologs in other species has been precluded for almost a decade due to its low degree of sequence conservation. Only the N-terminal coiled-coil region and the C-terminal basic motif are weakly conserved. This fact, combined with yeast genetic screens led to the discovery of MEI-S332 homologs in other eukaryotic genomes (Katis et al., 2004; Kitajima et al., 2004; Rabitsch et al., 2004). MEI-S332 homologs were named "shugoshin" (Sgo) - Japanese for the Samurai's guardian spirit. While *S. cerevisiae* and flies express only one shugoshin, both *S. pombe* and mammals have two.

3.8.1. Cohesin protection by human Sgo1 in mitosis

The function of the mammalian Sgo1 has first been studied by siRNA mediated depletion from cultured cells (McGuinness et al., 2005). Sgo1 depleted cells separate their sister chromatids already in early mitosis. Premature sister chromatid separation is not a result of separase activity since it also occurs under conditions, in which separase is inactive. Sister chromatid cohesion in Sgo1 depleted cells can be rescued by the expression of a mutant form of SA2 that is resistant to the prophase pathway (McGuinness et al., 2005). This SA2 mutant lacks a series of potential phosphorylation sites required for cohesin removal by the prophase pathway. It was therefore assumed that Sgo1 interferes with SA1/2 phosphorylation by the prophase pathway (Fig. 3A). Interestingly, Sgo1 interacts with protein phosphatase 2A (PP2A), the major cellular Ser-/Thr-phosphatase (Kitajima et al., 2006; Riedel et al., 2006).

The PP2A holoenzyme consists of the three subunits A, B and C. The A subunit constitutes a scaffold of PP2A. It consists mainly of HEAT repeats and is a founding member of this protein family. The PP2A-A subunit entertains interactions with both the B and the C subunit. The C subunit is the smallest PP2A subunit and harbors the catalytic phosphatase activity of the enzyme. A manganese ion bound to the C subunit is essential for the enzymatic hydrolase activity. Substrate specificity and subcellular localization are determined by the choice of the mutually exclusive regulatory B subunit. Several coding genes as well as alternative splicing give rise to at least 16 different B subunits. Based on sequence homology they are grouped into the three main categories B, B' and B''.

Cells expressing a mutant version of Sgo1 that cannot bind PP2A have similar cohesion defects as Sgo1 depleted cells (Tang et al., 2006). The main function of mammalian Sgo1 is thus the recruitment of PP2A to centromeres. Here, it is thought to keep cohesin dephosphorylated, thereby protecting it from phosphorylation dependent displacement. Sgo1 is dispensable for mammalian meiosis. Depletion of Sgo1 from *in vitro* cultured mouse oocytes did not result in any cohesion defects (Lee et al., 2008).

3.8.2. Cohesin protection by Sgo2 during meiosis

Sgo2 is mainly required during meiosis. While separase removes cohesin complexes from the arms of homologous chromosomes in anaphase I, Sgo2 protects cohesin at centromeres (Fig. 3B). Oocytes lacking Sgo2 lose sister chromatid cohesion already at the metaphase I to anaphase I transition (Lee et al., 2008; Llano et al., 2008). Sgo2 co-localizes both with PP2A and with the cohesin subunit Rec8 at the centromeres of meiotic chromosomes (Gomez et al., 2007; Lee et al., 2008; Llano et al., 2008). It has been proposed that Rec8 cleavage by separase depends on prior Rec8 phosphorylation (Brar et al., 2006). The current model suggests dephosphorylation of Rec8 by Sgo2 associated PP2A as the molecular basis of meiotic cohesin protection. Evidence for this theory stems from experiments in yeast and mouse meiosis. Normally, only centromeric cohesin is protected by PP2A in meiosis I. If PP2A is artificially forced to generic chromatin in *S. pombe*, all cohesin becomes resistant to separase in meiosis I (Riedel et al., 2006). Furthermore, meiotic *S. pombe* shugoshin with a mutated PP2A binding site is non-functional (Xu et al., 2009). Also in mammalian (mouse) meiosis, PP2A seems to be important. Treatment of mouse oocytes with the PP2A inhibitor okadaic acid leads to premature sister separation of chromatids already in meiosis I (Mailhes et al., 2003). To the contrary, forced overexpression of mitotic Sgo1 in mouse oocytes results in the

recruitment of PP2A along the whole length of chromosome arms. In this case, cohesin will not be removed from these chromosome arms in anaphase of meiosis I (Xu et al., 2009). However, it has not yet been formally shown, that PP2A binding to mammalian Sgo2 is indeed required for Sgo2-dependent cohesin protection. A more precise characterization of PP2A binding to Sgo2 could therefore provide a tool to study the effects of the Sgo2-PP2A interaction in mammalian meiosis.

3.8.3. Localization of shugoshin

In human mitotic cells, two factors have been identified that are important for the subcellular localization of Sgo1 as well as Sgo2: the kinases Aurora B and Bub1. Depletion of any of these two factors leads to complete dissociation of both Sgo1 and Sgo2 from chromatin (Huang et al., 2007). However, Sgo2 localization is far more complex. While Sgo2 is found at centromeres in meiosis I, it relocates to kinetochores in metaphase of meiosis II (Gomez et al., 2007). The change of localization has been proposed to deprotect centromeric cohesin in meiosis II and to enable separate to cleave this remaining chromosomal subfraction of cohesin in order to trigger sister chromatid separation in anaphase of meiosis II.

A similar relocalization pattern has been observed for Sgo2 at metaphase of mitosis in human cultured cells. So far, studies on Sgo2 relocalization have been purely descriptive. Cellular factors regulating the decision of Sgo2 binding to either centromere or kinetochore have not yet been identified. Above all, it remains unknown if the relocalization of Sgo2 has anything to do with its ill-understood inactivation between meiosis I and II.

3.9. *The spindle assembly checkpoint (SAC)*

The metaphase to anaphase transition has to be extremely well regulated. Due to its irreversible nature, any spindle defects present at anaphase onset will invariably lead to chromosome missegregation. As a consequence of the resulting aneuploidy, the daughter cells will either be inviable or they will head towards oncogenic transformation due to an inappropriate ratio of tumor suppressors versus protooncogenes (Weaver and Cleveland, 2006).

The spindle assembly checkpoint (SAC) is a safety mechanism that halts mitotic cells until they have attached all kinetochores to the mitotic spindle and more precisely have done so in an amphitelic fashion. The SAC is not absolutely crucial in mitosis of some organisms like *D. melanogaster* (Buffin et al., 2007). There it only becomes essential if

cells are challenged with conditions disturbing the MT cytoskeleton. In mammalian cells however, the SAC is essential even in unperturbed cell cycles and it is triggered in each and every mitosis until correct spindle assembly has taken place (Wassmann and Benezra, 1998).

3.9.1. Attachment and tension

Two main branches of the SAC can be distinguished: On the one hand the detection of unattached kinetochores and on the other hand the detection of inappropriately attached kinetochores. But how can a cell measure inappropriate attachments? If both kinetochores of a chromosome are attached to the same spindle pole, no pulling force can occur between kinetochores. The tension that the mitotic spindle exerts on a correctly attached chromosome is a physical property which - at least in theory - can be measured by cells (Stern and Murray, 2001). Nevertheless, the molecular nature of the "tension sensor" has remained elusive. In yeast, the Sli15-Bir1 complex linking kinetochores and microtubules has been implicated in tension sensing (Sandall et al., 2006). In agreement with this finding, studies in higher eukaryotes suggest that tension is measured within the kinetochore rather than at centromeres (Maresca and Salmon, 2009; Uchida et al., 2009). An important distinction between attachment and tension SAC is the requirement of the kinase Ipl1/Aurora B. Ipl1 mutant yeast cells as well as Aurora B depleted human cells are no longer able to arrest in response to lack of tension but they are still proficient in detecting unattached chromosomes (Biggins and Murray, 2001; Ditchfield et al., 2003; Hauf et al., 2003). Aurora B could indirectly trigger the SAC by converting mis-attached kinetochores into unattached kinetochores (Pinsky et al., 2006). However, at present the literature is not clear as to whether there could be a direct signal from Aurora B to the SAC (Vader et al., 2007).

For SAC research, chemicals also referred to as spindle poisons, have been extremely helpful. One class of compounds leads to depolymerization of microtubules. These include for example nocodazole, vinblastine and colcemid. Cells treated with MT depolymerizing drugs will exhibit unattached kinetochores and therefore trigger the attachment sensing branch of the SAC. The other class of spindle poisons (e.g. paclitaxel/taxol) leads to stabilization of microtubules, abolishing microtubule dynamics. MTs will still attach to kinetochores but they are no longer exerting forces. Consequently, kinetochores lack tension and cells arrest in mitosis via activation of the tension sensing SAC.

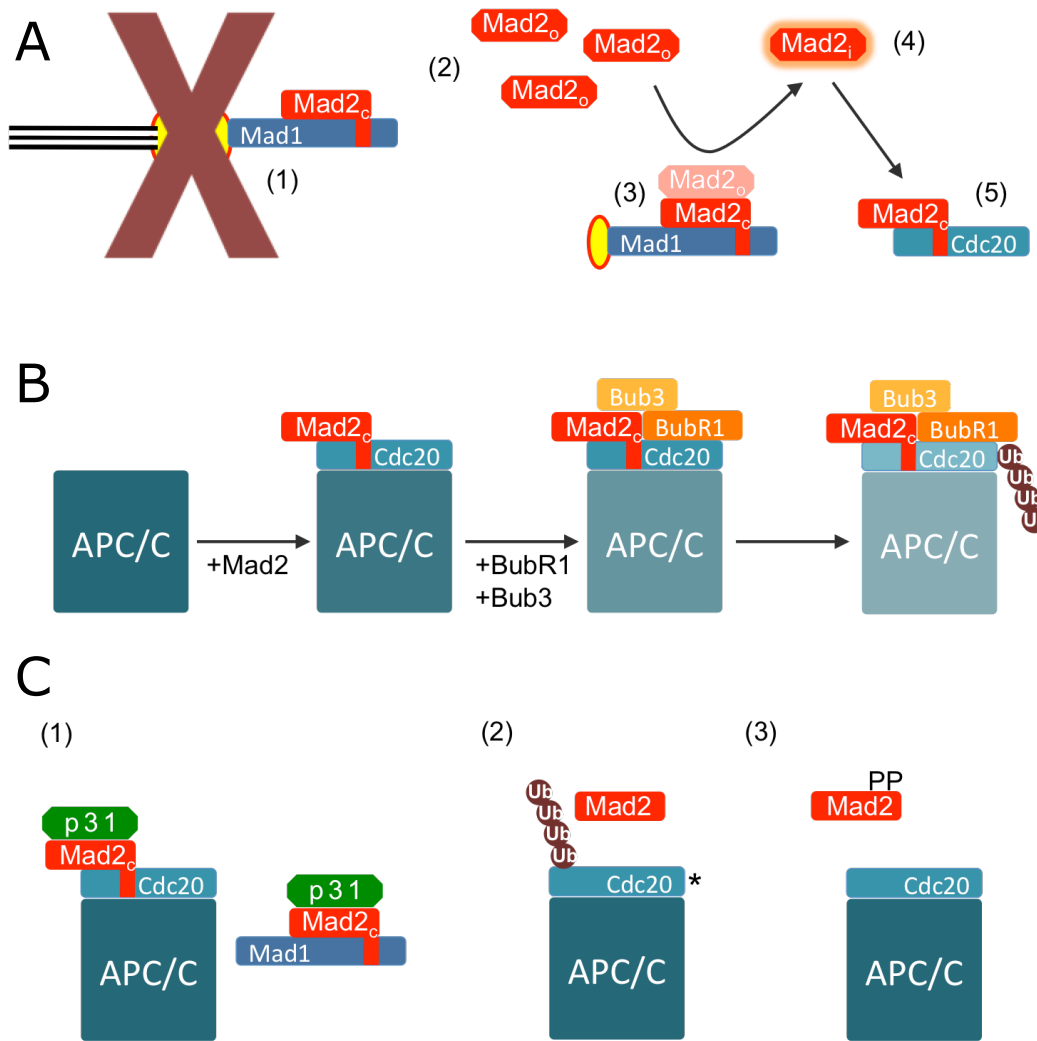


Fig. 5: The mitotic spindle assembly checkpoint (SAC). (A) The SAC template model. Unattached kinetochores attract a complex of Mad1 and Mad2 (1). Mad2 is in its closed (C) conformation in this complex. An additional (open, O) Mad2 molecule (2) binds to Mad1 associated Mad2 (3). In a catalytic mechanism, open Mad2 is activated to a hypothetical structural intermediate (I) between open and closed state (4). Now, it can efficiently bind to Cdc20, adopting the closed conformation (5). (B) Formation and function of the mitotic checkpoint complex (MCC). Once the Mad2-Cdc20 complex has been formed, additional checkpoint proteins (BubR1, Bub3) associate and build the MCC. This complex is more potent in APC/C^{Cdc20} inhibition than Mad2 alone. A further step in APC/C inhibition is MCC induced ubiquitylation of Cdc20 by the APC/C. (C) Current models for inactivation of the SAC. (1) p31 specifically binds to closed Mad2. On the one hand, this blocks Mad2 activation by the Mad1-Mad2 template complex, on the other hand, APC/C^{Cdc20} can be active despite bound Mad2. (2) Cdc20 ubiquitylation might contribute to the dissociation of Mad2 from Cdc20. (3) The phosphorylation of several serine/threonine residues of Mad2 negatively influences binding to Mad1 and Cdc20 and could therefore be a negative regulator of SAC.

3.9.2. Kinetochores as signaling hubs of the SAC

Already quite early it has become clear that unattached chromosomes induce a mitotic delay and that the centromere/kinetochore region of the chromosomes is essential for the arrest. Live cell imaging experiments elegantly demonstrated that the kinetochore of the

last unaligned chromosome is sufficient for mediating a mitotic arrest (Rieder et al., 1995; Rieder et al., 1994). In order to achieve robustness and an appropriate signal-to-noise ratio, it seemed logical that erroneously attached chromosomes generate a negative "wait" signal rather than correctly attached chromosomes sending a positive signal. The fact that a single unattached kinetochore is able to trigger the SAC suggested a catalytic nature of SAC signaling.

3.9.3. The molecular components of the SAC

In an attempt to identify genes required for the drug induced mitotic arrest in yeast, two genetic screens have been performed in the early 1990s (Hoyt et al., 1991; Li and Murray, 1991). Mutants isolated from the screens were named "mitotic arrest deficient" (Mad) and "budding uninhibited by benzimidazole" (Bub). The Mad and Bub genes are widely conserved among eukaryotes.

The SAC delays anaphase in response to spindle defects by directly targeting the Cdc20 co-factor of APC/C. Mad2, a 24 kDa protein, is the core component of the SAC. Mad2 binds to Cdc20 that remains associated with the APC/C. APC/C^{Cdc20} activity is inhibited in this complex and the bulk of substrates like securin or cyclin B1 will not become ubiquitylated (Fang et al., 1998; Li et al., 1997). In order to achieve full inhibition, the assembly of the so-called mitotic checkpoint complex (MCC) is required (Sudakin et al., 2001; Tang et al., 2001). In this complex, in addition to Mad2, also BubR1 and Bub3 are bound to APC/C^{Cdc20} (Fig. 5B). In the MCC, Cdc20 itself can become ubiquitylated by the APC/C and subsequently degraded. This Cdc20 destabilization during a SAC arrest is thought to further reduce APC/C activity (Nilsson et al., 2008). Inhibition of APC/C^{Cdc20} is subject to precise regulation since the Mad2-Cdc20 complex only forms with slow kinetics by itself (Sironi et al., 2001). How Mad2 is activated to only bind Cdc20 when the SAC becomes triggered, is explained by the currently most accepted view of the SAC, the "template model" (Nasmyth, 2005).

The template model requires an additional checkpoint factor: Mad1, an 83 kDa coiled-coil protein that interacts with Mad2. Briefly, the template model constitutes a signaling pathway with Mad1 as an upstream component, localized at unattached kinetochores. One of the most downstream steps of SAC signaling is the inhibitory binding of Mad2 to Cdc20. To delineate the template model, first some crucial findings will be summarized and subsequently put into a common framework.

(1) In contrast to most other proteins, Mad2 can adopt two distinct native folds. Due to different surface-exposed residues, the two Mad2 conformers can be separated by ion exchange chromatography (Luo et al., 2004). An interchange between the two conformations is possible and involves global structural rearrangements (Luo et al., 2000; Mapelli et al., 2007). The Mad2 conformations are referred to as "open" and "closed". (2) Mad2 physically interacts with the upstream SAC component Mad1 as well as with the downstream target Cdc20. The Mad1-Mad2 and the Cdc20-Mad2 interaction are highly similar. Both Mad1 and Cdc20 contain a conserved four amino acid Mad2 interaction motif (MIM). When Mad2 binds to either of the two interactors, it switches to its closed conformation (Luo et al., 2002; Luo et al., 2004). A C-terminal loop of Mad2 entraps Mad1 or Cdc20 in an almost topological fashion analogous to a car's safety belt locking the passenger (Sironi et al., 2002). (3) Mad1 and Cdc20 binding to Mad2 is competitive. Nevertheless, Mad1 is able to stimulate the formation of Cdc20-Mad2 complexes (Kulukian et al., 2009; Sironi et al., 2001). (4) Mad2 in its open conformation can bind to closed Mad2 which is associated with Mad1 (De Antoni et al., 2005; Mapelli et al., 2007). This gives rise to a Mad1-Mad2^{closed}-Mad2^{open} complex. Closed Mad2, which is bound directly to Mad1, is kinetically stable, while the second, open Mad2 molecule in the trimeric complex shows a high turnover rate (Vink et al., 2006).

According to the template model of the SAC (Fig. 5A), a complex of Mad1 and closed (C) Mad2 is recruited to unattached kinetochores. Open (O) Mad2 from a cytosolic pool transiently binds to closed Mad2 associated with Mad1. The Mad1-Mad2 complex serves as a "template" to catalytically transform this open Mad2 molecule into closed Mad2, which facilitates its binding to Cdc20. Alternatively, Mad2 transformation involves an activated "intermediate" (I) conformation that adopts its closed fold only upon Cdc20 binding.

Once all requirements for proper spindle formation have been fulfilled, the SAC has to be switched off. There are several pathways implicated in SAC inactivation (Fig. 5C). (1) The p31 protein mimicks the structure of open Mad2 (Yang et al., 2007). It can bind to both Mad1-Mad2 and Cdc20-Mad2 complexes. By that means it blocks the Mad1-Mad2 template and thus the source for any further "wait anaphase" signal. Furthermore, it enables APC/C^{Cdc20} to regain activity despite the continued presence of active Mad2 (Xia et al., 2004). (2) Another method of SAC inactivation is ubiquitylation of Cdc20. This is thought to displace Mad2 from Cdc20 which in turn re-activates the APC/C (Reddy et al., 2007; Stegmeier et al., 2007). It should be mentioned that this finding clashes to some

extent with the aforementioned positive effect of Cdc20 ubiquitylation on the SAC (Nilsson et al., 2008) (3) Mad2 becomes increasingly phosphorylated as cells progress towards the metaphase-anaphase transition, most probably owing to the activation of mitotic kinases. Specifically the phosphorylation of a series of serine/threonine residue at the C-terminus of Mad2 inhibits its binding to Mad1 and abrogates its SAC function (Wassmann et al., 2003a). Mad2 phosphorylation could therefore act as a negative regulator of SAC. Mechanisms (1) and (2) might act as constitutive buffers of the SAC that poise the system for rapid inactivation once the SAC is satisfied. Another, inherently regulated, SAC inactivation mechanism (not depicted in Fig. 5) involves a complex of cytoplasmic dynein and dynactin. This complex can use microtubule based transport to move Mad1-Mad2 complexes away from kinetochores and towards the spindle poles once microtubules have become attached (Howell et al., 2001).

So far, the SAC signaling pathway is essentially linear. Mad1 is the only upstream signal source feeding into the pathway and Cdc20 is the only target of SAC signaling.

3.10. Implications of yeast shugoshin homologs in the SAC

The first evidence that members of the shugoshin family play a role in the SAC came from *S. cerevisiae*. Mutants in the *SGO1* gene are partially SAC deficient. They are capable to arrest, when the mitotic spindle is completely depolymerized but they lack a checkpoint when chromosomes are not under tension (Indjeian et al., 2005). This led to the theory that Sgo1p is required for the tension sensitive branch of the SAC. In contrast to *S. cerevisiae*, fission yeast has two shugoshin homologs. The shugoshin SAC function seems to be conserved among yeast species since also *S. pombe* Sgo2 is involved in SAC signaling. A loss of cohesin function in mitosis normally triggers the tension sensitive SAC. However, *S. pombe* strains lacking the *SGO2* gene fail to arrest in response to lack of tension (Kawashima et al., 2007). Also the human shugoshin homolog Sgo2 has been discussed in connection with the SAC. Yen and coworkers report that Sgo2 depleted human cells exit mitosis in spite of spindle defects and lagging chromosomes (Huang et al., 2007).

Nevertheless, the above findings do not provide a link between shugoshin and the mitotic checkpoint on a molecular level.

3.11. Clinical relevance of human shugoshin homologs

Human shugoshin homologs have been implicated in a series of cancers. Human Sgo1 has been shown to be overexpressed in a series of breast cancers (Scanlan et al., 2001).

Another example is downregulation of hSgo1 in colon cancer patient samples, compared to unaffected adjacent tissue (Iwaizumi et al., 2009). When hSgo1 is depleted from HCT116 colon cancer tissue culture, a delay in mitosis is observed. However, if Sgo1 depletion is continued for longer periods of time, mitotic slippage occurs that can lead to tetraploidy and an increased centrosome number (Iwaizumi et al., 2009). Such tetraploid intermediates are prone to chromosomal instability in case they undergo another round of cell division. Mainly the higher number of centrosomes causes an increase in merotelic attachments due to altered spindle geometry (Ganem et al., 2009). Merotelic attachments in turn pose a high risk to chromosome missegregation (Cimini, 2008).

3.12. Aim of this work

The analysis of protein complexes can provide insight into how a protein can perform its cellular tasks. For the human Sgo1 protein, an unbiased biochemical approach was taken to identify new interaction partners. Sgo1 was overexpressed in human cell culture and subsequently purified by a two step affinity strategy. Out of the Sgo1 interactors identified by mass spectrometry, mainly the protein phosphatase 2A (PP2A) was characterized further. Since PP2A can interact with both human shugoshin homologs Sgo1 and Sgo2, it was investigated whether the two interactions are structurally similar. Furthermore a potential influence of Sgo2 on the catalytic activity of PP2A was measured. Data from other research groups showed that the interaction of shugoshin family members with PP2A contributes to the protection of centromeric cohesin. Besides that, shugoshin family members have also been implicated in the spindle assembly checkpoint (SAC), at least in yeast. Since no molecular details of the SAC function of shugoshin were known, the hypothesis of direct binding of shugoshin to a component of the SAC was tested for *X. laevis* Sgo1. The SAC component Mad2 was found to directly bind to xSgo1. In the following, it was tested whether the interaction was conserved also in mammalian cells. This was the case for human hSgo2. The structural features of the hSgo2-Mad2 interaction were further analyzed. For this purpose, aspects of the well characterized Mad1-Mad2 and Cdc20-Mad2 complexes were compared to the novel Sgo2-Mad2 interaction. Following precise mapping of the respective binding sites, the interplay of the two newly identified Sgo2 interactors PP2A and Mad2 was investigated. In a second part of this work, determinants of Sgo2 subcellular localization were investigated. The localization of Sgo2 to subdomains of mitotic chromosomes changes during mitosis and meiosis. This feature of Sgo2 has been temporally correlated with its cohesin protective activity in a previous report. However, no regulators involved in fine-

tuning of the Sgo2 localization pattern have been identified so far. Of special interest were the relative contributions of microtubule-chromosome attachments on the one side and spindle pulling forces on the other side. Furthermore, an involvement of mitotic kinases in the regulation of Sgo2 localization was tested.

4. Results

4.1. *Identification of new shugoshin interaction partners*

Initially, it was unclear how shugoshin can fulfill its cohesin protective function. It neither contains known catalytic protein domains nor does it have any apparent enzymatic activities. Furthermore, despite its implication in the mitotic spindle assembly checkpoint (SAC), no molecular link between shugoshin and the SAC had been established. Therefore, different approaches were taken to identify potential new interaction partners of shugoshin proteins. First, human Sgo1 was purified from transiently overexpressing 293T cells and assayed for interaction partners by mass spectrometry (see chapter 4.1.1). Second, a candidate *in vitro* binding screen was performed to test SAC components for binding to *Xenopus laevis* shugoshin (see chapter 4.1.6).

4.1.1. **Interaction partners of hSgo1 identified by mass spectrometry**

Due to the absence of catalytic domains in shugoshin family members, it was hypothesized that associated factors could mediate shugoshin functions. To identify such factors, human Sgo1 with tags at its N- and C-termini was overexpressed by transient transfection in 293T cells. hSgo1 and associated factors were purified by two step affinity chromatography (Fig. 6A). Samples were then separated by SDS-PAGE and Coomassie stained bands that appeared specifically in the Sgo1 pulldown and not in the control lane were cut out and sent for identification by mass spectrometry. Fig. 6B shows the most significant hits for each band.

A majority of the candidates belong to the group of protein phosphatase 2A (PP2A) subunits. Specifically B' PP2A subunits were identified while none of the other B subunit classes (B, B'') were found. Besides, a PP2A inhibitory protein SET/I-2 (PP2A) and the protein kinase CK2 (formerly known as casein kinase 2) were found. Identification of protein kinase CK2 as a potential interactor of the mitotic regulator Sgo1 was intriguing since CK2 also performs mitotic functions. For example, CK2 phosphorylates and regulates topoisomerase II (Ackerman et al., 1985). CK2 is a heterotetrameric Ser/Thr kinase consisting of two catalytic alpha subunits and two regulatory beta subunits.

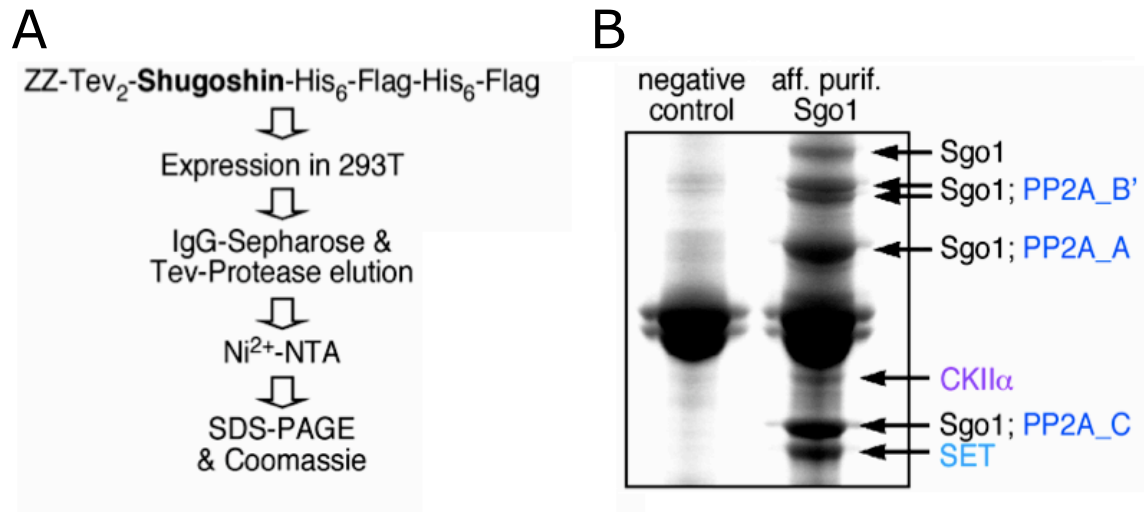


Fig. 6: Identification of Sgo1 interaction partners by mass spectrometry. (A) hSgo1 was overexpressed in 293T cells using a construct encoding an N-terminal ZZ- (Protein A) tag that could be removed by TEV protease and a C-terminal (His₆-Flag)₂-tag. In a first affinity purification step Sgo1 was bound to IgG sepharose beads via its ZZ-tag. Following elution by TEV protease cleavage, NaCl (400 mM) and Imidazole (10 mM) were added and a second purification step using Ni²⁺-NTA agarose was carried out. Following extensive washing, proteins bound to beads were eluted with SDS-PAGE sample buffer. (B) Samples were run on an SDS-PAGE gel, Coomassie stained and bands specifically present in the Sgo1 lane but not in the control (empty vector) were sent for identification by mass spectrometry (H. Urlaub, MPI Goettingen). The most significant hits (peptide coverage) are indicated.

Data obtained from mass spectrometric analysis are statistical predictions of potential interaction partners. Hence, the results needed confirmation by an independent method. To confirm the interaction between Sgo1 and protein kinase CK2, a co-I.P. (co-immunoprecipitation) approach was used (Fig. 7A). The beta subunit of CK2 (CK2beta) was expressed in 293T cells together with Sgo1. When Sgo1 was isolated from cell lysates, CK2beta co-purified. The interaction was specific, since it did not occur in a mock control without Sgo1. This finding could also be confirmed in a yeast-2-hybrid assay (Fig. 7B, "Sgo1 full"). The beta subunit of CK2 also showed interaction with Sgo1 in this experimental system, . The yeast-2-hybrid assay was also used to map the binding of CK2beta within Sgo1. Towards this end, fragments representing N-terminal, middle and C-terminal thirds of human Sgo1 were probed for binding of CK2beta. Only for the N-terminal fragment of Sgo1 an interaction with CK2beta could be observed.

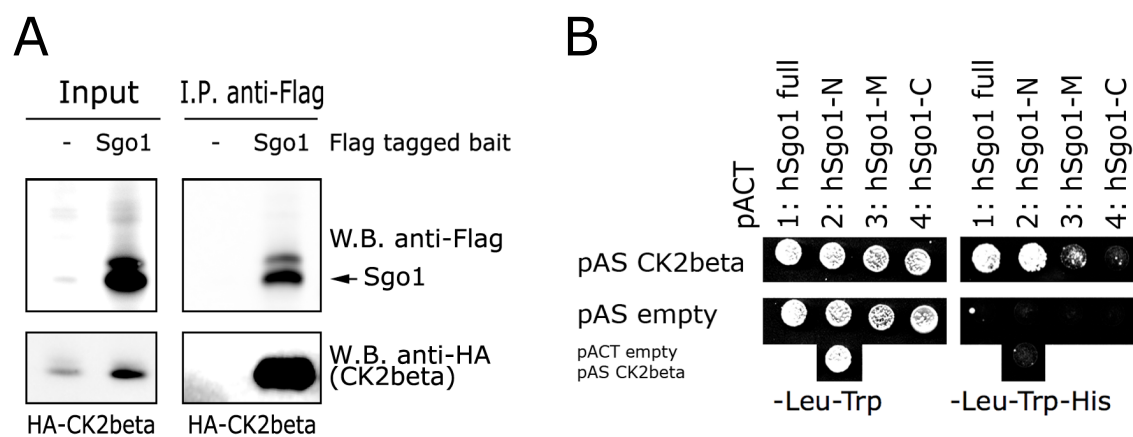


Fig. 7: Confirmation and mapping of the Sgo1-CK2 interaction. (A) Co-I.P. experiments from transiently transfected 293T cells expressing HA-tagged CK2beta, alone or together with Flag-tagged hSgo1. Flag-hSgo1 was isolated from cell lysates with anti-Flag agarose beads. Immobilized proteins were analyzed by SDS-PAGE and immunoblotting using anti-HA and anti-Flag antibodies. (B) The Sgo1 N-terminus interacts with CK2 in a yeast-2-hybrid assay. Full-length Sgo1 ("full") as well as non-overlapping fragments representing the Sgo1 N-terminus ("N"), middle part ("M") or C-terminus ("C") were expressed from pACT (in fusion with the activation domain of Gal4). In all cases, interaction with CK2beta expressed from pAS (fused to the DNA binding domain of Gal4) was tested. All constructs were tested for the absence of autoactivation in combination with the corresponding empty vector.

Thus, the beta subunit of protein kinase CK2 is an N-terminal interactor of human Sgo1. Also a specific interaction of the catalytic alpha subunit of CK2 with Sgo1 could be detected in a co-I.P. experiment (data not shown).

In contrast, the other human shugoshin homolog Sgo2 only showed weak interaction with CK2beta and no interaction above background levels with CK2alpha (data not shown). This suggests that CK2 interaction is a specific property of the human Sgo1 homolog.

The interaction between Sgo1 and PP2A could be confirmed in a yeast-2-hybrid assay (Fig. 8, "fl."). This assay was also used to map the Sgo1-PP2A interaction. To this end, fragments of Sgo1 were cloned that together covered the whole length of the Sgo1 sequence. The fragments were designed to encode polypeptides with a length of about 66 amino acids and a mutual overlap of 33 amino acids (Fig. 8, "1"- "16"). As an interaction partner, the PP2A regulatory subunit B'delta was chosen, which was considered the most likely direct binding PP2A subunit. Only fragment "2" in combination with PP2A-B'delta led to growth of the test strain on selective medium. Therefore, the Sgo1-PP2A interaction maps to the N-terminus of Sgo1, more precisely to a region between amino acid residues 33 and 100.

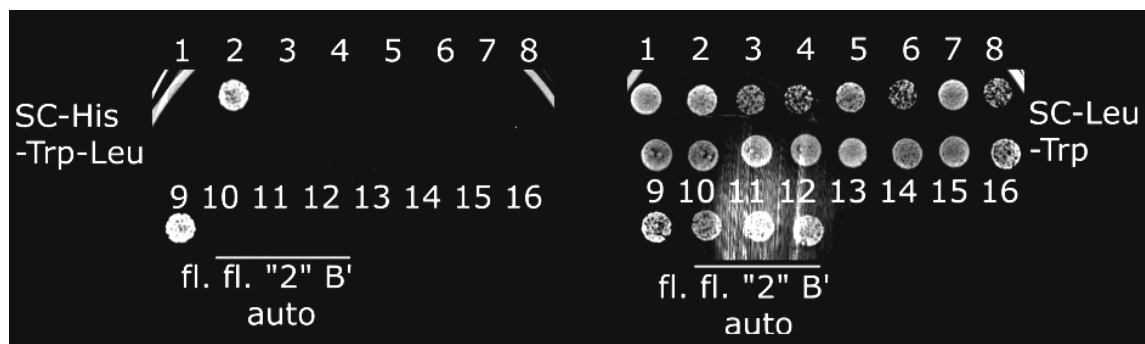


Fig. 8: PP2A is a specific interactor of the Sgo1 N-terminus. Yeast-2-Hybrid assay to confirm and to map the binding of PP2A to hSgo1. Full-length hSgo1 (f.l.) as well as fragments of 100 amino acid residues (a.a.) with an overlap of 33 a.a. covering the whole length of hSgo1 (1-16) were expressed from pACT. As a counterpart, the PP2A subunit B'delta was expressed from pAS. All constructs involved in positive interactions - "2" (pACT-hSgo1³³⁻¹⁰⁰), "f.l." (pACT-hSgo1), and "B'" (pAS-PP2A-B'delta) - were tested for absence of auto-activation ("auto").

4.1.2. Conserved binding mode of PP2A between Sgo1 and Sgo2

Shortly after my discovery, it was reported by other researchers that PP2A interacts with Sgo1 and Sgo2 (Huang et al., 2007; Kitajima et al., 2006; Riedel et al., 2006; Tang et al., 2006). As these competing groups had functionally characterized the Sgo1-PP2A interaction, I focused my attention on a more detailed analysis of the Sgo2-PP2A interaction.

First, to confirm the Sgo2-PP2A interaction, a co-I.P. experiment was performed. Endogenous Sgo2 was affinity isolated from HeLa cell lysate using a specific antibody. Western blot analysis showed that the catalytic subunit of PP2A indeed bound to Sgo2 (Fig. 9A). This was further confirmed in a yeast-2-hybrid assay. Full-length Sgo2 showed specific interaction with the PP2A B'delta subunit (Fig. 9B). PP2A binding to the human Sgo1 homolog is mediated via the Sgo1 N-terminus. In order to test whether this also holds true for human Sgo2, again a yeast-2-hybrid assay was used. Indeed, a fragment comprising the N-terminal 250 amino acid residues (a.a.) of the 1265 a.a. protein Sgo2 retained interaction with PP2A (Fig. 9B). Thus, the Sgo2 N-terminus is sufficient for PP2A binding, similar to what has been described for Sgo1.

The binding site of PP2A had been previously mapped for human Sgo1 (Tang et al., 2006). Mutation of Asn 61 to Ile in Sgo1 (Sgo1-N61I) leads to a complete loss of PP2A binding. Sequence alignment (Fig. 9D, red box) showed that the residues around the PP2A binding site of Sgo1 are well conserved in Sgo2. Especially, the characteristic di-asparagine motif required for PP2A binding to Sgo1 is present in both Sgo1 and Sgo2. It

was therefore conceivable that a conserved PP2A binding site might be present in both human shugoshin homologs.

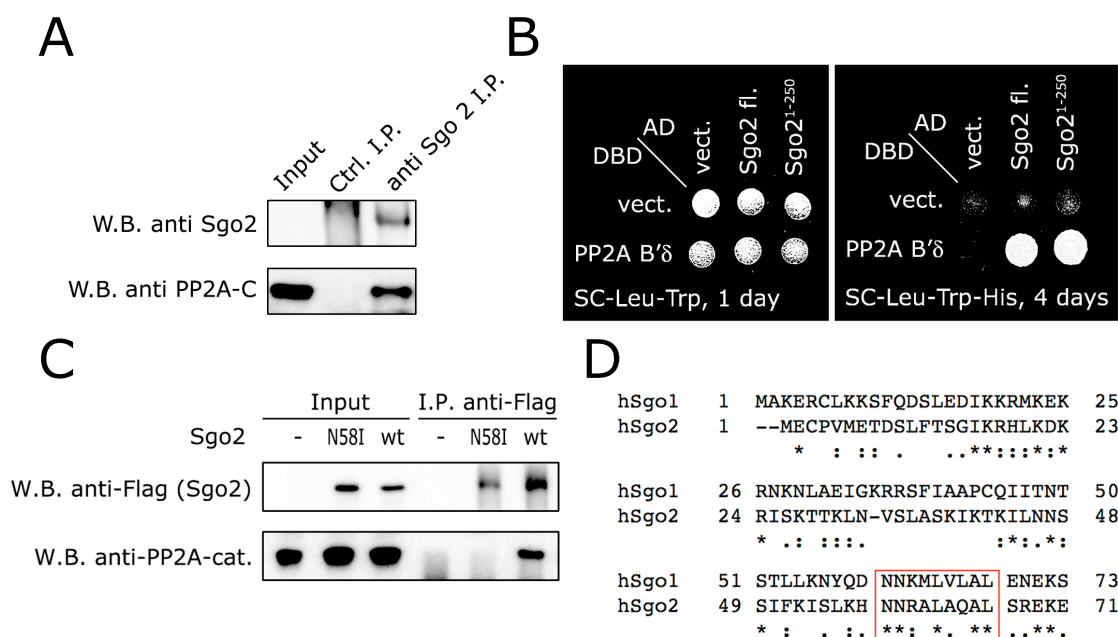


Fig. 9: Identification of the PP2A binding site of Sgo2. (A) Endogenous hSgo2 was immunoprecipitated from lysate of approx. 10^8 HeLa cells using 5 μ g of immobilized anti-Sgo2 antibody. Non-specific rabbit IgG served as negative control. Immunoprecipitates were probed by immunoblotting for Sgo2 and PP2A-C. (B) hSgo2 full-length or hSgo2¹⁻²⁵⁰ fused to Gal4-AD were tested for binding to PP2A-B' fused to Gal4-DBD. The left panel shows equal plating by growth on selective medium for the transformed plasmids. (C) 293T cells were transfected with plasmids encoding Flag-tagged wild-type (wt) hSgo2 or hSgo2-N58I. Following anti-Flag-I.P., material bound to the beads was analyzed by immunoblotting using anti-Flag and anti-PP2A antibodies. (D) The PP2A binding motif is conserved between Sgo2 and Sgo1. The N-termini of human Sgo1 and Sgo2 were aligned using the Clustal-W algorithm. The red box indicates conserved residues surrounding the shugoshin PP2A binding site. The asterisk denotes an asparagine residue important for PP2A binding in both Sgo1 and Sgo2.

To test this possibility, a Sgo2 mutant (Sgo2 N58I) - analogous to Sgo1-N61I - was created and assayed for PP2A binding. Tagged versions of wild-type Sgo2 and the potential PP2A binding mutant were immunoprecipitated from lysates of transfected 293T cells. While wild-type Sgo2 specifically bound to PP2A-C, Sgo2-N58I no longer interacted with PP2A-C (Fig. 9C). This result shows that the mode of PP2A binding is conserved between hSgo1 and hSgo2. Xu et al. (2009) have very recently solved the crystal structure of hSgo1 in complex with the PP2A holoenzyme. PP2A binds to a coiled-coil region around N61. Consistent with the findings presented here, bioinformatic analysis indicated that also the Sgo2 N-terminus can form a coiled-coil structure (data not shown).

4.1.3. Sgo2 regulates PP2A

Phosphorylation is an important post-translational modification that regulates protein function. Mitosis is characterized by increased kinase activity and the extensive phosphorylation of many target proteins. In terms of regulation of protein phosphorylation, the prevalent opinion had been that kinases are tightly controlled while the counteracting phosphatases are more or less constitutively active. This view has recently been challenged by the discovery of several tightly regulated functions of PP2A (Trinkle-Mulcahy and Lamond, 2006). The trimeric PP2A is well suited for regulation due to a variety of different isoforms of its subunits (especially the regulatory B subunit). So far, mainly recruitment of specific PP2A subtypes to distinct subcellular compartments has been proposed to confer specificity of PP2A (Trinkle-Mulcahy and Lamond, 2006). One example is the recruitment of PP2A-B' to the centromere of mitotic cells by Sgo2 (Kitajima et al., 2006).

But is there also a direct regulation of PP2A activity by shugoshin binding? To shed light on this issue, the activity of Sgo2 associated PP2A was studied in more detail. First, it was determined whether Sgo2 showed any associated phosphatase activity. Towards this end, overexpressed Sgo2 was isolated from 293T cells. Phosphatase activity was measured using a malachite green based peptide dephosphorylation assay. Wild-type Sgo2 showed a much higher phosphatase activity than PP2A binding deficient Sgo2-N58I (Fig. 10). Thus, Sgo2 was associated with phosphatase activity and more specifically with PP2A activity in human cells.

Next, phosphatase activity of Sgo2-less PP2A of the B' subtype was compared to the activity of Sgo2 bound PP2A. The protein complexes were isolated from 293T cells transiently transfected with plasmids encoding tagged versions of PP2A-B' Δ or Sgo2, respectively. Due to the strong overexpression, PP2A-B' Δ samples could be considered essentially free from Sgo2. After competitive elution using a Flag₃ peptide, free PP2A and Sgo2-PP2A were subjected to malachite green phosphatase assay (Fig. 10). Sgo2-PP2A had an about 3-fold higher phosphatase activity compared to PP2A-B' Δ alone. The observed differences were not due to the presence or absence of the Flag-tag on a PP2A subunit since a similar result was obtained when tags were removed using TEV protease cleavage (Suppl. fig. 1)

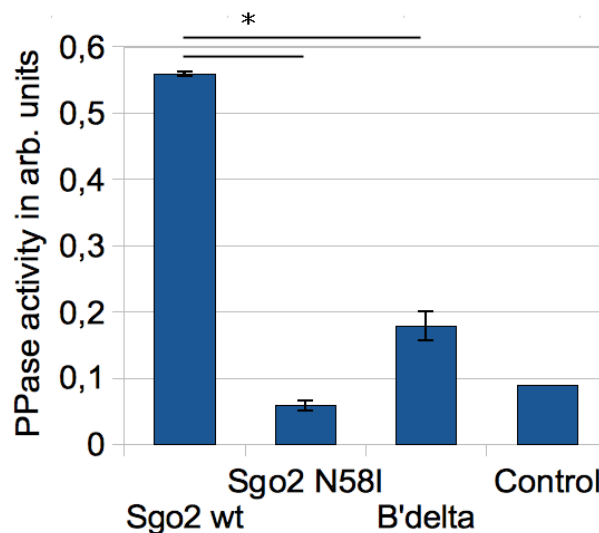


Fig. 10: Sgo2 is specifically associated with phosphatase (PPase) activity and stimulates PP2A activity *in vitro*. Flag-tagged versions of wild-type Sgo2 (wt), Sgo2-N58I (PP2A binding deficient) or PP2A-B'delta were expressed in 293T cells. The proteins were isolated from cell lysates using anti-Flag agarose beads and eluted by competition with Flag₃ peptide. Semi-quantitative immuno-blotting was used to adjust equal Sgo2 concentrations (to compare between Sgo2-wt and Sgo2-N58I) or equal PP2A-C concentrations (to compare between Sgo2-wt and PP2A-B'delta). Subsequently, Ser-/Thr PPase activities were measured using a peptide dephosphorylation assay followed by detection of free phosphate using the malachite green method. Control indicates a PPase assay without enzyme addition. Stimulation of PP2A by Sgo2 association was statistically significant. Error bars show standard deviation of three independent measurements. (Student's t-test: *: $p < 0.001$).

Sgo2 is therefore able to stimulate PP2A *in vitro*. A potential function on the cellular level could be that Sgo2 is not merely a recruiting factor for PP2A but also locally increases its catalytic activity.

4.1.4. Human Sgo1 but not Sgo2 is required to protect centromeric cohesin in mitosis

While human Sgo1 is dispensable for cohesin protection in meiosis (Lee et al., 2008), it is essential for protection of mitotic cohesin from the prophase pathway (McGuinness et al., 2005). In the case of human Sgo2, the published literature is less clear. There is one report stating that depletion of Sgo2 from mitotic human cells leads to a considerable degree of cohesion loss. The authors also show that PP2A is downstream of Sgo2 in terms of centromeric localization (Kitajima et al., 2006). However, similar experiments were published by the laboratory of Tim Yen. According to their findings, knock-down of Sgo2 in human cells leaves cohesion unaffected (Huang et al., 2007). Consistent with the latter report, *sgo2*^{-/-} mouse embryonic fibroblasts are perfectly able to execute a precise mitosis without suffering premature sister chromatid separation (Llano et al.,

2008). However, this result should be taken with care since mice express another Sgo2 homolog from a different genomic locus.

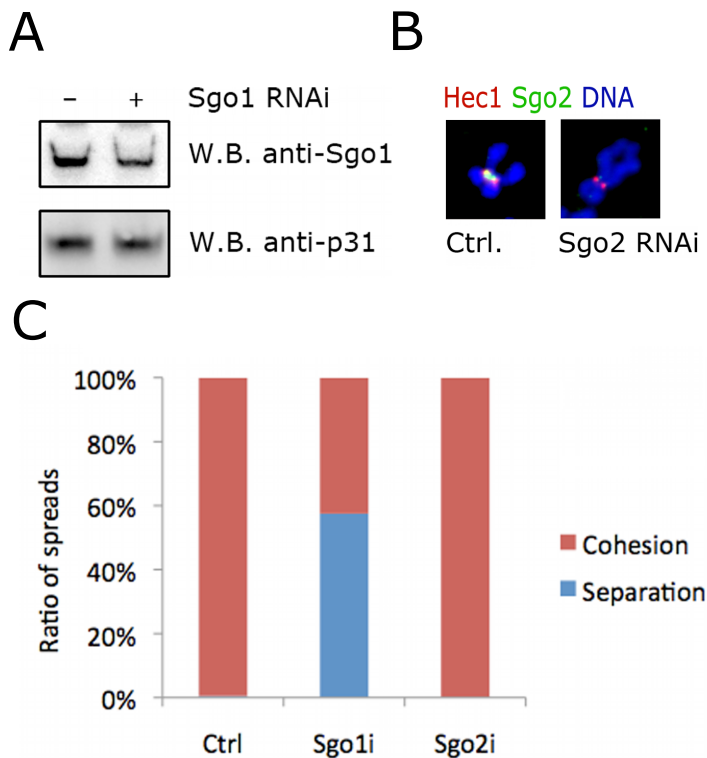


Fig. 11: Sgo2 is dispensable for cohesion in mitosis. (A) HeLa cells were transfected with Sgo1 siRNA (40 nM) or mock transfected (-) and immediately synchronized using a thymidine-nocodazole protocol. Lysates of mitotic cells were analyzed by SDS-PAGE and immunoblotting for p31 as an input control and for Sgo1. In addition, chromosome spreads were prepared as described in the Materials and Methods section. (B) HeLa cells were transfected with Sgo2 siRNA (40 nM) or mock transfected (Ctrl.). 24 h later cells were synchronized via a thymidine-nocodazole protocol. Chromosome spreads were prepared from mitotic cells as in (A). Spreads were stained with Hoechst 33342 (blue) and by immunofluorescence

(I.F.) against the outer kinetochore marker Hec1 (red) and against Sgo2 (green). (C) Quantification of sister chromatid cohesion in spreads from (A) and (B). Spreads comprising predominantly cohesed or separated chromosomes were assigned to the respective categories. For Sgo2 depletion, only spreads were selected that were devoid of Sgo2 in immunofluorescence.

In order to get insight into the relative contribution of Sgo1 and Sgo2 to sister chromatid cohesion in mitosis, the two factors were depleted using specific siRNAs. Subsequently, mitotic cells were prepared for chromosome spreads. Immunofluorescence staining of the kinetochore marker Hec1 and fluorescence labeling of DNA enabled a reliable differentiation of cohesed or separated sister chromatids. The depletion efficiency for Sgo1 was determined by immunoblotting. Compared to the input control p31, merely a mild reduction of Sgo1 levels by RNAi was observed (Fig. 11A). Nevertheless, in chromosome spreads about 60% of Sgo1 RNAi cells showed premature sister chromatid separation, while the control revealed intact cohesion (Fig. 11C).

Next, the contribution of Sgo2 to mitotic cohesion protection was assayed. Here the siRNA efficiency was determined by co-staining of chromosome spreads with antibodies specific for Sgo2 (Fig. 11B). For the Sgo2 RNAi sample, only cells that did not show a detectable signal were counted. None of the Sgo2 depleted cells analyzed had signs of

premature sister chromatid separation (Fig. 11C). These results show that hSgo1 but not hSgo2 is required to protect centromeric cohesin in mitosis.

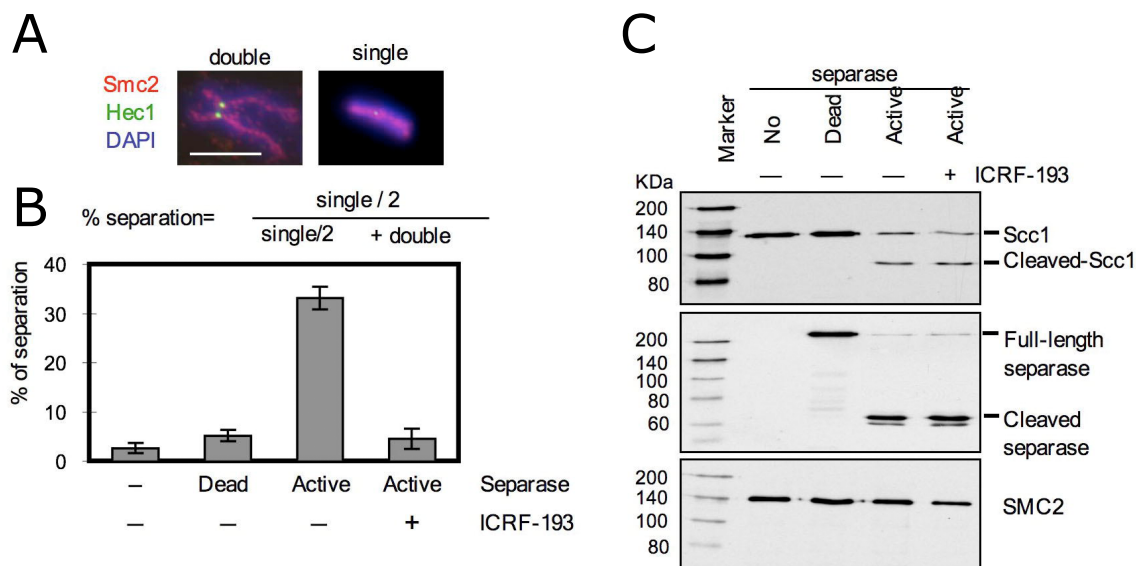
4.1.5. Cohesin protects DNA catenations until the metaphase-anaphase transition

The proposed mechanism by which Sgo2 fulfills its protective function involves cohesin dephosphorylation via associated PP2A. While this process is crucial in meiosis (Lee et al., 2008; Llano et al., 2008), Sgo2 is not required for protection of centromeric cohesin in mitosis (Llano et al., 2008). Cohesin is not the only entity that has been implicated in keeping sister chromatids together from S-phase until mitosis. Long before the components of the cohesin complex had been identified, DNA catenation has been suggested as a potential source of chromatid cohesion (Murray and Szostak, 1985; Nasmyth and Haering, 2005). Like the proteinacious cohesion, DNA catenation arises during S-phase along with DNA replication (Sundin and Varshavsky, 1980). Findings from yeast showing that minichromosomes are decatenated before anaphase (Koshland and Hartwell, 1987) argue against an essential role of catenation in cohesion of chromatids. However, in mammalian cells, DNA catenation at centromeres is only resolved during anaphase (Baumann et al., 2007; Wang et al., 2008). Topoisomerase II (TOPO II) is the main enzyme involved in decatenation in mitosis. During prophase it resolves arm catenation but spares residual catenation at centromeres (Porter and Farr, 2004). How centromeric catenation is protected from TOPO II has been unclear, however its resolution correlates in time with the removal of cohesin complexes. Furthermore, TOPO II is a mitotic phosphoprotein (Taagepera et al., 1993) which serves as a substrate for kinases like Aurora B and CK2 (Ackerman et al., 1985; Morrison et al., 2002). CK2 phosphorylation stimulates TOPO II activity *in vitro* (Ackerman et al., 1985).

Two main factors were tested as candidates for the protection of centromeric catenation: (1) Sgo2, which together with PP2A could dampen the activity of centromeric TOPO II by keeping it dephosphorylated, and (2) cohesin, which might represent a "road-block" for TOPO II.

The first model was tested by siRNA mediated depletion of Sgo2 from HeLa cells. Cells were fixed and the degree of catenation in anaphase cells was determined. To this end, an immunofluorescence staining was performed using an antibody directed against the helicase PICH, which is a marker for persistent anaphase DNA threads (Baumann et al., 2007). Both in control as well as in Sgo2 depleted cells an equal number of PICH

positive DNA threads was observed (Suppl. fig. 2). Therefore, Sgo2 is not responsible for the protection of centromeric catenation.



Experiment in collaboration with Lily H.C. Wang

Fig. 12: Cohesin counteracts TOPO II at centromeres of metaphase chromosomes. (A) Immunofluorescence staining of isolated metaphase chromosomes using antibodies directed against the condensin subunit Smc2 and against the kinetochore marker Hec1. Together with Hoechst 33342 labeling of DNA, precise judgement of sister chromatid cohesion ("double") or separation ("single") was possible. (B) *In vitro* sister chromatid separation assay: Purified metaphase chromosomes were treated with wild-type ("active") or protease-dead mutant separase in the presence or absence of the TOPO II inhibitor ICRF-193. Immunofluorescence staining as in (A) was used to quantify separated and cohesed chromosomes. (C) SDS-PAGE analysis of the samples from (B) using antibodies against Scc1 (to detect cohesin cleavage), separase (to detect separase self-cleavage as a measure of activity) and SMC2 (input control).

The second hypothesis, a potential involvement of cohesin complexes in catenation protection, was tested in collaboration with Lily Wang (Nigg laboratory, MPI for Biochemistry, Martinsried). As a tool, an *in vitro* sister chromatid cohesion assay was used. Human prometaphase chromosomes were purified from cultured cells arrested with nocodazole (Fig. 12A). These typical X-shaped chromosomes still maintain cohesin complexes including the Scc1 subunit at their centromeres (Waizenegger et al., 2000) as well as presumably also catenations (Wang et al., 2008). Moreover, they were associated with TOPO II, which proved to be highly active upon chromosome extraction (data not shown).

If cohesin complexes were an impediment for TOPO II, then removal of cohesin should enable decatenation, i.e. physical separation of sister chromatids. To remove cohesin, chromosomes were treated with recombinant active separase or with a protease-dead separase mutant as negative control. While in the control most chromosomes stayed paired, addition of active wild-type separase led to sister chromatid separation in more than 30% of cases (Fig. 12B). This result was consistent with the removal of catenation following cohesin cleavage. Nevertheless, a formal proof for the presence of DNA catenation on isolated metaphase chromosomes was required. To achieve this, the cleavage assay was performed in the presence of the TOPO II inhibitor ICRF-193. Now, separase could no longer induce sister chromatid separation (Fig. 12B). Immunoblotting for the cohesin subunit Scc1 revealed an equally efficient cleavage by separase, independent of ICRF-193 addition (Fig. 12C).

Therefore, separase mediated cohesin removal is sufficient for sister chromatid separation *in vitro*. Together with the failure to separate chromatids upon TOPO II inhibition, it can be concluded that cohesin indeed blocks TOPO II mediated resolution of centromeric catenations during metaphase.

4.1.6. Candidate binding screen - Mad2 interacts with *X. laevis* Sgo1

Motivated by the temporal correlation between SAC activity and shugoshin functions in mitosis and meiosis, a candidate screen had been carried out in the Stemmann lab. *X. laevis* Sgo1 (xSgo1) and various checkpoint proteins were recombinantly expressed, purified and used for *in vitro* binding assays. As a result a new interaction between xSgo1 and Mad2 was found (Olaf Stemmann, personal communication). Since recombinant full-length xSgo1 derived from *E. coli* is prone to degradation, the initial experiment was repeated in a different setup. Full-length xSgo1 was produced by coupled *in vitro* transcription/translation ("IVT") in the presence of [³⁵S]methionine. Then, Mad2 was immobilized on beads and incubated with xSgo1 IVT. Empty beads served as negative control. Material bound to beads was assayed via SDS-PAGE and autoradiography (Fig. 13). Significant xSgo1 binding to beads could only be detected in the presence of Mad2. Thus, Mad2 could be identified as a new interaction partner of the shugoshin xSgo1.

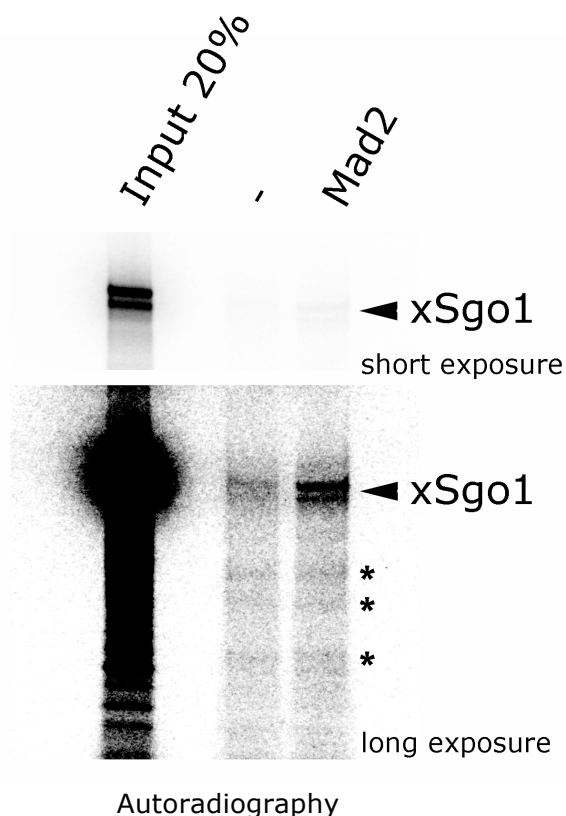


Fig. 13: *X. laevis* Sgo1 (xSgo1) is a specific interaction partner of the mitotic checkpoint factor Mad2. 10 μ l of Ni²⁺-NTA beads were incubated with buffer DP1 alone (-) or with 5 μ g His₆-Mad2 for 2 h at 4°C. Then beads were washed, incubated with 8 μ l each of [³⁵S]methionine labeled xSgo1 for 2 h at RT and washed again. Bound material was finally eluted with SDS-PAGE sample buffer and analyzed by SDS-PAGE and autoradiography. Asterisks highlight unspecific bands that were present in both control and Mad2 pulldown.

4.1.7. Human Sgo2 but not Sgo1 interacts with Mad2

Searches in the annotated genome of *X. laevis* only revealed the existence of one shugoshin family member (xSgo1). Since higher vertebrates (mammals) contain two distinct shugoshin genes, frogs could in fact either lack the second homolog or annotation of the *X. laevis* genome is incomplete with respect to shugoshin genes. In collaboration with Kay Hofmann (Miltenyi Biotech, Cologne) it could be demonstrated that, surprisingly, a second shugoshin is indeed missing in the genus *Xenopus* as well as in zebrafish. In an evolutionary context, it is remarkable that *D. melanogaster* and *S. cerevisiae* also harbor only one shugoshin gene, whereas *S. pombe* contains two. Potential explanations include an independent gene duplication in mammals and fission yeast (convergent evolution) or – less likely - selective deletion of one of two shugoshin genes once present in an archetypal common ancestor. A special situation in mice is worthwhile mentioning. In contrast to humans, they have two independent genes encoding Sgo2 homologs: Sgo2.1 and Sgo2.2.

With respect to the interaction of xSgo1 and Mad2 the following questions arose: is the interaction also conserved in human cells and if so, which of the two human shugoshin homologs interacts with Mad2? The putative binding of hSgo1 and hSgo2 to Mad2 was first investigated in a yeast-2-hybrid assay. Growth on selective medium indicated

physical interaction between Sgo2 and Mad2 (Fig. 14) but not between Sgo1 and Mad2. This finding was validated by showing that the individual constructs did not give rise to non-specific growth ("auto-activation") and that PP2A B'delta subunit interacted with both Sgo1 and Sgo2, as expected.

Thus, Sgo2 has acquired the conserved Mad2 interaction in human cells. This is surprising since xSgo1 is more closely related to hSgo1 (28% identity, 33% gaps) than to hSgo2 (13% identity, 60% gaps). The evolutionary conservation of shugoshin-Mad2 indicates an important role of this interaction in vertebrates.

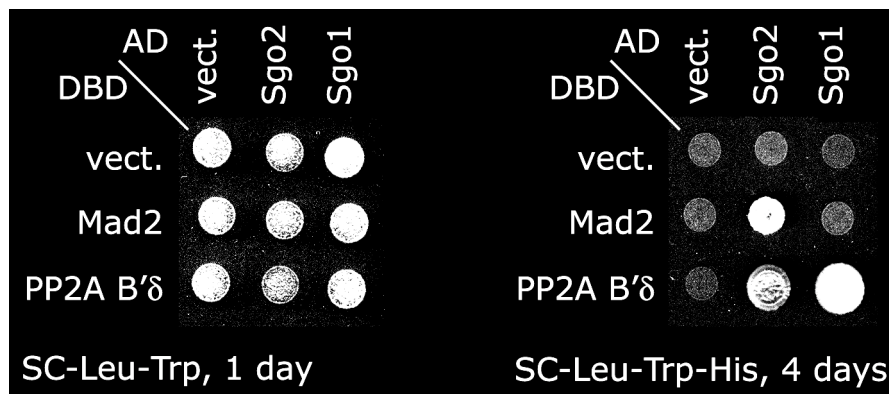


Fig. 14: Interaction with Mad2 is conserved in human Sgo2 but not Sgo1. For yeast-2-hybrid analysis, Sgo1 or Sgo2 were fused to the Gal4 activating domain, while Mad2 and PP2A B'delta were linked to the Gal4 DNA binding domain. Plasmids were transformed in the indicated combinations into the *S. cerevisiae* strain PJ69-4A. Comparable amounts of cells were spotted on SC-Leu-Trp plates (input control) and SC-Leu-Trp-His plates (selective medium for interaction). Transformations of single constructs together with the corresponding empty vector were used to control for autoactivation.

4.2. *Sgo2 is dispensable for mitosis*

4.2.1. *Sgo2 does not cause an override of a short-term SAC arrest*

There is evidence from different yeast species that shugoshin family members are required for the tension sensitive branch of the SAC (Indjeian et al., 2005; Vanoosthuysen et al., 2007). Nevertheless, no mechanistic explanation for the shugoshin-SAC connection has been demonstrated to date. In addition, there are no direct data showing an involvement of higher eukaryotic shugoshin homologs in the SAC. A role of mammalian Sgo1 can almost certainly be excluded here because Sgo1-less human cells show premature separation of sister chromatids followed by a robust, SAC mediated arrest (McGuinness et al., 2005). It has been reported that Sgo2 depleted HeLa cells, although delayed in mitosis, finally exit mitosis despite persistence of erroneous kinetochore-microtubule attachments (Huang et al., 2007). Although this would be consistent with a Sgo2-Mad2 interaction, it contrasts with the report that murine cells lacking Sgo2.1 (but not Sgo2.2) do not suffer from mitotic defects and remain fully SAC proficient (Llano et al., 2008). Thus, the putative positive role of mammalian Sgo2 in the mitotic SAC response has remained controversial.

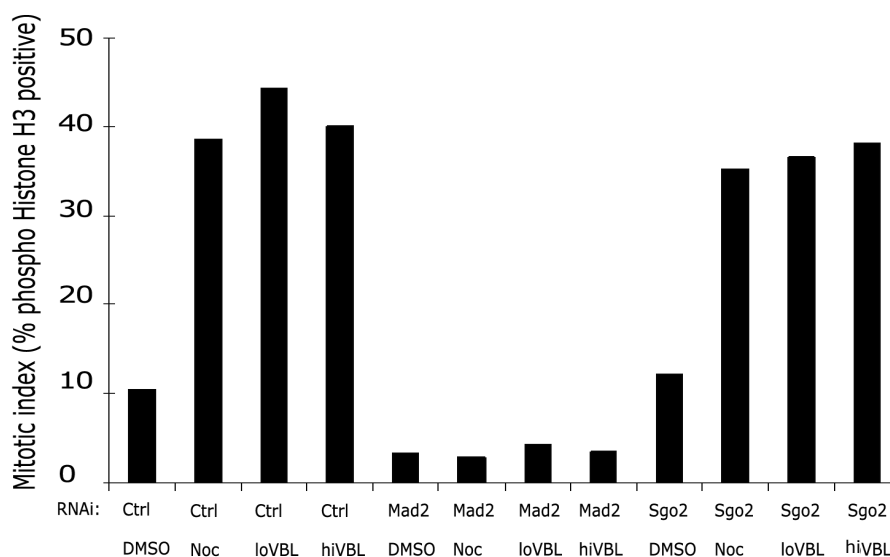


Fig. 15: Mad2 depletion but not Sgo2 depletion causes an override of a short-term SAC arrest. HeLa cells were transfected with control (Ctrl), Mad2, or Sgo2 siRNAs (40 nM) and presynchronized with thymidine. 6 h after release, DMSO (as control) or drugs were added (Noc: 200 ng/ml, loVBL (low conc. vinblastine): 6.7 nM, hiVBL (high conc. vinblastine): 0.5 μ M). Another 8 h later, the mitotic index was determined by immunofluorescence staining for phosphorylated Histone H3 (as a mitotic marker) and counterstaining of DNA with Hoechst 33342. The mitotic index was calculated as ratio of phospho-Histone H3 positive over all Hoechst 33342 labeled cells. The relatively low mitotic indices were most probably due to an inefficient thymidine release, i.e. only about half of the cells entered mitosis in the first place.

To clarify this issue, Sgo2 function was tested in a first assay for SAC function. HeLa cells were released from a thymidine arrest into a synchronous mitosis in the absence or presence of different spindle poisons to trigger a SAC arrest. The mitotic index was determined about 3 h after mitotic entry, when untreated control cells had already completed mitosis (mitotic index 10%). Upon addition of various SAC inducing drugs, about 40% of cells remained arrested in mitosis at this time point. While loss of Mad2 caused a dramatic decrease of the mitotic index under these conditions, a Sgo2 depleted cell population maintained a high mitotic index. Thus, Sgo2 is not required to establish a short-term mitotic checkpoint arrest. This is true for loss of attachment (nocodazole, 0.5 μ M vinblastine) as well as for loss of tension (6.7 nM vinblastine (Skoufias et al., 2001)).

4.2.2. Sgo2 is not required for maintenance of a prolonged mitotic SAC arrest

A short term response of cultured cells to spindle poisons constitutes quite a simple situation with predictable outcomes. However, when spindle poisons are applied for longer periods of time, several factors have to be considered. Cells can undergo various fates including apoptotic cell death or adaptation resulting in "mitotic slippage" into G1 phase (Weaver and Cleveland, 2005). Mitotic cell death upon prolonged drug treatment indeed shows classical signs of apoptosis like activation of caspase-3 (Tao et al., 2005). It has been shown that mitotic slippage happens in spite of an active SAC via slow continued cyclin B1 degradation (Brito and Rieder, 2006). Which fate decision is taken depends on the type of spindle poison applied and also on the cell type (Gascoigne and Taylor, 2008; Orth et al., 2008).

To study a possible involvement of Sgo2 in the subtle fate decisions upon prolonged mitotic arrest, the response of Sgo2 depleted cells to long-term nocodazole or taxol arrest was studied. Thereby, the ability to maintain a prolonged SAC arrest was tested. HeLa cells pre-synchronized with thymidine were released into nocodazole containing medium. The mitotic index was determined by flow cytometry 17, 25 and 30 h thereafter (Fig. 16A).

At the early time point, the mitotic index was found to be slightly lower for Sgo2 RNAi compared to the control. Nevertheless, the difference did not become more pronounced during the arrest. It was hence attributed to a less efficient thymidine release and/or mitotic entry. 30 h after release, control as well as Sgo2 RNAi cells showed a comparable decrease of the mitotic index, presumably due to mitotic slippage. In

conclusion, depletion of Sgo2 did not significantly affect a prolonged arrest in nocodazole.

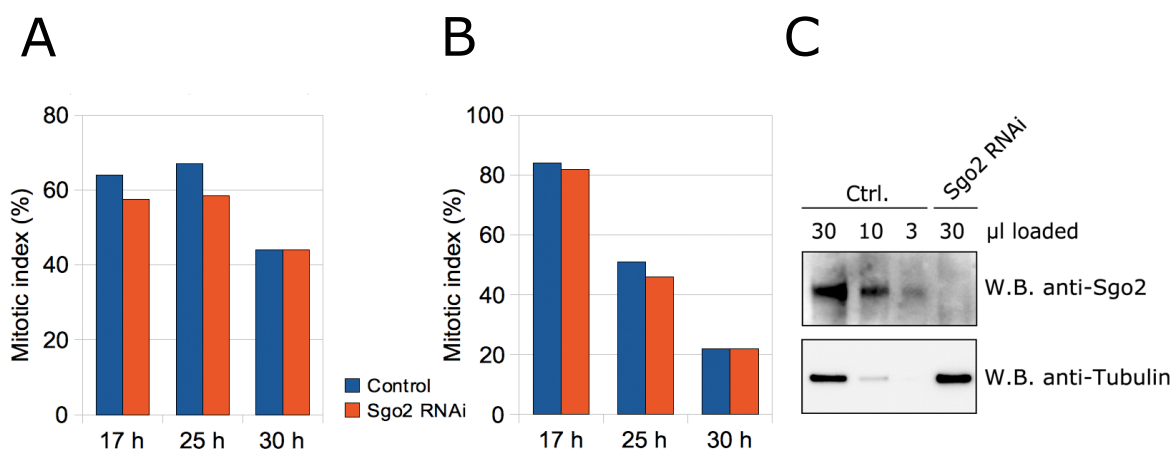


Fig. 16: Sgo2 is not required to maintain a prolonged mitotic checkpoint arrest. HeLa cells were presynchronized at the G1/S transition with thymidine and subsequently released for the indicated time periods into medium containing spindle poisons (A) 200 ng/ml nocodazole or (B) 200 ng/ml taxol. (A) and (B) The mitotic index was determined using immunostaining for phospho-Histone H3 and flow cytometry. (C) Sgo2 RNAi efficiency was determined by immunoblotting. Comparison of the Sgo2 depleted sample to a dilution series of the control shows a >90% depletion of Sgo2 by siRNA. Tubulin staining was used to confirm equal loading.

When the response to taxol was measured, similar observations were made (Fig. 16B). Comparable mitotic indices were found 17 h after thymidine release for Sgo2 depleted samples and the control. At later time points the taxol arrest turned out to be less robust than the nocodazole arrest. At the 30 h time point, only a minor fraction of cells remained in mitosis. Again Sgo2-less cells behaved similar to control cells. The highly efficient depletion of Sgo2 of more than 90% is documented in Fig. 16C.

Thus, even under conditions of prolonged drug treatment, Sgo2 is not required to maintain the mitotic checkpoint arrest.

4.2.3. Sgo2 does not regulate mitotic checkpoint complex composition

In vitro, both Mad2 and BubR1 inhibit the APC/C on their own (Li et al., 1997; Tang et al., 2001). However, they were shown to be much more efficient in APC/C inhibition when acting together with Bub3 in the mitotic checkpoint complex (MCC) which includes Cdc20 (Sudakin et al., 2001). Recently, it became clear that Mad2, despite acting upstream of BubR1, might only be a minor or transient component of the final

MCC once this has formed (Nilsson et al., 2008). The question therefore arose whether Sgo2 as a novel interactor of Mad2 might be involved in the regulation of MCC composition.

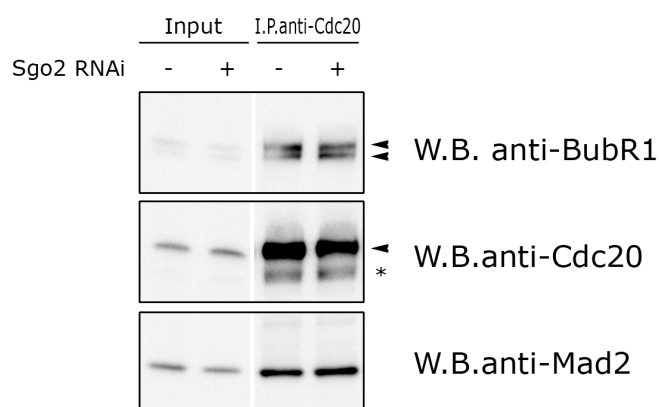


Fig. 17: Depletion of Sgo2 does not affect binding of Mad2 or BubR1 to Cdc20. HeLa cells were transfected with control or Sgo2 siRNA for a total of 50 h and synchronized using a thymidine-nocodazole protocol. Endogenous Cdc20 was immunoprecipitated from lysates and associated Mad2 and BubR1 were detected by immuno-blotting.

To test this possibility, Cdc20 was immunoprecipitated from mitotic HeLa cells and the amount of associated BubR1 and Mad2 was measured by immunoblotting (Fig. 17). Cdc20 could be efficiently isolated from control cells as well as from Sgo2 depleted cells. In both cases, comparable amounts of BubR1 and Mad2 were bound to Cdc20. Thus, Sgo2 depletion did not influence MCC composition.

4.2.4. Cdc20 is the only known Mad2 binding partner that becomes destabilized in mitosis

A newly described function of the mitotic checkpoint complex is targeting of Cdc20 for APC/C mediated ubiquitylation followed by proteasomal degradation (Ge et al., 2009; Nilsson et al., 2008). This dropping of Cdc20 levels helps to sustain a robust checkpoint arrest. Mad2 binding is essential for this SAC mediated instability of Cdc20. However, whether the stability of the other known Mad2 binding partners, Mad1 and the newly discovered Sgo2, would also change in a SAC arrest, has not yet been tested. To clarify this issue, mitotic HeLa cells were treated with the translation inhibitor cycloheximide (CHX) and protein levels were followed in a time course by immunoblotting (Fig. 18). In agreement with the literature, Cdc20 levels dropped during the experiment to about 20% (densitometry, data not shown), while the controls Actin and Mad2 did not change (Fig. 18).

Now, the stability of the two other Mad2 interactors Mad1 and Sgo2 was determined during a SAC arrest. Mad1 was stable in the cycloheximide shutoff. This was not

unexpected since Cdc20 instability requires Cdc20's C-terminal "IR" motif, which allows for direct APC/C binding. Mad1 does not contain such a motif. In the case of Sgo2 the situation was less clear, since its C-terminus consists of the amino acid residues "MRR". Nevertheless, no drop of Sgo2 protein levels could be detected when translation was blocked in SAC arrested cells (Fig. 18).

This shows that Sgo2 is stable during a mitotic arrest. The function of the Sgo2-Mad2 interaction is therefore not to destabilize Sgo2.

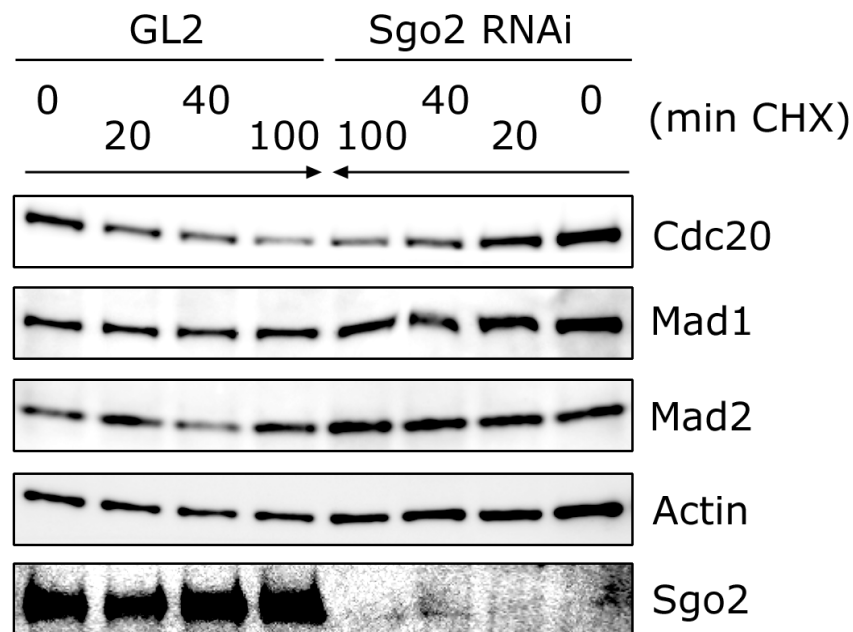


Fig. 18.: Cdc20 is degraded in prolonged mitosis while Mad1 and Sgo2 are stable. HeLa cells were transfected with control (GL2) or Sgo2 siRNAs for a total of 50 h and synchronized using a thymidine-nocodazole arrest. Mitotic cells were enriched by shake-off and incubated with 20 μ g/ml cycloheximide for the indicated periods of time. Thereafter, cells were lysed in SDS-PAGE sample buffer, resolved by SDS-PAGE and analyzed by immuno-blotting.

The Sgo2-Mad2 interaction could also influence mitotic protein stability by other means. For example, it could modulate the other Mad2 interactions with Mad1 or Cdc20 in a way that either Mad1 would become unstable or that Cdc20 would be stabilized.

The hypothesis was tested by comparing protein stability in control cells to that in Sgo2 depleted cells. Therefore, again a cycloheximide shutoff experiment was carried out in nocodazole treated cells. Sgo2 depletion was successful as determined by immunoblotting. However, no change in protein stability could be detected for Mad1 or Cdc20 upon Sgo2 depletion compared to the control (Fig. 18). From the above experiment, it can be concluded that Sgo2 and hence also its interaction with Mad2 do not modulate the stability of either Mad1 or Cdc20 in a SAC arrest.

4.2.5. Sgo2 is not required for normal mitotic progression

In the current literature, there are conflicting data on the importance of Sgo2 in mitosis. The Tim Yen laboratory has published experiments showing a strong mitotic phenotype characterized by a significantly prolonged mitosis (about 3-fold) upon Sgo2 depletion by siRNA (Huang et al., 2007). This phenotype has been attributed to a downstream mislocalization of the microtubule depolymerizing kinesin MCAK. This in turn was proposed to lead to the accumulation of erroneous microtubule-kinetochore attachments. These errors, sensed by the tension sensitive SAC, were the authors explanation for the mitotic delay. Contrasting results arose from studies on mouse *sgo2*^{-/-} embryonic fibroblasts (MEFs), which did neither show a mitotic delay nor a SAC defect (Llano et al., 2008). Yet, this later study suffered from the fact that two closely related Sgo2s are expressed in mouse but that only one of the corresponding genes was targeted.

To resolve the question whether or not Sgo2 influences mitotic timing, the original Yen laboratory experiments were revisited. The duration of mitosis was measured in HeLa cells treated with an siRNA oligo directed against Sgo2 (Huang et al., 2007). If Sgo2 played a role in mitotic spindle formation, a prolonged mitosis would be expected. However, live cell imaging data show comparable mitotic timing of about 30 min from nuclear envelope breakdown (NEBD) to anaphase onset for both control and Sgo2 depleted cells (Fig. 19A). When cells were additionally challenged with a low dose of taxol (10 ng/ml) they responded with a prolonged mitosis, as expected. Also under these conditions, Sgo2 depletion had no significant effect on the duration of mitosis (Fig. 19B). Another phenotype reported by Yen and coworkers was a significant increase in the percentage of cells undergoing anaphase with lagging chromosomes (about 40% upon Sgo2 depletion compared to 10% in control cells). This finding could also not be reproduced. Both control cells as well as Sgo2 depleted cells showed slightly less than 20% of aberrant anaphases (lagging chromosomes or chromatin bridges, Fig. 19C). Depletion of Sgo2 was greater than 90% and thus comparable to the level achieved by Huang et al. (2007). The observed results were validated by showing highly efficient Sgo2 depletion by immunoblotting (Fig. 19D).

It could not be resolved why the results shown here strongly contradict previously published findings from the Yen laboratory. One possible reason could be variations between different lines of HeLa cells which had been cultivated independently for many years. Nevertheless, similar results were also obtained with HCT-116 human colon

cancer cells (data not shown). In summary, the results presented here strongly argue against an overt role of Sgo2 in mitotic progression in human cancer cells.

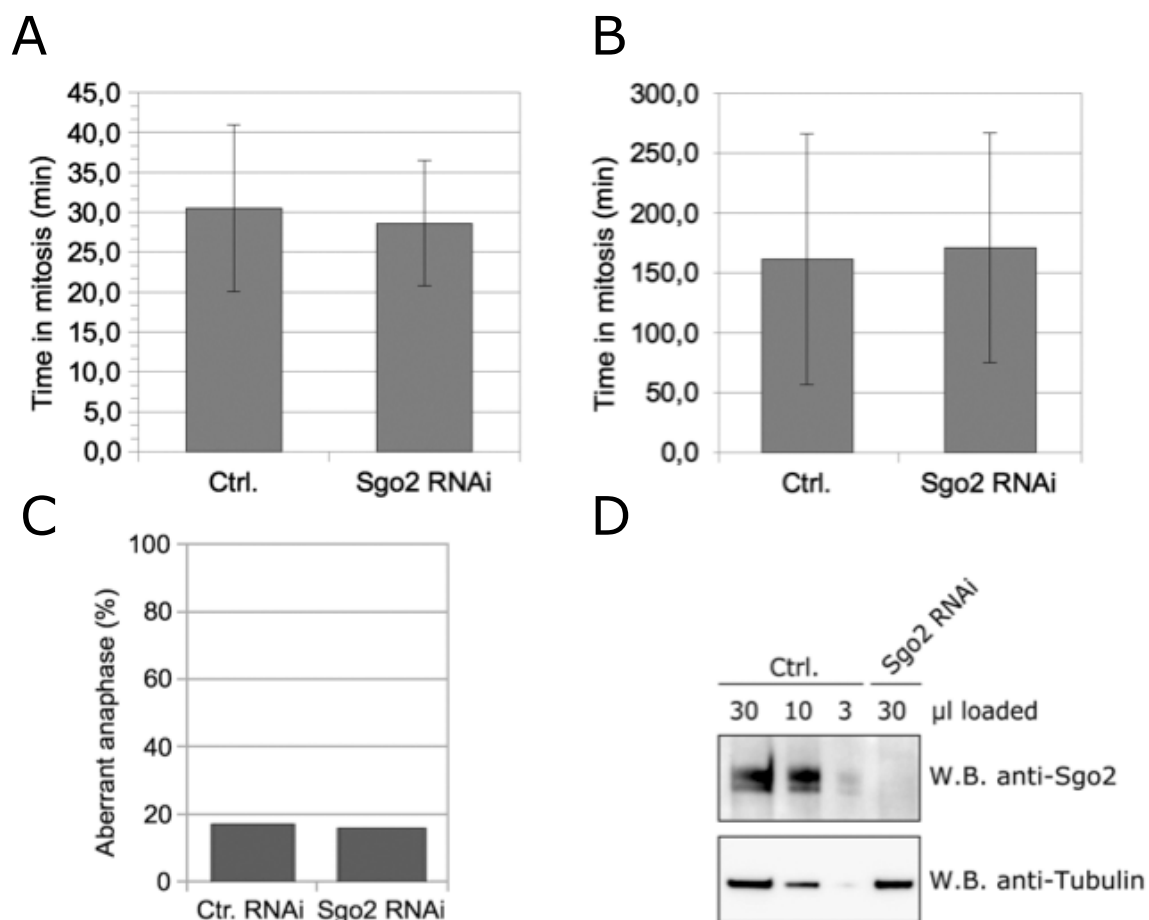


Fig. 19: Sgo2 is dispensable for normal mitotic progression in human cultured cells. (A)-(D) Cells were treated with control or Sgo2 siRNA (40 nM) for a total of 55 h. Live cell imaging was performed following release from a single thymidine block. (A and B) HeLa cells were imaged by phase contrast microscopy at a time resolution of 5 min per frame. Duration of mitosis was determined as the time interval between the first signs of cell rounding and initiation of cleavage furrow ingression. Error bars show standard deviation. Cells were cultured either in (A) DMEM or in (B) DMEM with 10 ng/ml taxol. (C) HeLa cells stably expressing histone 2B-eGFP were imaged using fluorescence microscopy. (D) Sgo2 depletion efficiency was determined semi-quantitatively by immunoblotting of different amounts of lysate. Detection of tubulin served as a loading control. Number of cells counted per data point: (A) $n > 100$, (B) $n > 70$, (C) $n > 60$.

4.3. *The Sgo2-Mad2 complex resembles the SAC complexes Mad1-Mad2 and Cdc20-Mad2*

4.3.1. The Sgo2-Mad2 complex can be isolated from living cells

So far, only yeast-2-hybrid data were available to demonstrate the Sgo2-Mad2 interaction for human proteins. Considering the lack of obvious mitotic phenotypes, further proof was required to demonstrate the specificity of the interaction. Therefore, it was tested whether Sgo2 and Mad2 also interacted at the level of endogenous proteins in human cell culture. Lysates were prepared from nocodazole arrested 293T cells and Sgo2 was immunoprecipitated using a specific antibody. Non-specific IgG was used as a negative control. By immunoblotting, Mad2 could be specifically found in the Sgo2 immunoprecipitate (I.P.) but not in the control (Fig. 20A). Thus, Mad2 binds Sgo2 in human cells.

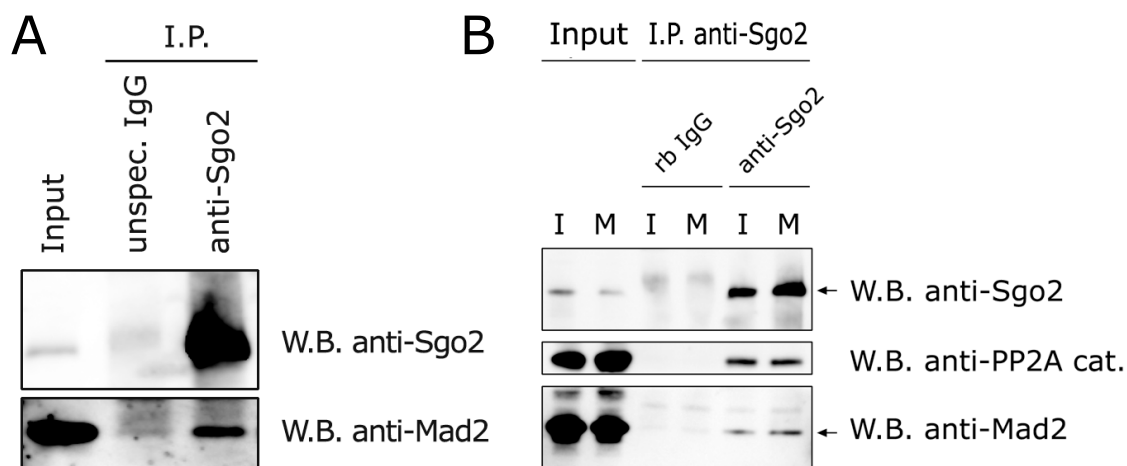


Fig. 20: The Sgo2-Mad2 exists in cells under endogenous conditions. (A) and (B) For each sample, 293T cells from 750 cm² confluent culture dish area were lysed (LP2+ with additional 250 mM NaCl) and subjected to immunoprecipitation using antibodies directed against Sgo2 (4 µg) bound to 20 µl of Protein G beads. Non-specific IgG was used as negative control. Samples were eluted using SDS-PAGE sample buffer and resolved by SDS-PAGE. Immunoblotting was used to detect Sgo2, Mad2 and PP2A. (A) Co-I.P. experiment of endogenous Sgo2 from nocodazole arrested cells. (B) The co-I.P. of Sgo2 and Mad2 was compared between interphase ("I", 15 h treatment with 2 mM thymidine) and mitosis ("M", 15 h treatment with 200 ng/ml nocodazole). Detection of the PP2A catalytic subunit (PP2A-C) served as a positive control.

A potential caveat of an interaction between two at least partially chromosome associated factors is that the interaction could be bridged via chromatin. This possibility was largely excluded by the addition of ethidium bromide at a high concentration (200 µg/ml) to the co-I.P. experiment, a method commonly used to displace proteins from DNA (Lai and

Herr, 1992). The Sgo2-Mad2 interaction was stable under these condition, supporting that it was not chromatin bridged (Suppl. fig. 3).

Given the mitosis specific function of Mad2, it was also of interest whether the Sgo2-Mad2 interaction was confined to mitosis or present also during other cell cycle phases. To distinguish between the two possibilities, HeLa cells were arrested either in interphase (G1/S-transition) using thymidine or in mitosis using nocodazole. Then, interaction between Sgo2 and Mad2 was studied by co-I.P. of endogenous Sgo2. In both samples, comparable amounts of Mad2 associated with Sgo2. The same was true for the Sgo2-PP2A interaction (Fig. 20B). In conclusion, Sgo2 and Mad2 interact in a cell-cycle independent manner.

Mad2 is a member of a protein family characterized by the presence of the so-called HORMA domain (Aravind and Koonin, 1998; Luo et al., 2000). This domain has been identified by sequence analysis in proteins involved in meiosis, DNA repair and the SAC and has been named with an acronym using the initials of its founding members (Hop1, Rev7 and Mad2).

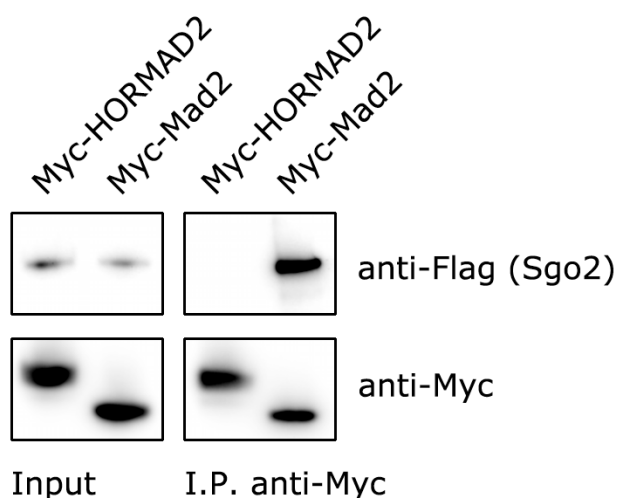


Fig. 21: Mad2 binding to Sgo2 is not a common feature of HORMA domain containing proteins. 293T cells were transfected with plasmids coding for tagged versions of Sgo2 (Flag), HORMAD2 and Mad2 (both Myc). Myc-tagged proteins were affinity isolated using anti-Myc beads and samples were probed for binding of Sgo2 by immunoblotting against the Flag-epitope.

In mouse, two meiosis specific members of the protein family have recently been identified, HORMAD1 and HORMAD2 (Fukuda et al., 2009; Wojtasz et al., 2009). Interestingly, in metaphase of meiosis I they co-localize with Sgo2. Therefore the question had to be resolved whether Sgo2 can interact with HORMA domain containing proteins in general or whether the interaction is confined to Mad2. Towards this end, either HORMAD2 or Mad2 were co-expressed with Sgo2 in 293T cells. Subsequently, HORMAD2 and Mad2 were affinity-isolated from cell lysates and checked for associated Sgo2 by immunoblotting (Fig. 21). Sgo2 was specifically detected only in the

Mad2 I.P. but not in the HORMAD2 I.P. Thus, Sgo2 binding is not mediated by HORMA domains *per se* but is instead a specific property of Mad2.

4.3.2. The Mad2 binding site is located between amino acid residues 101 and 200 of xSgo1

A point mutation that disrupts binding is one of the best proofs for specificity of a newly found protein-protein interaction. A first step towards finding such a shugoshin mutant was the mapping of the Mad2 binding site.

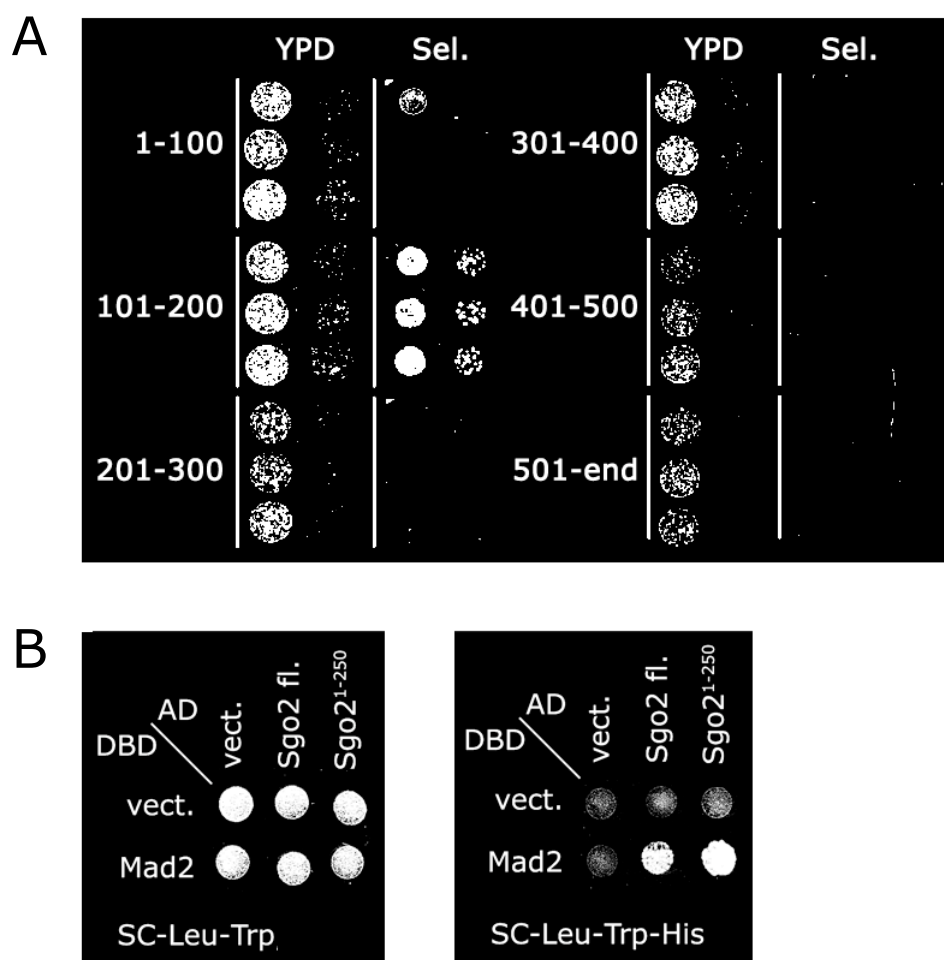


Fig. 22: Mapping of Mad2 binding sites. (A) The Mad2 binding site of *Xenopus* Sgo1 (xSgo1) is located between amino acid residues 101 and 200. Fragments of xSgo1 (length indicated in amino acid residues) fused to the Gal4 transactivating domain (AD) were tested for interaction with Mad2 fused to the Gal4 DNA binding domain (DBD) in a yeast-2-hybrid assay. Equal amounts of three independent clones were spotted for each construct on either YPD (input control) or SC-Leu-Trp-His ("Sel.", selective medium for interaction) (B) The N-terminal 250 amino acid residues of human Sgo2 (hSgo2) are sufficient for Mad2 binding. The indicated AD and DBD fusions were tested for auto-activation and specific interaction in a yeast-2-hybrid assay. Full-length Sgo2 served as positive control.

To this end, fragments of about 100 a.a. covering the whole length of xSgo1 were tested in a yeast-2-hybrid-assay for interaction with Mad2 (Fig. 22A). Only a fragment encoding a.a. 101-200 of xSgo1 showed growth on selective medium when Mad2 was simultaneously expressed, indicating that this N-terminal part of xSgo1 harbors the Mad2 binding site. It was further of interest whether Mad2 binding to the N-terminus of the shugoshin partner was evolutionary conserved. Therefore it was tested if an N-terminal 250 amino acid fragment of hSgo2 retains the ability to interact with Mad2 (Fig. 22B).

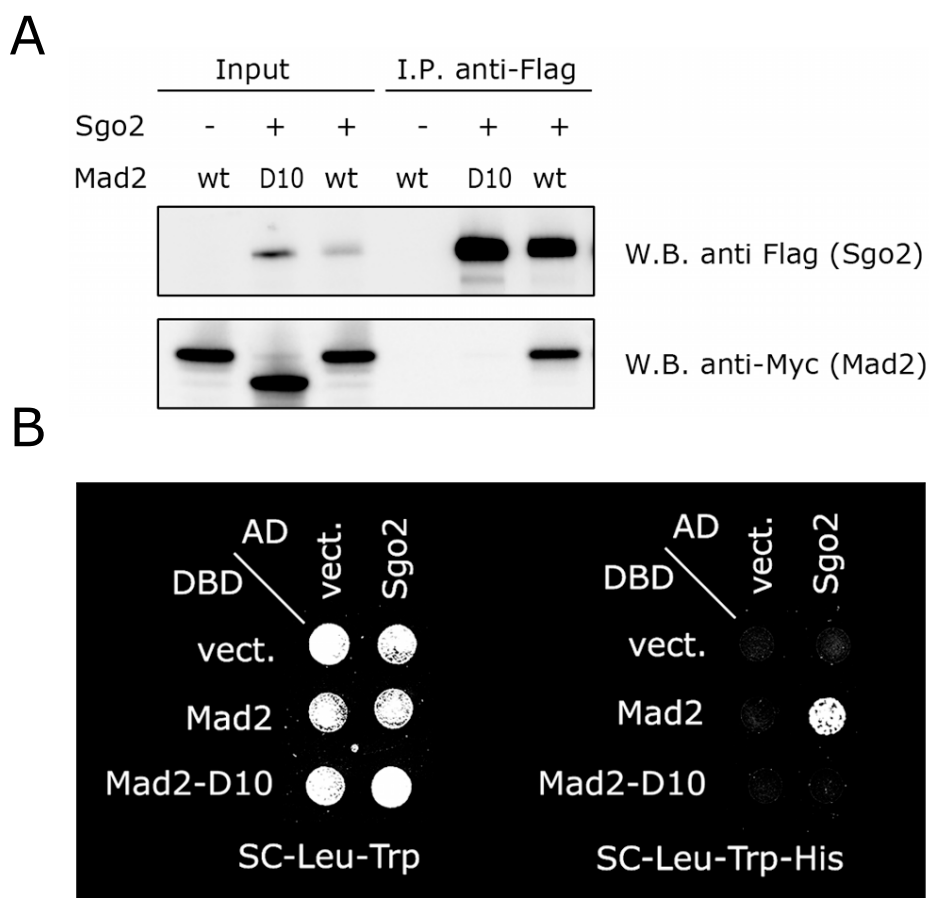


Fig. 23: The Mad2-D10 mutant is interaction deficient for Sgo2. (A) Co-I.P. experiment: 293T cells were transfected with plasmids encoding Flag-Sgo2 as well as Myc-tagged Mad2-wt or Mad2-D10. Sgo2 was immunoprecipitated from cell lysates with anti-Flag agarose. Beads were washed and then eluted with SDS-PAGE sample buffer. Following SDS-PAGE, tagged proteins were visualized by immunoblotting as indicated. (B) Yeast-2-hybrid experiment: *S. cerevisiae* strain PJ69-4A was transformed with the indicated plasmids. Yeast suspensions of positive transformants were plated either on SC-Leu-Trp plates (control for comparable cell numbers) or on SC-Leu-Trp-His plates (selection for protein-protein interaction). Note that single constructs did not show non-specific growth, i.e. auto-activation.

While none of the constructs gave rise to false-positive signals on their own, co-transformation of 2-hybrid vectors coding for Mad2 and Sgo2¹⁻²⁵⁰ enabled growth on

selective medium. The interaction between full-length Sgo2 and Mad2 served as a positive control. Therefore, also in the human system, the N-terminus of the Mad2-binding Sgo2 is sufficient for interaction.

4.3.3. Only Mad2 in its closed conformation can bind to Sgo2

The interactions of Mad2 with Mad1 and Cdc20 have been characterized in great detail and, surprisingly turned out to be highly similar (Luo et al., 2000; Sironi et al., 2002). This raised the question whether the newly identified Sgo2-Mad2 complex might also share mutual aspects of Mad1-Mad2 and Cdc20-Mad2. A series of Mad2 mutants have been identified that compromise its function. One example is a deletion of 10 amino acid residues from its C-terminus (Fang et al., 1998) which renders the resulting Mad2-D10 unable to interact with Mad1 and Cdc20 (Chen et al., 1999; Sironi et al., 2001). This is because Mad2-D10 is permanently locked in its "open" conformation (Luo et al., 2004). If the Sgo2-Mad2 interaction resembled the known complexes of Mad2, then Sgo2 should be unable to interact with Mad2-D10. The question was first resolved by a co-I.P. experiment. 293T cells were transfected with plasmids encoding tagged versions of Sgo2 along with wild-type Mad2 (Mad2-wt) or Mad2-D10. When Sgo2 was affinity isolated from cell lysates, only co-transfected Mad2-wt but not Mad2-D10 was found to be associated (Fig. 23A). In a negative control, no unspecific binding of transiently expressed Mad2-wt to the affinity matrix was detected.

Therefore, quite similar to the known Mad2 interactions, the newly identified Sgo2-Mad2 complex does not form when Mad2 is constitutively locked in the "open" conformation. The same conclusion could be drawn from a yeast-2-hybrid assay. Also in this system, specific interaction between Sgo2 and Mad2-wt but not Mad2-D10 could be observed (Fig. 23B).

4.3.4. Mad2 phosphorylation is incompatible with Sgo2 binding

Once a functional mitotic spindle has assembled, the SAC is switched off to allow cells to exit from mitosis. Among other mechanisms, phosphorylation of Mad2 has been suggested as a negative regulator of the SAC (Wassmann et al., 2003a). In the same study, a mutant version of Mad2 has been described, in which 3 serine/threonine residues are mutated to either aspartate or alanine residues in order to mimic a constitutively phosphorylated or de-phosphorylated state, respectively. The phosphorylation mimicking mutant lost binding to Mad1 while the alanine mutant retained full Mad1 binding capacity.

Again, the question arose whether the Mad2 phosphorylation site mutants would show similar behavior towards the new interactor Sgo2. Since the kinase Plk1 has been implicated in Mad2 regulation (Katja Wassmann and Olaf Stemmann, personal communications) two additional mutations in Plk1 consensus motifs were introduced (Mad2-5xD or Mad2-5xA).

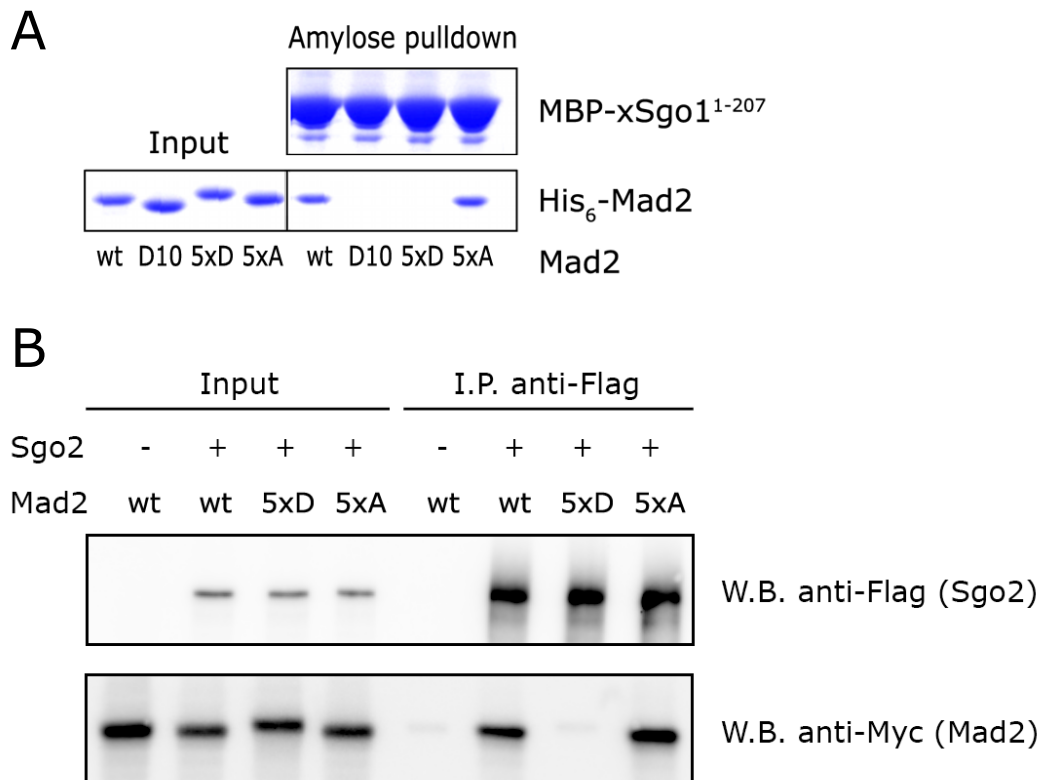


Fig. 24: A phosphorylation mimicking mutant of Mad2 does not bind to Sgo2. (A) *In vitro* pull-down assay: 10 μ g recombinant MBP-xSgo1¹⁻²⁰⁷ were bound to 10 μ l of amylose resin prior to incubation with 5 μ g each of either His₆-tagged recombinant Mad2-wt, Mad2-D10, Mad2-5xD or Mad2-5xA. After washing, proteins that eluted upon boiling of the beads in 50 μ l SDS-PAGE sample buffer were analyzed by SDS-PAGE and Coomassie staining. (B) Co-I.P. experiment: 293T cells were transfected with the indicated combinations of plasmids. Anti-Flag agarose beads were used to affinity purify Flag-tagged Sgo2 and associated proteins. SDS eluates were resolved by SDS-PAGE and analyzed by immunoblotting against the Flag-(Sgo2) and Myc-(Mad2) epitopes.

First, the mutants were tested in an *in vitro* pull-down assay. Therefore, Mad2-wt, Mad2-5xD, Mad2-5xA and, as a negative control, Mad2-D10 were expressed as His₆-tagged proteins in *E. coli* and purified. A recombinant N-terminal fragment of *Xenopus laevis* Sgo1 (xSgo1¹⁻²⁰⁷) was immobilized on beads and incubated with the different versions of Mad2. Material bound to the beads was analyzed by SDS-PAGE and Coomassie staining (Fig. 24A). As expected, Mad2-wt interacted with xSgo1 (positive control) while the

Mad2-D10 mutant did not bind (negative control). Interestingly, no binding was observed for Mad2-5xD while Mad2-5xA bound to xSgo1 with wild-type characteristics. A similar finding for human Sgo2 (hSgo2) could be obtained using co-I.P. experiments performed on lysates from transfected 293T cells (Fig. 24B). When hSgo2 was immobilized on beads, only co-transfected Mad2-wt and Mad2-5xA bound while Mad2-5xD did not.

Hence, mimicking phosphorylation of Mad2 negatively influences its binding to Sgo2. This is a similar binding behavior as it has been observed for the Mad1-Mad2 as well as for the Cdc20-Mad2 interaction by Wassmann et al. (2003a). Given that one of the mutated residues lies within the C-terminal safety belt, it is conceivable that phosphorylation induces Mad2 to adopt an open conformation.

4.3.5. xSgo1 and Cdc20 compete for Mad2 binding

If complex formation between shugoshin and Mad2 resembled the known checkpoint complexes like Cdc20-Mad2, then also the binding site on Mad2 should be the same. If this really were the case then Mad2 should not be able to bind xSgo1 and Cdc20 at the same time. Towards an experimental test of this hypothesis, an *in vitro* pulldown assay was performed. Recombinant xSgo1, Cdc20 and Mad2 carrying three different tags were mixed and incubated to allow binding. Subsequently, in separate pulldown experiments each of the factors was immobilized on beads via its specific affinity tag. When Mad2 was immobilized (Ni²⁺-NTA pulldown), both Cdc20 and xSgo1 could interact (Fig. 25), a result still consistent with mutually exclusive binding or a trimeric complex.

However, when xSgo1 (Amylose pd.) or Cdc20 (GSH pd.) were bound to beads, only Mad2 was found in the eluate. The fact that the respective other Mad2 interactor could not be identified in both cases showed that xSgo1 and Cdc20 bind to Mad2 in a mutually exclusive manner.

The result is consistent with xSgo1 and Cdc20 occupying the same or a similar binding site on Mad2. Strictly, from this experiment it cannot be excluded that the two factors each induce conformational changes of Mad2 that prevent binding of the other interactor. However, this second hypothesis could be ruled out by a 2D-NMR experiment shown in chapter 4.

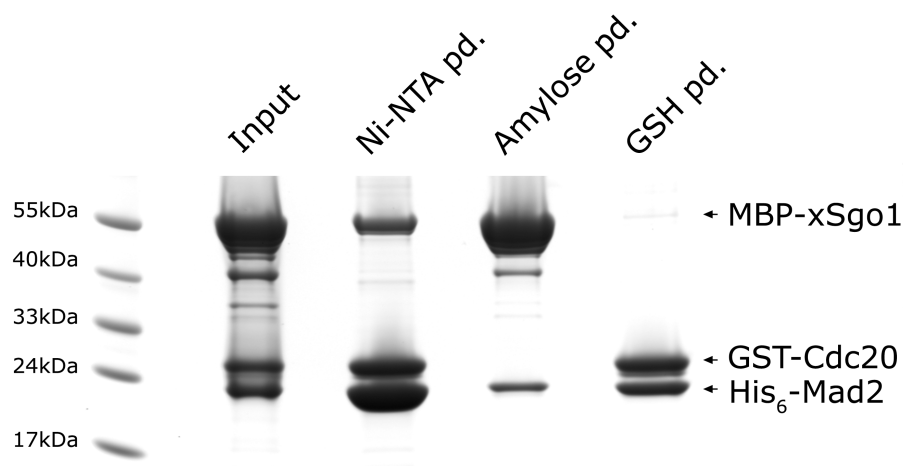


Fig. 25: Binding of Cdc20 and xSgo1 to Mad2 is mutually exclusive. *In vitro* binding assay: for each sample, recombinant MBP-xSgo1¹⁻²⁰⁷ (10 μ g), GST-Cdc20 (5 μ g) and His₆-Mad2 (5 μ g) were incubated for 4 h at 4°C. An input sample was directly mixed with SDS-PAGE sample buffer. For the pulldown assays, either 10 μ l each of Ni²⁺-NTA agarose, amylose or glutathione(GSH)-sepharose beads (10 μ l) were added for 1 h. After washing the beads, all bound proteins were eluted with SDS-PAGE sample buffer. The figure shows a Coomassie stained SDS-PAGE gel of the samples.

4.3.6. A conserved putative Mad2 binding motif in xSgo1 and hSgo2

For both Mad1 and Cdc20, the Mad2 binding sites have been mapped. Interestingly, Mad1 as well as Cdc20 contain a well conserved motif of four amino acids which is required for the interaction with Mad2 (Hwang et al., 1998; Luo et al., 2000; Luo et al., 2002). In the solved crystal structure of the Mad1-Mad2 complex, the Mad2 interacting motif (MIM) of Mad1 is in close contact with residues of Mad2 including those of the C-terminal safety belt (Sironi et al., 2002)(see also Fig. 26B).

Considering the similarities of complex formation, it was possible that also Mad2 binding to Sgo2 was mediated by a MIM. Sequence alignments were carried out comparing the known MIMs with amino acid residues 101-200 of xSgo1, to which Mad2 binding had been mapped (see chapter 4.3.2). Indeed, a short conserved stretch comprising four characteristic MIM residues was identified in xSgo1 (a.a. 168-171). Additionally, this sequence was followed by a proline residue, which also occurs downstream of most known MIMs (Luo et al., 2002). Next, it was tested whether the MIM was conserved between Mad2 binding shugoshin proteins. Using an alignment of the N-termini of xSgo1 and hSgo2, a potential MIM could be located in hSgo2 (a.a. 151-154) (Fig. 26A). This raised the possibility that the shugoshin-Mad2 interaction is mediated by a motif similar to the ones present in Mad1 and Cdc20.

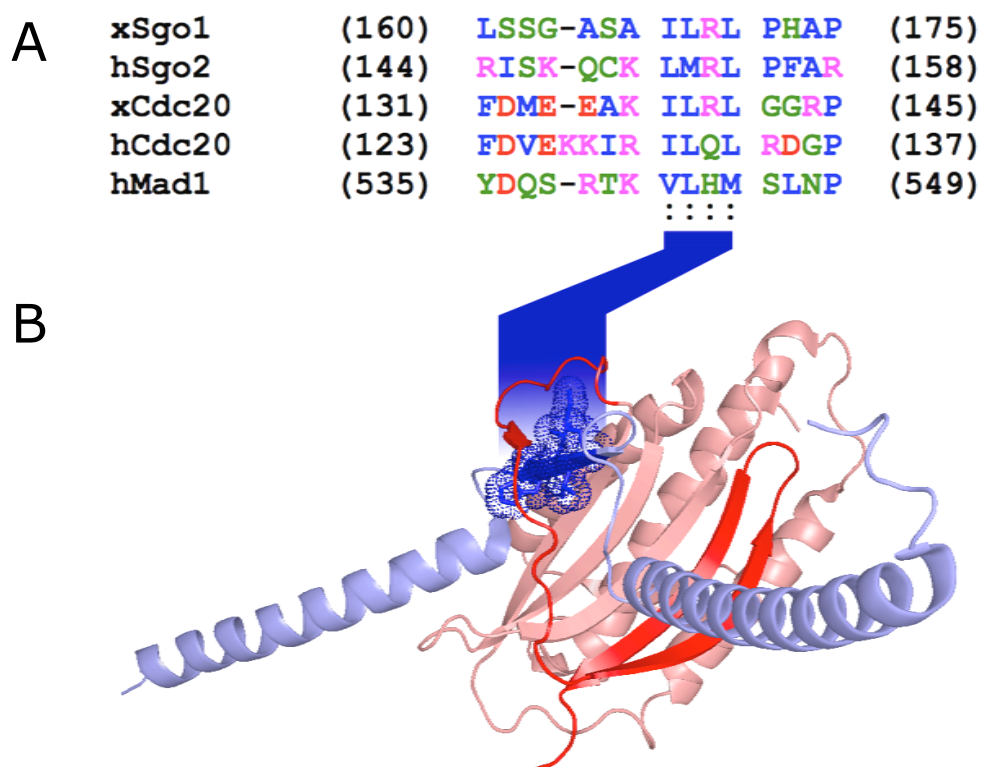


Fig. 26: A conserved putative Mad2 interacting motif (MIM) in *X. laevis* Sgo1 and *H. sapiens* Sgo2. (A) Sequence alignment of MIMs from human and *X. laevis* Mad1 and Cdc20 as well as xSgo1 and hSgo2. (B) Modified ribbon visualization of the hMad1-hMad2 crystal structure (Sironi et al., 2002) showing Mad2 in shades of red and a Mad1 fragment in shades of blue. The safety belt of Mad2 is drawn in dark red while the MIM is colored in dark blue.

A comparison of the Sgo1 and Sgo2 protein sequence shows that the MIM sequence present in Sgo2 is not well conserved in Sgo1 (data not shown). This result is consistent with the finding that Sgo1 is not a Mad2 interactor (see chapter 4.1.7).

4.3.7. The MIM is required for Mad2 binding to hSgo2

The MIM of known SAC factors Mad1 and Cdc20 is essential for their function. For example Cdc20 mutants leading to SAC deficiency have been mapped to its MIM (Hwang et al., 1998). In addition, mutations in the MIMs of Mad1 or Cdc20 abolished Mad2 binding (Luo et al., 2002). If the putative MIM sequence in Sgo2 would be the critical determinant for Mad2 binding then mutations within this motif should interfere with Mad2 binding. To test this hypothesis, a conserved arginine residue within the hSgo2 MIM (R153) was changed to alanine using site-directed mutagenesis of the Sgo2 coding DNA sequence. To test the mutant binding capacity, first a co.I.P. experiment was carried out. Towards this end, 293T cells were depleted from endogenous Sgo2 using

siRNA and at the same time siRNA resistant versions of wild-type Sgo2 or the MIM mutant Sgo2-R153A were overexpressed together with HA-tagged Mad2. Sgo2 was immunoprecipitated from cell lysates using a specific antibody.

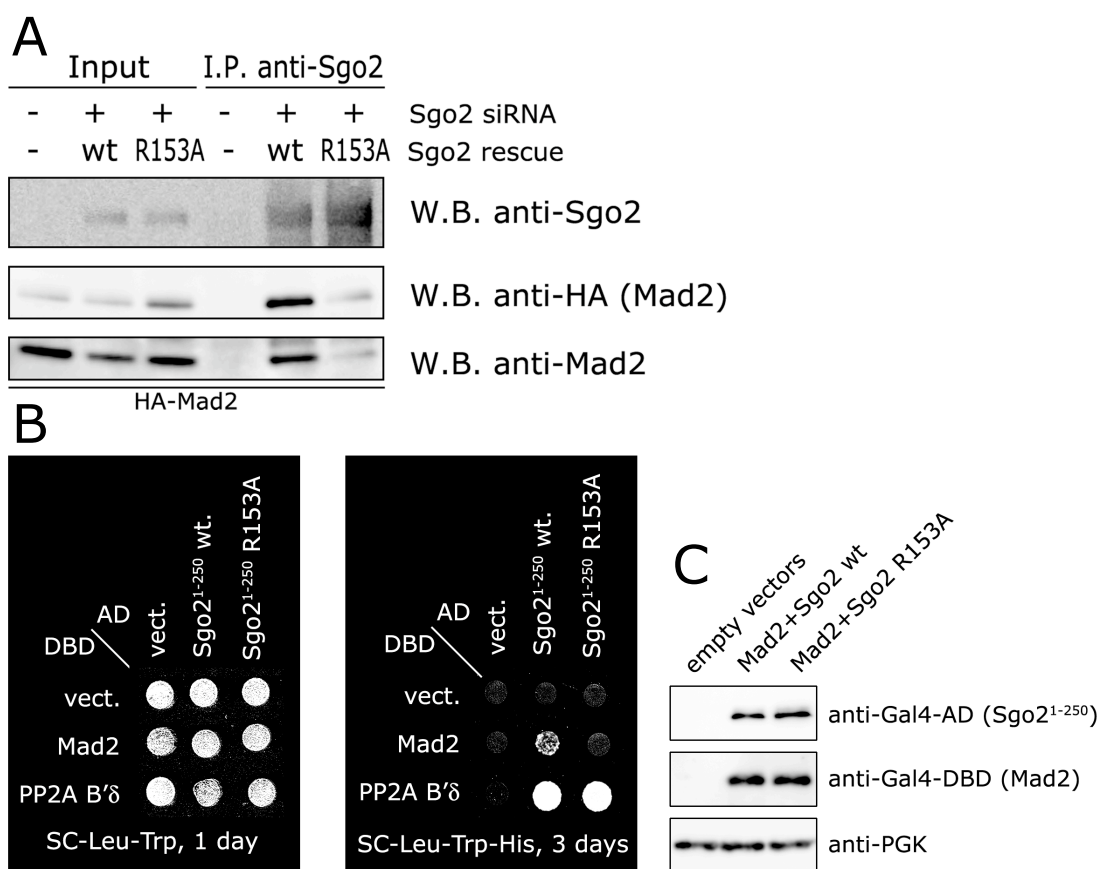


Fig. 27: Mutation of the Sgo2 MIM strongly reduces its interactions with Mad2. (A) 293T cells were co-transfected with Sgo2 siRNA and plasmids coding for HA-Mad2 along with wild-type or R153A mutant Sgo2. Sgo2 was affinity-isolated from cell lysates (LP2+ with additional 200 mM NaCl) using an anti-Sgo2 antibody. Precipitated proteins were eluted with SDS-PAGE sample buffer, resolved on an SDS-PAGE gel and analyzed by immunoblotting with anti-Sgo2, anti-HA (transfected Mad2) and anti-Mad2 antibodies. (B) In a yeast-2-hybrid assay, the indicated DBD or AD fusion constructs were transformed into the *S. cerevisiae* strain PJ69-4A. Comparable amounts of positive transformants were spotted either on SC-Leu-Trp agar plates (spotting control) or on SC-Leu-Trp plates (selective medium for interaction) and incubated at 30°C for the indicated periods of time. (C) Yeast cells transformed with the indicated constructs (Mad2: DBD-Mad2, Sgo2: AD-Sgo2) were grown over night in SC-Leu-Trp liquid cultures. Whole cell lysates were analyzed by SDS-PAGE and immunoblotting using antibodies against the Gal4 AD or DBD tags.

The degree of Mad2 binding was measured by immunoblotting for the HA-tag as well as for endogenous Mad2 (Fig. 27A). Both Sgo2 constructs were expressed at comparable levels but in the I.P. samples much less Mad2 was detected bound to the R153A mutant compared to wild-type Sgo2. Therefore, Sgo2 contains a functional MIM that enables its interaction with Mad2.

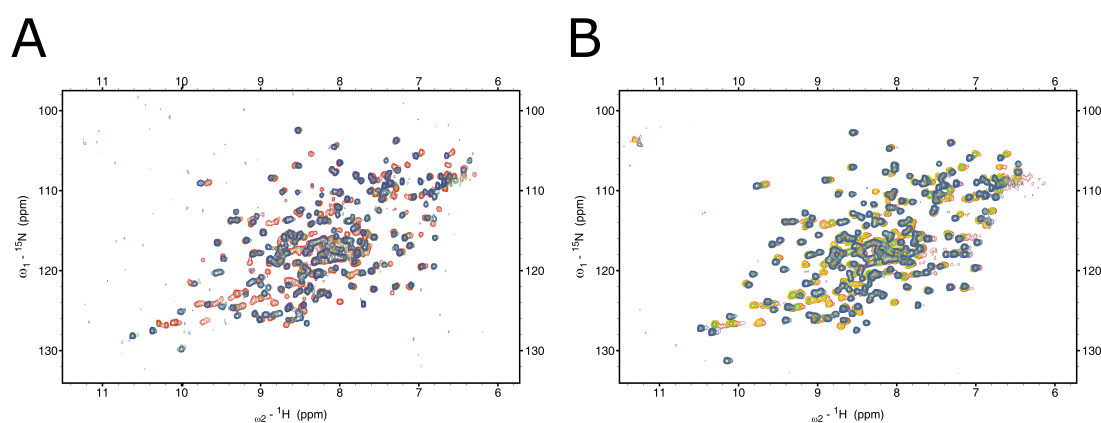
This finding was further supported by a yeast-2-hybrid experiment using N-terminal 250 a.a. fragments of hSgo2 containing the MIM (Fig. 27B). Wild-type Sgo2 and Sgo2-R153A were compared for their ability to interact with Mad2. After 3 days, wild-type Sgo2 but not Sgo2-R153A allowed for growth on selective medium. All constructs were expressed at equal levels as determined by Western blotting (Fig. 27C). It should be mentioned that at later time points also for the R153A mutant growth was detected, which could have been caused by residual binding (data not shown).

One possible, undesirable explanation could be that the R153A mutation affected the global protein structure of Sgo2 or at least of its N-terminus. To exclude this possibility, binding of another N-terminal Sgo2 interactor, PP2A was determined in the yeast-2-hybrid assay (Fig. 27B). Both wild-type Sgo2 and the R153A mutant gave rise to growth on selective medium in combination with PP2A-B' Δ . Therefore, the R153A mutation specifically affects Mad2 binding and does neither interfere with expression levels of Sgo2 nor with PP2A binding to Sgo2. This indicates that the R153A amino acid exchange is compatible with structural integrity of Sgo2.

4.3.8. Sgo2 binding induces a global conformational change of Mad2

The structure of Mad2 has been visualized in 2D NMR spectra, in which chemical shift peaks can be assigned to distinct amino acid residues (Luo et al., 2000). When a ^{15}N labeled version of Mad2 is used, an unlabeled peptide can be titrated in to perform binding studies using a ^1H - ^{15}N -HSQC experiment. The resulting changes of chemical shifts in the 2D spectrum give an indication as to which amino acids are involved in the protein-protein interaction. In a previous study, unbound Mad2 was compared to Cdc20 bound Mad2 in 2D-NMR. There, many chemical shifts changed, indicating a global structural change of Mad2 (Luo et al., 2000). This has been attributed to a switch of Mad2 from its open into the closed conformation upon Cdc20 binding. Furthermore, comparative 2D-NMR has been used to demonstrate similar changes of chemical shifts upon formation of Mad1-Mad2 and Cdc20-Mad2 complexes and, hence, similar binding modes for both (Luo et al., 2002). Binding behavior of Mad2 mutants to shugoshin suggested that there might be a similarity in complex formation compared to Cdc20-Mad2 or Mad1-Mad2 (see above). Since this should also be reflected in the 2D-NMR spectrum, binding of either a Mad1 peptide or a xSgo1 peptide to Mad2 was studied in collaboration with the laboratory of Tad Holak (MPI for Biochemistry, Martinsried). Reproducing the original finding (Luo et al., 2000), global structural rearrangements

were detected for binding of Mad2 to a Mad1 peptide (Fig. 28A). Strikingly, when an xSgo1 peptide harboring the Mad2 binding site was titrated to Mad2, highly similar changes of the 2D-NMR spectrum were observed (Fig. 28B). Formation of the Sgo2-Mad2 complex is therefore comparable to that of the well characterized Mad1-Mad2 complex. The 2D-NMR data strongly suggest that Mad2 undergoes a structural rearrangement from open to closed conformation upon association with shugoshin. Furthermore, strong splitting of NMR peaks during titration indicated a high binding affinity of xSgo1 and Mad2 (estimated $K_D < 1 \mu\text{M}$).



Experiment performed by U. Rothweiler and T. Holak

Fig. 28: Similar amino acid residues of Mad2 are involved in binding of Mad1 and xSgo1 peptides. His₆-Mad2 expression was performed in minimal medium with [¹⁵N]ammonium chloride as the only nitrogen source and purified as described in the Methods section. For the NMR experiments, protein concentrations of 0.2 mM Mad2 in PBS containing 10% D₂O were used. (A) Mad1 peptide (Sequence: TKVIHLSLN) was added in 4 steps to the Mad2 protein solution leading to a molar ratio of: 2.5:1; 1,25:1; 0.8:1; 0.2:1 Mad2:Mad1; red: reference spectrum; green: 1,25:1, blue: final step) (B) xSgo1 peptide (Sequence: SAILRLPIH) was added in 4 steps to the Mad2 protein solution leading to a molar ratio of: 2.5:1; 1,25:1; 0.8:1; 0.2:1 Mad2:Mad1; red: reference spectrum; yellow: 2.5:1; green: 1,25:1, blue: final step). Note that some of the final peak positions upon titration might differ due to different compositions of the peptides and hence different chemical environments.

4.3.9. p31 binding to Sgo2 is modulated by Mad2 levels

p31 has been described as a factor contributing to inactivation of the SAC. Its mechanism of action involves the binding to a preformed Mad1-Mad2 complex. This in turn blocks the catalysis of Mad2 conformational activation. Importantly, only Mad2 in the closed conformation, i.e. bound to Mad1 or Cdc20, is a cognate binding partner for p31 (Xia et al., 2004; Yang et al., 2007). This qualifies p31 as a molecular probe for detection of closed Mad2. If Sgo2 bound Mad2 were indeed in the closed conformation, then Sgo2 should be able to interact with p31 in the cellular context. To test this hypothesis, binding

was tested in a co-I.P. experiment using lysates from 293T cells transfected with plasmids coding for Myc-Sgo2 and Flag-p31 or with a Flag-p31 plasmid alone (negative control). When Sgo2 was bound to beads, co-I.P. of p31 could be detected while in the control only a very weak signal for p31 was observed (Fig. 29A).

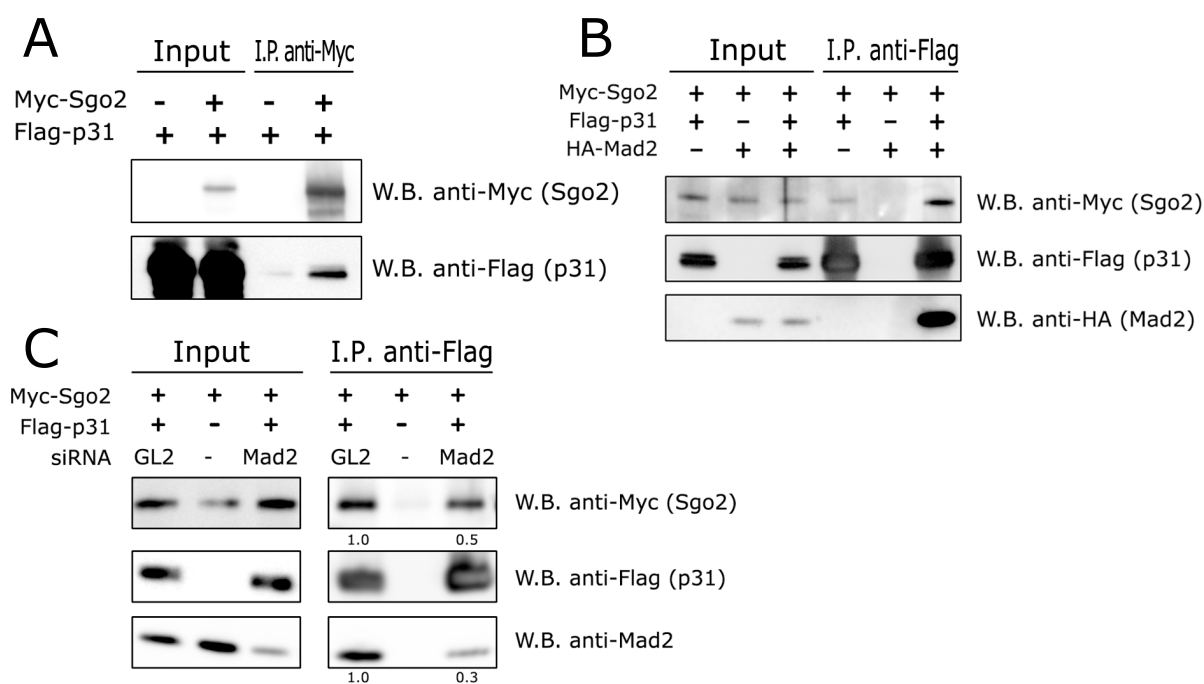


Fig. 29: p31 interaction strength with Sgo2 correlates with Mad2 levels. (A)-(C) 293T cells were transfected with plasmids coding for Sgo2 (Myc-tag), p31 (Flag-tag) or Mad2 (HA-tag). Myc-Sgo2 (A) or Flag-p31 (B and C) was isolated from cell lysates by bead-coupled epitope specific antibodies (10 μ l beads per sample). Detection was carried out by immunoblotting for the epitope tags or for endogenous Mad2 (A)-(C). (C) When indicated, control (GL2) or Mad2 siRNA was transfected along with the plasmids using the calcium phosphate method (Final concentration of dsRNA oligo in the culture medium: 50 mM). Densitometric measurements of Western blots referenced to the GL2 control were performed to measure relative amounts of Sgo2 and Mad2.

p31 is therefore able to interact with Sgo2. Considering the known p31 complexes, it was assumed that Sgo2-p31 interaction was bridged via Mad2. If this were the case, then changing the levels of Mad2 should proportionately affect Sgo2-p31 binding. This was tested by two different approaches. (1) *Mad2 overexpression*: in a co-I.P. experiment, p31 was immobilized on beads and binding of Sgo2 was determined by immunoblotting. When the experiment was performed with lysates from cells overexpressing Sgo2, p31 and Mad2, the Sgo2-p31 interaction was enhanced compared to samples without concomitant Mad2 overexpression (Fig. 29B). (2) *Mad2 depletion*: to study the effect of

decreased Mad2 levels on the Sgo2-p31 interaction, cells were transfected either with control (GL2) or Mad2 siRNA along with the plasmids. Decreased Mad2 levels were observed upon Mad2 siRNA transfection in the input sample, confirming successful RNA interference (Fig. 29C). As expected, less Mad2 (approx. 3-fold) was associated with p31 in the Mad2 siRNA sample compared to the GL2 control. At the same time, about twofold less Sgo2 was bound to p31 upon Mad2 depletion (Fig. 29C). In conclusion, Mad2 overexpression and depletion experiments are consistent with a heterotrimeric Sgo2-Mad2-p31 complex in which Sgo2 and p31 interact only indirectly via Mad2 in the closed conformation. The complex very likely comprises a direct Mad2-p31 interaction, indicating that Sgo2 bound Mad2 is in its closed conformation.

4.3.10. xSgo1 forms a trimeric complex with Mad2 and PP2A *in vitro*

PP2A binding (N58, Fig. 9) and Mad2 binding (R153, Fig. 27) have been mapped to closely juxtaposed positions within Sgo2's primary sequence. Two scenarios can be envisioned: first, both binding partners are able to interact at the same time on one Sgo2 molecule. Second, steric constraints allow binding of either Mad2 or PP2A but not of both.

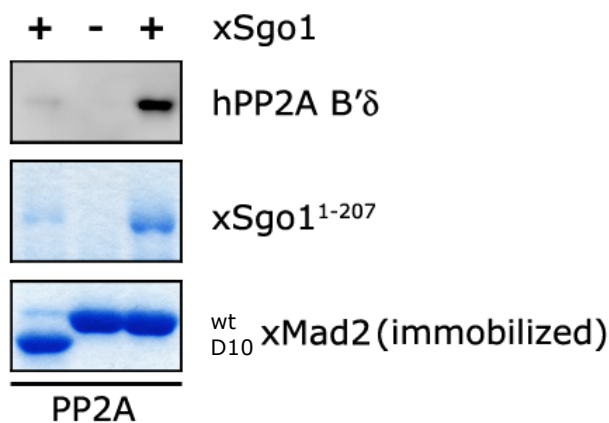


Fig. 30: xSgo1 can bind to Mad2 and PP2A at the same time. 5 μ g of His₆-Mad2 (wt or D10 mutant) were immobilized on 10 μ l of Ni²⁺-NTA agarose. To these, 100 μ l of cell extract from Myc-PP2A-B' δ overexpressing 293T cells were added in the presence or absence of 10 μ g MBP-xSgo1¹⁻²⁰⁷. Following incubation and extensive washing of the beads, immobilized proteins were eluted with SDS-PAGE sample buffer and analyzed by SDS-PAGE. Mad2 and xSgo1 were visualized by Coomassie staining, while PP2A-B' δ was detected by immunoblotting using anti-Myc antibodies.

To distinguish between the two models, *in vitro* pull-down experiments were performed. The following proteins were used: hMad2 and an N-terminal xSgo1 fragment were purified from bacterial expression cultures, while a lysate of 293T cells overexpressing Myc-tagged PP2A-B' δ served as a source of PP2A. First, Mad2 was immobilized on beads and incubated with PP2A alone. No binding of PP2A to Mad2 was detected (Fig. 30). Consistently, no interaction between the two proteins has been described in the

literature. However, when immobilized Mad2 was incubated with PP2A and xSgo1 together, both proteins were found in association with Mad2. Binding of xSgo1 to Mad2 was specific, since it was strongly reduced for the binding deficient Mad2-D10 mutant. This finding is most consistent with a model, in which the interaction of PP2A with Mad2 is bridged by xSgo1. Furthermore, it implies that xSgo1 can interact with both Mad2 and PP2A simultaneously.

4.3.11. Sgo2 can form multimers

A common characteristic of shugoshin family members is the presence of a coiled-coil region at their N-termini (Kerrebrock et al., 1995; Rabitsch et al., 2004). In many cases, coiled-coil regions mediate protein-protein interactions, such as homodimerization or formation of higher multimers.

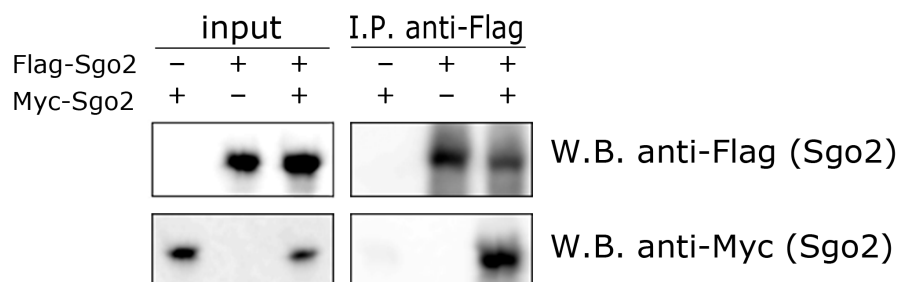


Fig. 31: Sgo2 interacts with itself. 293T cells were transfected with plasmids encoding Flag-tagged and/or Myc-tagged Sgo2. Following an anti-Flag-I.P. from cell lysates, beads were eluted with SDS-PAGE sample buffer. The samples were separated on an SDS-PAGE gel and analyzed by immunoblotting using antibodies directed against the Flag- and Myc-epitopes.

To clarify whether Sgo2 might also interact with itself, a co-I.P. experiment was carried out using as a starting material transfected 293T cells expressing Flag- and Myc-tagged Sgo2 either together or individually. When anti-Flag beads were used for the I.P., Myc-Sgo2 could only be co-precipitated when Flag-Sgo2 was bound to the beads (Fig. 31). Therefore, human Sgo2 exhibits self-interaction. Whether it forms just homodimers or higher order multimers could not be resolved in this experiment. This result is consistent with a previous publication reporting that the only *Drosophila* shugoshin, Mei-S332, does also interact with itself (Tang et al., 1998).

4.4. Regulation of the Sgo2 subcellular localization

4.4.1. Localization pattern of Sgo2 during mitosis

Both in mitosis and in meiosis II, a change of Sgo2 localization has been observed (Gomez et al., 2007; Huang et al., 2007). While at centromeres throughout prometaphase, Sgo2 switches to the kinetochore as the cell reaches metaphase. In order to determine the subcellular localization pattern of Sgo2 in more detail, immunofluorescence microscopy was carried out using co-staining of Hec1 to visualize outer kinetochores (Fig. 32). Consistent with previous reports (Huang et al., 2007), localization to the centromere in prometaphase as well as to the kinetochore in metaphase could be reconciled. In interphase, Sgo2 displayed a diffuse nuclear localization (data not shown).

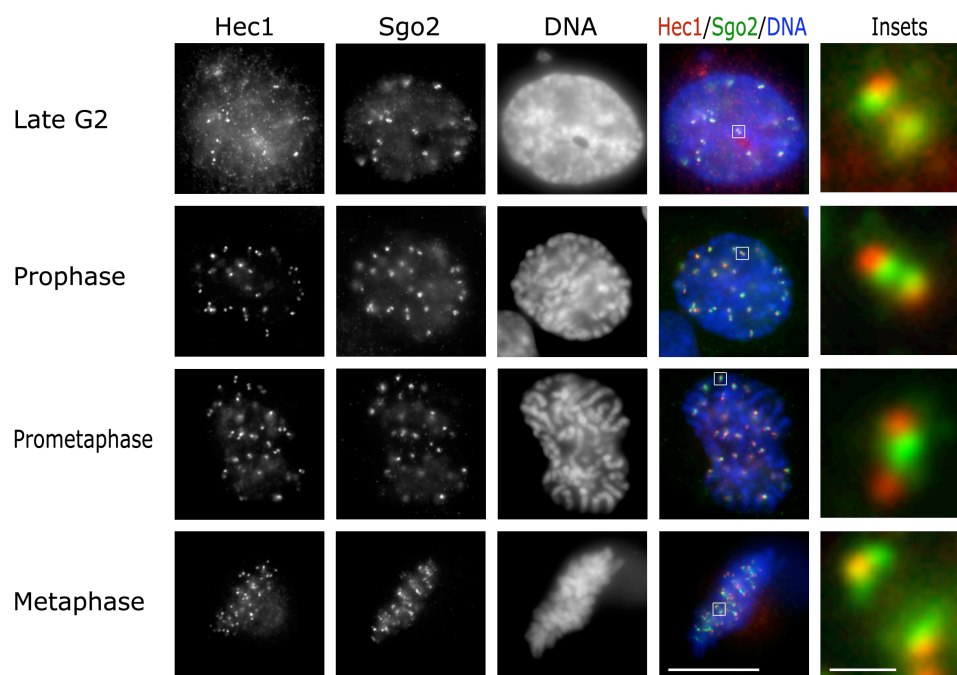


Fig. 32: Sgo2 localization pattern in mitosis. Asynchronous HeLa cells growing on glass coverslips were fixed with formaldehyde and stained with antibodies against Sgo2 (green) and the outer kinetochore marker Hec1 (red). DNA was counterstained with Hoechst 33342. Cell cycle phases were determined by chromatin morphology. The panels on the right show single kinetochore pairs at higher digital magnification. Scale bars are 8 μm for low magnification images and 1 μm for high magnification images.

When the first punctate Sgo2 localization could be observed, which presumably occurred in late G2 phase, interestingly, it partially colocalized with the kinetochore marker protein Hec1. This early recruitment of Sgo2 to the kinetochore has not been observed before. The reported concentration at centromeres took place only later, in prophase and

prometaphase. Thus, as cells progress from G2 via prophase into metaphase, Sgo2 travels from kinetochores to centromeres and back.

4.4.2. Microtubule attachment promotes Sgo2 relocation

Relocalization of Sgo2 in metaphase has been attributed to spindle forces pulling it away from centromeres and towards kinetochores (Gomez et al., 2007). Formally, other traits of metaphase could be responsible for the change of localization. Specifically, it was tested whether microtubule attachment to kinetochores is sufficient for Sgo2 relocalization or whether sister kinetochores also have to be under tension. To answer this question, HeLa cells were treated with different spindle poisons and the subcellular localization of Sgo2 was determined by immunofluorescence microscopy (Fig. 33).

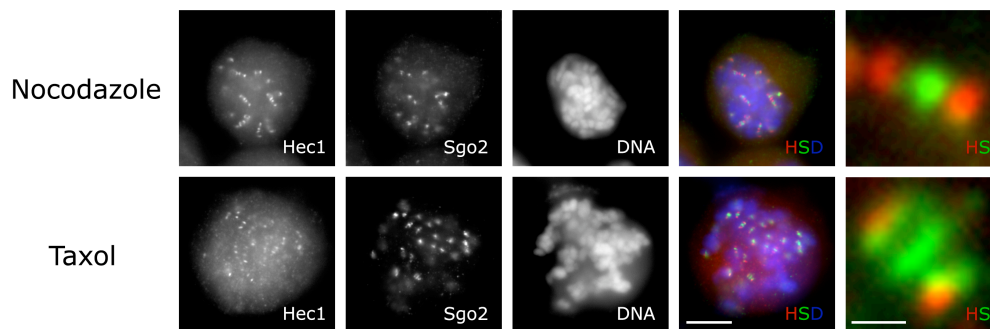


Fig. 33: Sgo2 partially translocates to kinetochores upon microtubule attachment. HeLa cells were treated with Nocodazole or Taxol (200 ng/ml each) for 6h, then fixed and stained with antibodies directed against Sgo2 (green, S) and Hec1 as a kinetochore marker (red, H). DNA, labeled with Hoechst 33342 staining is shown in blue (D). The panels on the right show single kinetochore pairs at higher digital magnification. Scale bars are 8 μm for low magnification images and 0.5 μm for high magnification images.

When cells were treated with nocodazole to depolymerize microtubules, Sgo2 localized to the centromere reminiscent of the prometaphase situation. In taxol treated cells Sgo2 was frequently found at the kinetochores while a fraction was still retained at centromeres. Taxol allows chromosome attachment to the mitotic spindle but inhibits spindle dynamics and hence tension across the centromeres. Consequently, this result shows that attachment alone is, at least in part, sufficient for Sgo2 relocalization to the kinetochores.

4.4.3. Sgo2 mutants localize correctly in mitotic human cells

As direct interactors of Sgo2, PP2A and Mad2 might influence its dynamic localization during mitosis. To test this possibility, recombinant PP2A and Mad2 binding deficient

mutants were compared to wild-type Sgo2 in their ability to replace the endogenous protein. To this end, HeLa cells were first transfected with corresponding siRNA (Fig. 34A, compare "Ctrl" and "Sgo2 RNAi"). Then, cells were transfected with one of different Sgo2 "rescue plasmids", in which the Sgo2 coding sequence had been altered to introduce four silent point mutations in the stretch targeted by the siRNA. Since RNAi requires a precise match, the rescue constructs were resistant to the respective siRNA oligo. Using this approach, wild-type and mutant (N58I or R153A) Sgo2s could be compared in terms of their subcellular localization by immunofluorescence microscopy (Fig. 34A). Cells transfected with rescue constructs could be easily identified since the vector used (pBOS SR-eGFP) also coded for soluble GFP. In nocodazole arrested cells, all three Sgo2 versions localized properly, i.e. to a single dot (green) in between Hec1-labeled kinetochores (red).

Therefore, neither binding of PP2A to Sgo2 nor its interaction with Mad2 are required for the characteristic centromeric localization of Sgo2 in prometaphase.

Huang et al. (2007) observed a delay in mitosis upon Sgo2 depletion. The defect was related to mislocalization of the microtubule depolymerase MCAK. In this work, Sgo2 could be depleted from human cells without much effect (see section 4.2). An immediate question was whether at least MCAK mislocalization in response to lack of Sgo2 could be reproduced. To test this, HeLa cells were depleted of Sgo2 as before and the localization pattern of MCAK was determined by immunofluorescence microscopy (Fig. 34B). In wild-type cells ("Ctrl") MCAK signals gave a punctate pattern. Individual dots being surrounded by two Hec1 signals indicated proper centromeric localization of MCAK. In the absence of Sgo2 ("Sgo2 RNAi"), only a diffuse cytoplasmic signal for MCAK was observed. Thus, the dependence of MCAK localization on Sgo2 could be reproduced. The MCAK mislocalization phenotype was indeed a specific effect, since it could be rescued by expression of wild-type Sgo2 in trans ("Sgo2 RNAi+Sgo2 wt").

In addition, the dependence of MCAK localization on binding of Mad2 or PP2A to Sgo2 was studied (Fig. 34B). Especially PP2A was an interesting candidate, since the phosphorylation status of MCAK can affect its localization to chromosomes (Zhang et al., 2007). However, the Mad2 ("R153A") and PP2A ("N58I") binding deficient mutants were both able to functionally replace endogenous Sgo2 in terms of MCAK localization.

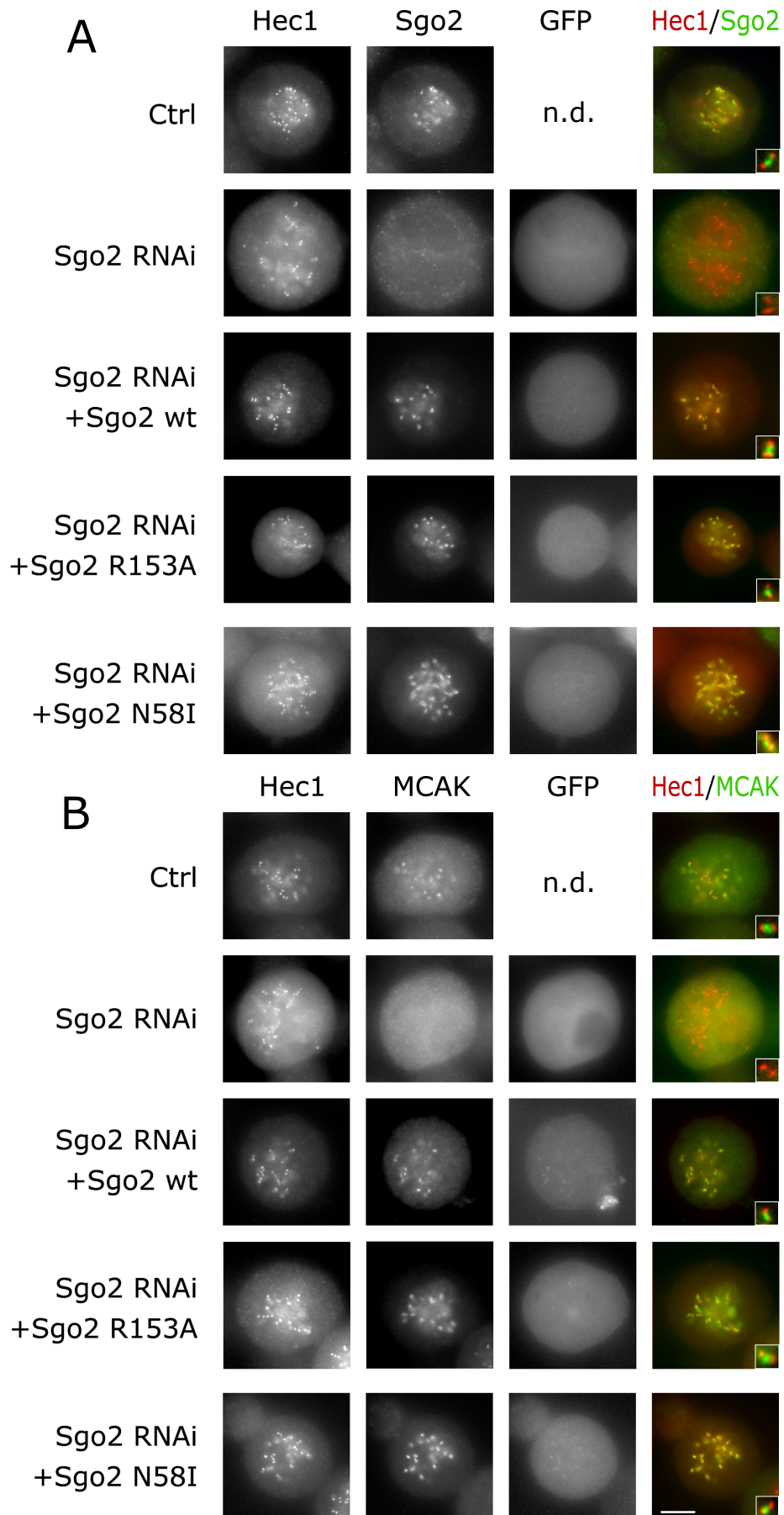


Fig. 34 (previous page): Analysis of the influence of Mad2 or PP2A binding to Sgo2 on the subcellular localization of Sgo2 and MCAK. (A) and (B) An siRNA rescue experiment was performed. Towards this end, Hela cells were either mock treated ("Ctrl", transfection reagent only) or transfected with siRNA directed against the endogenous Sgo2 mRNA. Then, rescue constructs were transfected, expressing wild-type Sgo2 ("wt"), Mad2 binding deficient Sgo2 ("R153A") or PP2A binding deficient Sgo2 ("N58I"). Cells were synchronized by a thymidine-nocodazole protocol and finally fixed with formaldehyde. (A) Subcellular localization of Sgo2. Immunofluorescence staining was done using antibodies against Sgo2 (green) and Hec1 (red, kinetochore marker). (B) Subcellular localization of MCAK. Immunofluorescence staining using antibodies against MCAK (green) and Hec1 (red). In both (A) and (B) Hoechst 33342 was used to label DNA. Cells transfected with rescue constructs or with the empty vector pBOS-SReGFP were identified by expression of soluble eGFP. n.d.: GFP fluorescence not determined. Scale bar is 8 μ m.

In summary, recruitment of MCAK to centromeres is the only detectable function of hSgo2 in mitosis. This function is properly executed irrespectively of whether or not PP2A or Mad2 can bind to hSgo2.

4.4.4. The C-terminus of Sgo2 is required for localization

The protein sequences of shugoshin homologs from different species are only weakly conserved. The central region is the most divergent while a somewhat better conservation is found at the N- and C-termini. Evolutionary conservation is often interpreted as an indication of functional relevance. Based on the findings from this work and from others, the shugoshin N-terminus is important for mediating protein-protein interactions.

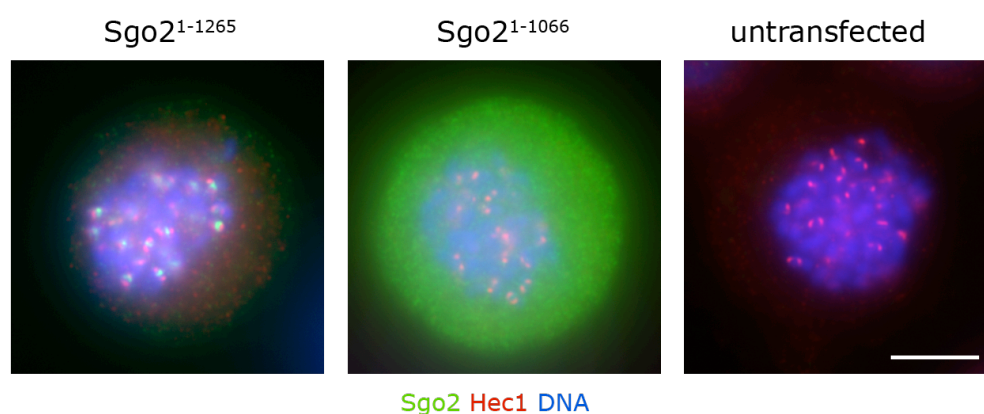


Fig. 35: The C-terminus of Sgo2 is required for its centromeric localization pattern in mitosis. In an siRNA rescue experiment, Hela cells were depleted from endogenous Sgo2 and subsequently transfected with rescue constructs encoding Myc-tagged full-length Sgo2¹⁻¹²⁶⁵ or a C-terminally deleted version, Sgo2¹⁻¹⁰⁶⁶. Localization was determined by immunofluorescence microscopy. Staining for Hec1 was used as a kinetochore marker. An untransfected cell which has been imaged using an equal exposure time for the green channel is shown as a negative control for background fluorescence. DNA is shown in blue and was visualized with Hoechst 33342 stain. Scale bar is 8 μ m.

In the case of hSgo2 binding of interaction partners like Mad2 or PP2A has been mapped to the N-terminal region (see chapter 4.3.2). Nevertheless, binding deficient Sgo2 mutants still show correct localization to centromeres. The hypothesis arose that Sgo2 chromatin localization could potentially be a conserved function of the C-terminus for the following reasons: the C-terminal conserved region is characterized by abundance of basic amino acids, a common feature of DNA binding proteins. In addition, point mutations within hSgo1's C-terminal part lead to its mislocalization (Yamagishi et al., 2008).

Quite similar, the hSgo2 C-terminus might be important for its recruitment to centromeres. To test this hypothesis, the C-terminal 199 amino acids were deleted from Sgo2 and the corresponding mutant Sgo2¹⁻¹⁰⁶⁶ was compared to the full-length protein Sgo2¹⁻¹²⁶⁵ in terms of centromeric localization (Fig. 35). Sgo2 depletion by siRNA combined with the transfection of rescue constructs was used to avoid effects due to interaction of endogenous Sgo2 with the truncation mutants (see chapter 4.3.11). While Myc-tagged wild-type Sgo2 localized like the endogenous protein, i.e. to centromeres in nocodazole arrested cells, Sgo2¹⁻¹⁰⁶⁶ was found to be completely cytoplasmic. In conclusion, the C-terminal 199 a.a. are required for Sgo2 to be recruited to its centromeric binding site. Interestingly, in the presence of endogenous Sgo2, the mutant Sgo2¹⁻¹⁰⁶⁶ localized properly, i.e. to centromeres (data not shown). This was most probably due to homotypic interaction between endogenous wild-type Sgo2 and the exogenous deletion construct, supporting functionality of the latter. Furthermore, it is a strong indication of multimeric Sgo2 at centromeres *in vivo*.

4.4.5. Sgo2 is a predominantly chromatin associated protein

From the immunofluorescence experiments, chromatin localization of Sgo2 was evident. However, no conclusions could be drawn as to the relative distribution between cytosol and chromatin. To resolve this issue, lysates from mitotic HeLa cells were prepared in the presence of increasing salt concentrations and separated into a soluble cytosol (S) and insoluble chromatin (C) fraction via centrifugation (Fig. 36). Staining for tubulin and core histones as markers for cytosol and chromatin, respectively, confirmed the success of this fractionation under all conditions. At lower salt concentrations, Sgo2 was almost exclusively recovered in the chromatin fraction. However, beginning at a NaCl concentration of 300 mM, Sgo2 was increasingly displaced from chromosomes with increasing ionic strength. In this regard, Sgo2 behaved similarly but not identically to

Topo II, which could be quantitatively solubilized at 400 mM NaCl. Sgo2 is therefore an almost exclusively chromatin associated protein that can be extracted from DNA at moderate salt concentrations.

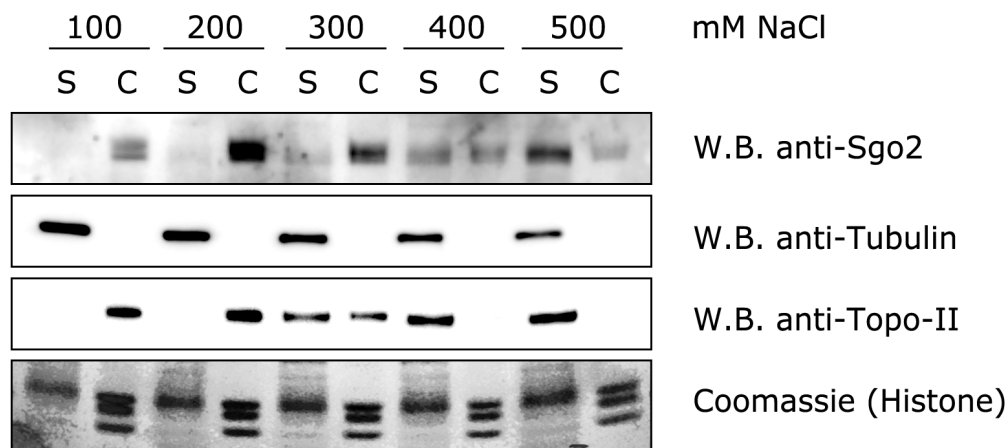


Fig. 36: The quantitative association of Sgo2 with mitotic chromosomes is sensitive to salt. HeLa cells were harvested and processed for chromatin fractionation, as described in the methods section. Buffer A was supplemented with the indicated NaCl concentrations. Detection of tubulin by Western blot and of core histones by Coomassie staining served as controls for the purity of the cytoplasmic and the chromatin bound fraction, respectively. Topoisomerase II was extracted at NaCl concentrations between 300 and 400 mM, while Sgo2 was solubilized between 300 and 500 mM NaCl.

4.4.6. Sgo2 is a mitotic phosphoprotein

The observed early mitotic relocalization of Sgo2 from kinetochores to the centromere correlates in timing approximately with the activation of mitotic kinases like Cdk1, Aurora B or Plk1. In order to test whether Sgo2 might be phosphorylated during mitosis, first the Sgo2 migration behavior was analyzed in SDS-PAGE. Phosphorylation of proteins often leads to a slower migration in SDS-PAGE due to diminished SDS binding. Indeed, Sgo2 from mitotic cells was detected at an apparently higher molecular weight compared to Sgo2 isolated from interphase cells (Fig. 37A). To confirm that the upshift was due to phosphorylation rather than other post-translational modifications, mitotic extracts were treated with Lambda phosphatase. This treatment reverted the apparent molecular weight of Sgo2 back to interphase level (Fig. 37A).

Which kinase contributes to Sgo2 phosphorylation? Aurora B was chosen as a first candidate since it had already been implicated in the regulation of Sgo2 and since it colocalizes with Sgo2 in prometaphase of mitosis (Huang et al., 2007). Aurora B loss of function experiments can easily be performed by specific chemical inhibition (Ditchfield

et al., 2003; Hauf et al., 2003). When mitotic HeLa cells were treated with Aurora B inhibitor for 30 min prior to lysis, Sgo2 migrated faster compared to the control with active Aurora B but slightly above interphase level (Fig. 37B).

In conclusion, Sgo2 becomes phosphorylated during mitosis and this depends at least in part on Aurora B.

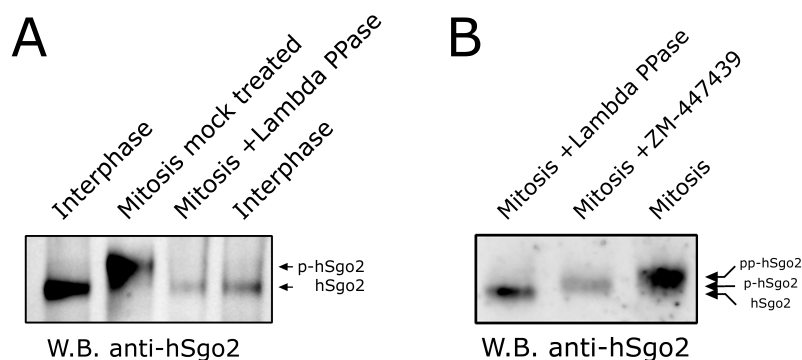


Fig. 37: Sgo2 is phosphorylated in mitosis. (A) HeLa cells were synchronized in mitosis or in interphase by a 15h treatment with nocodazole or thymidine, respectively. Cell lysates were prepared and treated with Lambda phosphatase when indicated. The relative migration behavior of Sgo2 was analyzed by SDS-PAGE and subsequent immunoblotting. (B) Cells were treated as in (A) but 10 μ M ZM447439 was added to the indicated sample 30 min before cell lysis. p-Sgo2 and pp-Sgo2 denote increasingly phosphorylated Sgo2 species.

4.4.7. Aurora B catalytic activity is required for proper Sgo2 localization

Aurora B starts to phosphorylate nuclear targets (e.g. Histone H3) in early mitosis (Giet and Glover, 2001). This correlates with the first relocation of Sgo2 from kinetochores to centromeres (see chapter 4.4.1). Direct or indirect influence of the Aurora B kinase could potentially be responsible for this change of localization.

To investigate whether Sgo2 localization is influenced by Aurora B activity, HeLa cells were synchronized in mitosis with nocodazole and then treated for 30 min with an Aurora B inhibitor or the corresponding solvent DMSO as a control. Immunofluorescence staining of control cells ("Ctrl.") revealed in most cases a single Sgo2 signal, which was located between the two kinetochores (Fig. 38A). Upon Aurora B inhibition ("ZM447439"), Sgo2 showed a more diffuse pattern and stretched between the two kinetochores. In some cases the signal even split into two dots close to the kinetochores, reminiscent of early mitosis or metaphase in unperturbed cells (overall mislocalization frequency about 60%, Fig. 38B).

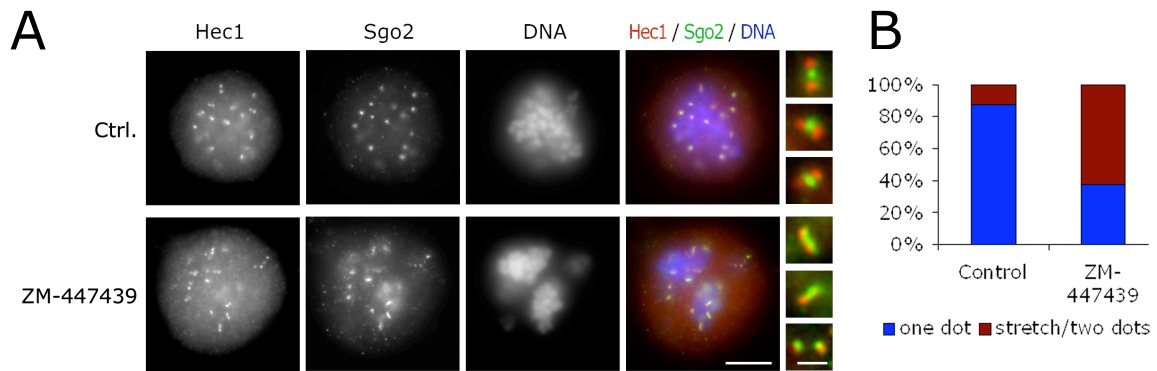


Fig. 38: Aurora B inhibition leads to premature kinetochore localization of Sgo2. HeLa cells were arrested in mitosis with nocodazole and collected by shake-off. Cells were then spun on coverslips and treated for 30 min with the Aurora B kinase inhibitor ZM4474439 (10 μ M) or the solvent DMSO (Ctrl.). (A) Immunofluorescence staining showing Sgo2 (green) and the kinetochore marker Hec1 (red). DNA stained with Hoechst 33342 dye is labeled in blue. Scale bars are 8 μ m for low magnification images and 1 μ m for enlarged kinetochore pairs. (B) Quantitative analysis of Sgo2 localization: correct centromeric localization (one dot) is shown as blue bars, diffuse localization including kinetochore signals (stretch/two dots) is shown in red.

Also, the localization of MCAK was analyzed in cells treated with Aurora B inhibitor. Very similar to Sgo2, MCAK mislocalized to kinetochores in prometaphase cells (Suppl. fig. 4).

Other studies have so far only used depletion of Aurora B by siRNA to study its impact on Sgo2 (Huang et al., 2007). While the loss of Aurora B abrogates Sgo2 chromatin localization completely, the short chemical inhibition presented here suggests that Aurora B catalytic activity is required to concentrate Sgo2 at the centromere in prometaphase.

5. Discussion

5.1. *The shugoshin-Mad2 interaction resembles the known SAC interactions Mad1-Mad2 and Cdc20-Mad2*

A role of shugoshin family members in the spindle assembly checkpoint has been demonstrated in the two yeast species *S. pombe* and *S. cerevisiae* (Indjeian et al., 2005; Kawashima et al., 2007). Specifically, yeast shugoshin is required for the function of the tension sensitive branch of the mitotic SAC. It is dispensable, however, for the attachment sensitive branch of SAC.

So far, only the phenotypes of shugoshin mutant yeast strains have been described. A putative involvement of shugoshin homologs in the SAC of higher eukaryotes has not yet been studied. Furthermore, it remains enigmatic how yeast shugoshin feeds into the SAC signaling pathway at the mechanistic level.

Shugoshin is conserved in higher eukaryotes: there is one shugoshin homolog in *X. laevis* (xSgo1) and two homologs in humans (hSgo1 and hSgo2). For both xSgo1 and hSgo2 a novel interaction with Mad2 was identified (Fig. 13, Fig. 14). This is the first direct link between shugoshin and a downstream component of the spindle assembly checkpoint. The following reasons argue for the specificity of the shugoshin-Mad2 interaction: (1) it is evolutionary conserved, (2) it can be isolated in co-I.P. experiments not only when Sgo2 and Mad2 are overexpressed but also at the level of endogenous proteins (Fig. 20, Fig. 21), and (3) it can be observed in diverse assays like yeast-2-hybrid (Fig. 14) and *in vitro* pulldown assays using recombinant proteins (Fig. 24). The latter experiment also proves that there is a direct interaction between Mad2 and Sgo2 that is not bridged by other proteins.

Mad2 can exist in two distinct native folds, named "open" and "closed". Mad2 interactions depend on its conformational state. Two types of Mad2 interactions can be distinguished: first, Mad2 in its open conformation can interact with Mad2 in its closed conformation to form an asymmetric homodimer (Mapelli et al., 2007). Second, Mad2 in its closed conformation can not only bind open Mad2 but also a partner that contains a Mad2 interaction motif (MIM). Up to now, Mad1 and Cdc20 have been the two only known Mad2 binding partners of this kind.

The shugoshin-Mad2 interaction can be assigned to this second class of closed-Mad2-MIM interaction. For example, hSgo2 fails to bind to a Mad2 mutant (Mad2-D10) that is

locked in its open conformation (Fig. 23). Identical behavior of the Mad2-D10 mutant towards Mad1 and Cdc20 has been described (Luo et al., 2000; Sironi et al., 2002). Another hint that Sgo2 associated Mad2 is in its closed conformation comes from the analysis of the p31 protein, a negative regulator of SAC, which structurally mimics open Mad2. It engages with closed Mad2 into a complex very similar to the asymmetric Mad2 dimer (Yang et al., 2007). However, p31 is unable to bind open Mad2 (Xia et al., 2004). Structural data suggest a trimeric complex, in which closed Mad2 bridges p31 and Mad1 (Yang et al., 2007). During this work a new interaction between p31 and Sgo2 could be identified (Fig. 29). The response of p31-Sgo2 complex formation to changing Mad2 levels was consistent with indirect p31-Sgo2 interaction, i.e. one that is bridged by Mad2. Given p31's preference for closed Mad2, this indicates that Mad2 bound to Sgo2 is in the closed conformation.

The Mad2 binding proficient shugoshin contains a conserved Mad2 interaction motif (MIM) both in *X. laevis* and in *H. sapiens* (Fig. 26). A point mutation (R153A) within the MIM of hSgo2 leaves shugoshin intact in terms of expression levels, cellular localization, ability to recruit MCAK and interaction with itself or PP2A (Fig. 27, 34, Suppl. fig. 5 and data not shown). All this indicates that the amino acid exchange has no gross effect on structure. Yet, the corresponding mutant is largely compromised in Mad2 interaction demonstrating that the MIM in shugoshin is functional and constitutes an important determinant of Sgo2's affinity for Mad2.

Nevertheless, this single point mutation does not completely abolish association of Sgo2 with Mad2 (Fig. 27). The residual binding could be due to the mutation leaving the MIM partially intact. This is unlikely since supposedly stronger MIM mutants were also tested and they, too, retained partial Mad2 binding ability. For example, no additional weakening of Mad2 binding was observed for Sgo2-4xAla (positions 150-153) compared to Sgo2-R153A. More likely, the residual Mad2 binding of Sgo2-R153A can be attributed to additional contacts between both partners. In binding assays it could be observed that the effect of the R153A mutation on Mad2 binding was weaker when full-length Sgo2 instead of an N-terminal fragment was analyzed (data not shown). However, attempts to further compromise Mad2 binding by additionally deleting parts of the Sgo2-R153A mutant were unsuccessful (data not shown). Therefore, the MIM around amino acid residue 153 of hSgo2 is an important Mad2 binding site, but there could be additional weaker contacts.

According to the template model of the SAC, Mad1 and Cdc20 can be assigned to a signaling pathway from unattached kinetochores to the APC/C. In this model, Mad1 is an upstream source of the "wait anaphase" signal while Cdc20 is the downstream target. It can only be speculated on the question whether shugoshin as a Mad2 interactor rather resembles Mad1 or Cdc20. While Cdc20 binds Mad2 only when the SAC is active (Wassmann and Benezra, 1998), the Mad1-Mad2 complex is constitutively present throughout the cell cycle (Chen et al., 1999). In that respect Sgo2 behaves like Mad1 (Fig. 20). Another difference between the known SAC interactors is that Cdc20 is destabilized by the SAC (Ge et al., 2009; Nilsson et al., 2008) while Mad1 is stable (Fig. 18). Again, Sgo2 behaves more like Mad1 than Cdc20. The data at hand suggest, therefore, that Sgo2 could play the role of an upstream source of SAC signal, like Mad1. In this work, the Sgo2-Mad2 interaction was identified and characterized. However, no cellular function of this complex could be demonstrated, so far. A current dogma in the mitotic checkpoint field is that the SAC signaling pathway is not branched. It has a single signal source (Mad1) and a single target (Cdc20). The finding of a Mad1/Cdc20 like interaction between shugoshin and Mad2 challenges this dogma and suggests branching of the SAC. Sgo2 could be an upstream checkpoint component which emits a "wait anaphase" signal in response to a spindle defect not sufficiently sensed by Mad1. Alternatively, Sgo2 might be a new downstream target of the SAC being regulated in its function by association with Mad2 (see chapter 5.7 for a more detailed discussion of these two hypotheses).

5.2. *The shugoshin recruitment cascade in human cells*

During this study, the binding site of PP2A in hSgo2 has been mapped (see chapter 4.3.2). This enabled the generation of a single point mutant of hSgo2 that is no longer able to interact with PP2A (Fig. 9). The PP2A binding deficient hSgo2-N58I was analyzed for its subcellular localization. In prometaphase cells, it showed a clear centromeric signal, like wild-type hSgo2 (Fig. 34A). For hSgo1, a different behavior has been described. A PP2A binding deficient version of hSgo1 is no longer able to bind to chromosomes and shows a diffuse signal (Tang et al., 2006). The fact that PP2A is dispensable for hSgo2 localization but required for hSgo1 localization is consistent with the published literature. hSgo1, hSgo2 and PP2A localize to the centromere of prometaphase cells. An interdependence of their localization has been described by siRNA depletion experiments (Kitajima et al., 2006). According to this study, hSgo2 is the most upstream of the three factors and PP2A localization depends on hSgo2. hSgo1

recruitment in turn depends on PP2A. A prediction would be that in cells expressing hSgo2-N58I as the only source of Sgo2, PP2A should not localize properly. Due to problems with PP2A immunostaining, this prediction could not be tested, so far. There are still open questions concerning the shugoshin recruitment cascade. Specifically, it is unclear in the light of the above findings why the absence of Sgo2 does not lead to mislocalization of Sgo1 (Kitajima et al., 2006). As a direct consequence, effects of the hSgo2-N58I mutant on PP2A localization can also not be indirectly assessed by Sgo1 immunostaining.

5.3. Evolutionary conservation of the PP2A binding motif

In both Sgo1 and Sgo2 from various vertebrate species, the protein sequence around the PP2A binding site is well conserved (see chapter 4.1.2). It frequently consists of two asparagine residues, followed by one positively charged and several hydrophobic amino acid residues. The di-asparagine motif is an especially crucial determinant of PP2A binding. Mutations within this motif interfere with PP2A binding to hSgo1 and hSgo2 (Tang et al., 2006; Fig. 9). However, it was not clear whether the respective asparagine residues are directly involved in molecular contacts with PP2A or whether the introduction of the bulky isoleucine residue sterically interferes with a nearby binding site. Meanwhile, the crystal structure of the mouse Sgo1-PP2A complex has been solved (Xu et al., 2009). The structure clearly shows that the di-asparagine motif of Sgo1 is in direct contact with amino acid residues of PP2A, more precisely, with its catalytic C-subunit. This fact strongly suggests that the corresponding amino acid residues in Sgo2 also engage in direct contacts with PP2A-C. Therefore, Sgo1 and Sgo2 contain an evolutionary conserved PP2A binding site.

The trimeric PP2A holoenzyme derives its specificity from a wide variety of regulatory B subunits, which fall into the three main categories B, B' and B'', that can be further subdivided according to isotypes and splice variants. Sgo1 has a clear preference for PP2A complexes containing regulatory B' subunits (Riedel et al., 2006). This can be explained by additional contacts between amino acid residues around E88 of Sgo1 and the B' subunit of the PP2A holoenzyme (Xu et al., 2009). Therefore, it can be assumed that the first binding site around N61 is responsible for basal binding to all forms of PP2A, while the second site around E88 confers specificity to a certain B subunit. Importantly, the second binding site is not able to sustain binding on its own, as demonstrated by the hSgo1^{N61I} mutant (Tang et al., 2006).

In contrast to Sgo1, Sgo2 is less specific in terms of preference for a certain type of PP2A. *In vitro*, it can bind B, B' and B'' equally well (Xu et al., 2009). The amino acids around E88 of Sgo1 are only weakly conserved in Sgo2, making the presence of a secondary PP2A binding site in Sgo2 questionable. Alternatively, Sgo2 might interact with PP2A exclusively via its NN-motif. In future experiments, this question could be elegantly resolved by exchanging the respective sequence motifs between Sgo1 and Sgo2 and subsequent analysis of binding specificity for PP2A subtypes.

Is the shugoshin-PP2A binding motif more commonly used for PP2A interaction or is it confined to the shugoshin protein family? Many cellular processes are regulated by PP2A and require binding of PP2A to specific substrates or locations. One example is the modulation of separase activity by PP2A (Holland et al., 2007). A stretch of amino acid residues within separase could be identified that faintly resembles the shugoshin-PP2A interaction motif. However, mutational analysis showed, that these residues are not crucial for binding of PP2A to separase (Benjamin Sünkel, Bachelor's thesis). In another approach, homology searches identified a series of proteins containing short sequence stretches similar to the shugoshin-PP2A binding motif (data not shown). However, in the few cases, in which the corresponding proteins were cloned and tested in I.P. experiments, no binding of PP2A could be detected (data not shown). Therefore, the shugoshin-PP2A motif is highly conserved among shugoshin orthologs and paralogs but there is no indication for it representing a general hallmark of PP2A interactors.

5.4. Sgo2 stimulates PP2A activity

In an *in vitro* pulldown experiment, a trimeric complex could be isolated, in which PP2A and Mad2 are linked by Sgo2 (Fig. 30). The binding sites of PP2A (N58) and Mad2 (R153) both map to the N-terminus of Sgo2. Nevertheless, Mad2 and PP2A apparently do not clash sterically when bound to Sgo2.

There is potential for mutual influences between the members of the trimeric complex. In this study it could be shown, that Sgo2 has a stimulatory effect on bound PP2A (Fig. 10). Considering the direct contacts between Sgo2 and the catalytic C-subunit of PP2A (PP2A-C) it is conceivable that binding of Sgo2 induces conformational changes within PP2A-C that increase its catalytic activity. When the two available crystal structures of Sgo1-bound and unbound PP2A-C were analyzed in an overlay (using MacPyMol, Suppl. fig. 6), most amino acid residues were hardly changed. A remarkable exception is Y90, which is rotated by about 90° around the axis of the hydroxyl group upon Sgo1 binding to PP2A. However, this residue is located rather far from the catalytic cleft,

making it hard to reconcile how this conformational change could influence phosphatase activity. Consistently, Xu et al (2009) did not detect an impact of their Sgo1 peptide on PP2A binding. Given the fact that a short shugoshin fragment was co-crystallized with PP2A and that Sgo1 instead of Sgo2 was used, it remains possible, however, that binding of full-length Sgo2 has a more profound influence on the PP2A-C active center.

In a phosphatase assay using purified Sgo2-PP2A complex, the effect of recombinant Mad2 on phosphatase activity was also investigated. In comparison with a Mad2 mutant, which does not interact with Sgo2 (Mad2-D10), wild-type Mad2 did not detectably change the phosphatase activity of Sgo2-PP2A (Suppl. fig. 7). Another possibility of mutual influence arose from the fact that mimicking phosphorylation of Mad2 has a negative influence on Sgo2 binding (Fig. 24). Thus, PP2A might stabilize the Sgo2-Mad2 complex *in vivo* by keeping Mad2 in a dephosphorylated state. As attempts to identify the relevant kinase failed (data not shown), this hypothesis could not be tested *in vitro*. Therefore, it was tested instead how much Mad2 was associated with PP2A binding deficient Sgo2-N58I relative to the wild-type protein upon immunoprecipitation from transfected cells (data not shown). As no differences in Mad2 binding could be detected, stimulation of PP2A catalytic activity by Sgo2 is the only detectable mutual influence within the trimeric Sgo2-Mad2-PP2A complex.

5.5. A three-step model for the removal of cohesive elements in mitosis

While DNA catenation is not sufficient to sustain sister chromatid cohesion in the absence of cohesin function, clearly, DNA catenation persists until the onset of anaphase (Baumann et al., 2007; Chan et al., 2007). This raised two main questions. First, what is the protective factor that blocks topoisomerase II (TOPO II) from acting on centromeric catenations until anaphase? Second, what are potential functions of residual catenations? The removal of catenations at anaphase onset could in theory be caused by multiple factors. Cdk1-Cyclin B1 activity drops and dephosphorylation events could activate centromeric TOPO II. Alternatively, an as yet unknown protector of catenation could act specifically at the centromere prior to anaphase onset. Finally, separase activation could directly stimulate centromeric TOPO II or do so indirectly via cohesin cleavage. Since these possibilities were difficult to resolve *in vivo*, an *in vitro* assay was chosen to test one of the hypotheses, i.e. the one that centromeric cohesin would interfere with decatenation (Fig. 12). This assay showed that in an isolated system with purified components, removal of cohesin precedes decatenation by TOPO II. The model most consistent with the experimental results is that cohesin itself protects centromeric

catenation. Cohesin could exert this function either by locally inhibiting TOPO II enzymatic activity or, more likely, by posing a sterical constraint to TOPO II. Another possibility is that the presence of cohesin still allowed TOPO II action but, by keeping the two DNA strands in close proximity, would prevent that microtubule dependent pulling on sister chromatids gives directionality to TOPO II's enzymatic activity. Though the *in vitro* chromatid separation assay relies on purified components, native metaphase chromosomes isolated from human cells come with a multitude of associated proteins. Thus, it cannot be completely excluded that another separase target distinct from cohesin is responsible for the observed effects. However, the only separase substrates known in mitotic mammalian cells are the cohesin subunit Scc1 and separase itself, which undergoes auto-cleavage.

In summary, resolving paired sister chromatids in mitosis is at least a three-step process. First, cohesin is phosphorylated and thus removed from chromosome arms by action of the "prophase pathway". Next, at the metaphase-to-anaphase transition, separase-mediated cohesin cleavage removes the remaining centromeric cohesin complexes. Finally, centromeric DNA catenations are resolved during anaphase.

Why should DNA catenations be preserved, if decatenation is not independently regulated but instead just passively follows cohesin removal? In fact, incomplete resolution of contacts between sister chromatids at anaphase onset might even result in DNA breakage, thereby threatening genome integrity. Persistent anaphase catenations could potentially contribute to continued silencing of the spindle assembly checkpoint (SAC). The SAC is switched off once all chromosomes have aligned properly on the metaphase plate. For this to happen, it is crucial that all centromeres/kinetochores are under tension. However, when separase cleaves cohesin complexes and sister chromatids spring apart, the tension at kinetochores would immediately dissipate. Hence, kinetochores of separating sister chromatids could in theory reactivate the SAC. Reactivation of the SAC in anaphase could stabilize residual securin and cyclin B1 and promote their re-accumulation by re-synthesis. Indeed, many aspects of anaphase can be reverted – even very late in mitosis – by artificial reactivation of Cdk1 (Potapova et al., 2006). DNA catenations might prolong the time period, in which kinetochores are under tension, thereby ensuring complete ubiquitylation and degradation of APC/C^{Cdc20} targets.

5.6. The roles of Sgo1 and Sgo2 in mitotic cohesin protection

The published data on mammalian shugoshin homologs led to conflicting ideas about the importance of Sgo2 for mitotic cohesin protection. While Kitajima et al. (2006) report a

significant loss of cohesion upon depletion of Sgo2, Huang et al. (2007) do not see such an effect. Both studies use different dsRNA oligos for targeting Sgo2's mRNA. Thus, the discrepancies might be explained by off-target effects in one but not in the other case. In this work (Fig. 11) it could clearly be shown that cells depleted of Sgo2 do not lose centromeric cohesion.

There is consent in the literature about the essential requirement of Sgo1 in mitotic cohesin protection. Also in this work, Sgo1 depletion has consistently led to premature sister chromatid separation (Fig. 11). That loss of Sgo2 does not compromise centromeric cohesion is difficult to reconcile with the report that the levels of PP2A at the centromere are markedly reduced when Sgo2 is depleted (Kitajima et al., 2006). It is also unexpected that Sgo1 depletion leads to premature sister chromatid separation without obviously affecting PP2A localization. These findings could only be reconciled if Sgo1 had a PP2A independent effect on cohesin protection, e.g. by physically shielding cohesin from access of kinases like Plk1. However, since depletion or chemical inhibition of PP2A does give rise to strong cohesion defects (Minshull et al., 1996), both Sgo1 and PP2A would have to collaborate to protect centromeric cohesin (Kitajima et al., 2006).

5.7. Potential implications of the Sgo2-Mad2 complex in meiosis

The following functions have been evoked for Sgo2 in mitosis: protection of centromeric cohesin (Kitajima et al., 2006), formation of spindles and proper microtubule-kinetochore interactions (Huang et al., 2007) and robustness of the SAC (Huang et al., 2007). The data presented in this work falsify all of these claims and are in agreement with more recent studies (Lee et al., 2008; Llano et al., 2008). The only "function" of mitotic Sgo2 that could be reproduced is the recruitment of the microtubule depolymerase MCAK to centromeres. Thus, the functions of Sgo1 and Sgo2 seem to be largely confined to mitosis and meiosis, respectively. As a consequence, the Sgo2-Mad2 interaction could potentially play a role in meiosis, affecting either Sgo2 and/or Mad2 functions. In the following, meiotic functions of Sgo2 and Mad2 - and possible mutual influence - will be discussed.

5.7.1. A role of Mad2 in meiotic cohesion is unlikely

Assuming that Sgo2 resembles a Cdc20-like downstream target of the SAC, it is – *a priori* – not obvious whether Mad2 will influence Sgo2 in a positive or negative way. Mad2 may act as a co-factor of Sgo2, thus helping to protect centromeric cohesin. Alternatively, Mad2 might be responsible for the mysterious inactivation of Sgo2 prior to

anaphase of meiosis II (see below). However, circumstantial evidences against both these models do exist. Murine oocytes depleted of Mad2 show missegregation of homologous chromosomes. However, when analyzed in metaphase of meiosis II, nearly all sister chromatids are still paired at centromeres indicating that Sgo2 function remains intact (Homer et al., 2005). SAC deficient oocytes also retain their ability to separate sister chromatids in anaphase of meiosis II, largely ruling out that Sgo2 cannot be switched off (Tsurumi et al., 2004). Taken together, there is currently no indication for a positive or negative role of Mad2 in cohesion of sister centromeres during meiosis. It is therefore unlikely that the function of the Sgo2-Mad2 complex lies in meiotic protection of centromeric cohesion.

5.7.2. Shugoshin 2 as a Mad1-like activator of the meiotic SAC?

A more promising hypothesis to test is an involvement of Sgo2 in the meiotic spindle assembly checkpoint. There has been some debate as to the importance of the SAC in meiosis. It seems that the meiotic SAC is more "sloppy" than the mitotic SAC since it ignores single chromosomes, which occur in X0 mice (Hunt et al., 1995; LeMaire-Adkins et al., 1997). The single X-chromosome can in theory be attached to the meiotic spindle but since it lacks its homologous counterpart, it will not experience tension. Apparently, this single tensionless chromosome is not detected by the meiotic SAC. However, the SAC in oocytes is able to detect loss of tension when several homologous chromosomes are unpaired. This is the case, for example, in *mlh1*^{-/-} mice that have defects in recombination and formation of chiasmata (Woods et al., 1999). Therefore, the meiotic SAC has difficulties detecting minor errors, which is in sharp contrast to its mitotic counterpart. A possible reason could be the diffusible nature of the "wait anaphase" signal together with SAC inactivation mechanisms that constitutively challenge this signal. With an increasing cytoplasm:DNA ratio, it will become more and more difficult to generate enough active Mad2 species to inhibit the APC/C in the entire cell. Similar effects are observed for the DNA damage checkpoint in early embryogenesis (Conn et al., 2004). Along these lines, mouse oocytes with a diameter of about 70 μm (Elder and Dale, 2000) can still respond to microtubule depolymerizing drugs by executing a SAC mediated arrest in meiosis I (Wassmann et al., 2003b). The much larger *Xenopus laevis* oocytes with a diameter of about 1 mm (Elder and Dale, 2000) are unable to do so. When the cytoplasm:DNA ratio is lowered in *X. laevis* egg extracts by addition of sperm chromatin at high concentrations, a SAC can readily be

established. All these findings lead to the conclusion that it is rather difficult to establish a robust spindle checkpoint response in oocytes.

Also in unperturbed murine meiosis, the SAC is triggered and required. Mouse oocytes that lack Mad2 will progress significantly faster from prophase to anaphase of meiosis I. This has dramatic consequences on the fidelity of homolog segregation (Homer et al., 2005).

While other components of the SAC, like Bub1 and Bub3, have also been found to be important in meiosis (Li et al., 2009; McGuinness et al., 2009; Yin et al., 2006), there are much less data about the upstream activator Mad1. While clear immunofluorescence data are available that show kinetochore signals of Mad2 (Wassmann et al., 2003b; Zhang et al., 2004), Mad1 localization in meiosis is apparently more diffuse (Zhang et al., 2005). This is consistent with a model, in which centromeric Sgo2-Mad2 can act in parallel to kinetochore bound Mad1-Mad2 as an alternative source for conformationally activated Mad2. Studying meiosis will be crucial to put this model to a test. More specifically, depletion of Mad1 and/or Sgo2 by microinjection of corresponding siRNAs should be combined with live cell imaging. If Sgo2 indeed took part actively in the meiotic SAC, one would expect faster progression of oocytes through meiosis I or their inability to arrest in response to spindle drugs. In addition, Sgo2 could play a role in the SAC of meiosis II. In male meiosis of *sgo2*^{-/-} mice, many spermatocytes progress beyond meiosis II despite the presence of separated sister chromatids and, hence, lack of kinetochore tension. Male *sgo2*^{-/-} mice are nevertheless sterile due to massive chromatid missegregation. The fact that the SAC seems to be inefficient in this special type of cell division is indicative of a potential SAC function of Sgo2.

5.8. The role of Aurora B in Sgo2 localization

Close examination of Sgo2 localization in normal mitosis revealed that Sgo2 first localized to kinetochores in prophase, then to centromeres in prometaphase and, finally, back to kinetochores in metaphase. How can this dynamic localization pattern be explained on a mechanistic level? Sgo2 localization in mammalian cells depends on Aurora B. The published phenotype for siRNA mediated depletion of Aurora B is a complete failure of Sgo2 to associate with chromatin (Huang et al., 2007). It had not been tested previously, whether the catalytic activity of Aurora B is necessary for its role in Sgo2 localization. In this work, catalytic inhibition of Sgo2 by the small molecule ZM447439 was used to analyze specifically the contribution of Aurora B kinase activity to Sgo2's subcellular localization. Surprisingly, Sgo2 was not lost from chromosomes

when mitotic cells were treated with ZM447439. Instead, premature relocalization of Sgo2 from centromeres to kinetochores was observed (see chapter 4.4.7). Even when the inhibitor was present during mitotic entry, the result was still kinetochore bound Sgo2 rather than complete delocalization (data not shown). Thus, Aurora B has a non-catalytic role in the initial recruitment of Sgo2 to chromosomes. Its kinase activity is required only later, i.e. to establish and to maintain the focused centromeric Sgo2 pattern during prometaphase.

The early requirement of Aurora B *protein* rather than kinase activity makes it tempting to speculate that Aurora B delivers Sgo2 to kinetochores by direct physical interaction. This prediction could now be tested by asking whether both proteins co-I.P. and whether Aurora B – like Sgo2 – transiently localizes to kinetochores in prophase before concentrating at centromeres. One can further speculate that Aurora B, like other mitotic kinases, reaches full enzymatic activity only by prometaphase. Consistent with the data shown in Fig. 37, it would now mediate Sgo2 phosphorylation, thereby creating an affinity of Sgo2 for some unknown centromeric structure.

But how then can Sgo2 relocalize from centromeres to kinetochores in metaphase when Aurora B kinase activity is still high? One possible explanation could be the activation of an as yet unknown phosphatase upon microtubule attachment to kinetochores. The exertion of tension as a triggering event is less likely here, since Sgo2 partially relocalizes in taxol- but not nocodazole-arrested cells (see chapter 4.4.2). Whatever the phosphatase, it is probably not PP2A, since PP2A binding deficient Sgo2 retains normal relocalization behavior. Instead, PP1, a known antagonist of other Aurora B functions, is a strong candidate because it localizes to kinetochores and dephosphorylates substrates like dynein at the time of SAC inactivation (Trinkle-Mulcahy et al., 2003; Whyte et al., 2008). A testable prediction would therefore be that a PP1 specific inhibitor should interfere with proper centromere-kinetochore traveling of Sgo2 in metaphase cells.

A corollary of the above model is that kinetochore- and centromere-localized Sgo2 should be hypo- and hyperphosphorylated, respectively. Raising peptide antibodies that specifically recognize only dephosphorylated or only phosphorylated Sgo2 might enable one to test this hypothesis by future immunofluorescence microscopy.

5.9. Downstream factors of Aurora B in the tension SAC

Many aspects of the tension sensitive branch of the SAC still remain unresolved. One example is the ongoing search for a molecular tension sensor. Another one concerns the events downstream of Aurora B, an essential component of the tension sensitive SAC.

There are two competing models. One model proposes that Aurora B takes part in the SAC in a rather active manner. It assumes that the signaling pathway, which is triggered by tensionless MT-kinetochore linkages, would branch downstream of Aurora B. One pathway would mediate the correction of erroneous kinetochore-microtubule attachments, but an additional one would directly trigger the SAC by an as yet unknown mechanism (Vader et al., 2007). A second, simpler model predicts that Aurora B *only* mediates depolymerization of false k-fibers. The resulting unattached kinetochores would then automatically recruit Mad1-Mad2 and trigger the SAC (Pinsky et al., 2006). A recent publication (Yang et al., 2009) indirectly supports the second model. Intermediate taxol concentrations stabilize erroneous kinetochore-microtubule attachments and hence trigger the tension sensitive SAC. In contrast, high taxol concentrations are a worse trigger of mitotic arrest. This finding is consistent with an excessive stabilization of attachments, impeding creation of free kinetochores. The remainder of this chapter will, therefore, deal with the nature of the pathway linking Aurora B with the creation of unattached kinetochore.

The microtubule depolymerizing kinesin MCAK has been evoked as the player chiefly responsible for the destabilization of tensionless k-fibers (Kline-Smith et al., 2004; Lan et al., 2004). This is based on experiments in the *Xenopus* system, in which the interference with MCAK apparently removes an essential microtubule depolymerase (Desai et al., 1999). In human cells, Aurora B recruits Sgo2, which in turn recruits MCAK to kinetochores/centromeres (Andrews et al., 2004; Huang et al., 2007; Lan et al., 2004). Consequently, Sgo2 depletion leads to delocalization of MCAK in mitotic HeLa cells. If human MCAK were essential to resolve kinetochore-microtubule contacts, such Sgo2-less cells should suffer from inability to correct erroneous attachments. However, this is clearly not the case, as Sgo2 depleted HeLa cells pass through mitosis with normal kinetics and no signs of lagging chromosomes (see chapter 4.2.5). This observation is consistent with the fact that depletion of MCAK from human cells likewise has little or no effect on error correction and chromosome segregation fidelity (Manuel Kaulich, personal communication). Thus, in marked contrast to Aurora B, Sgo2 and MCAK seem to be dispensable for correction of faulty attachments and triggering of the tension sensitive branch of the SAC in humans. Consequently, one has to propose the existence of an alternative route in humans that relays the signal from misattached chromosomes via Aurora B to error correction (Fig. 39). This could involve microtubule depolymerases other than MCAK and/or direct phosphorylation of microtubule-kinetochore attachment

sites. Consistently, a tension sensitive SAC was Aurora B dependent, even in the absence of Sgo2 (Suppl. fig. 8).

Given that MCAK seems to be indispensable for error correction in *X. laevis*, it seems worth studying potential mitotic roles of xSgo1 in the future. To this end, one would have to establish siRNA dependent knock-down in cultures of somatic frog cells and to then analyze mitosis and chromosome segregation by live cell imaging. As a downstream factor of xSgo1, MCAK also qualifies as a potential target of the newly identified xSgo1-Mad2 interaction. In future experiments, it should therefore be tested whether MCAK localization or function is modulated by Mad2 in *Xenopus* cell culture systems.

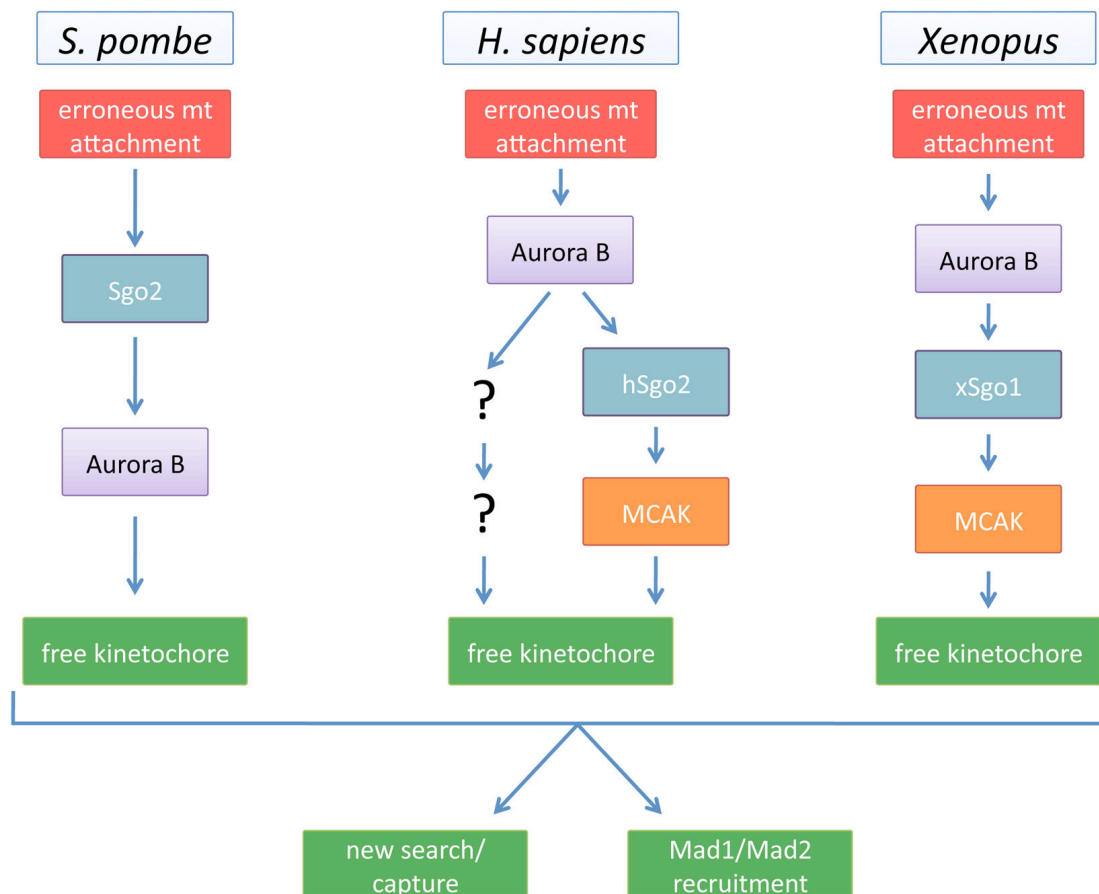


Fig. 39: Pathways linking the recognition of erroneous kinetochore-microtubule attachments with their correction. In the error correction pathway of *S. pombe*, Aurora B is downstream of Sgo2. In contrast, Aurora B is upstream of hSgo2 or xSgo1 in humans or *Xenopus*, respectively. While in *Xenopus* there is a strong requirement for MCAK in correcting erroneous kinetochore-microtubule attachments, in human cells MCAK is largely dispensable. This suggests an alternative pathway in parallel (marked by "?").

The mutual dependencies of shugoshin and Aurora B in terms of chromosomal localization differ from yeast to vertebrate cells. As mentioned above, Aurora B is upstream of hSgo2 in human cells. Similarly, Aurora B is upstream of xSgo1 in *X. laevis*

(Boyarchuk et al., 2007). Interestingly, the situation in *S. pombe* is the opposite: Here, Sgo2 is required for Aurora B localization (Kawashima et al., 2007). This might also account for the different Sgo2 loss of function phenotypes in terms of the tension sensitive branch of the SAC. So far, a role of a shugoshin homolog in the checkpoint dependent sensing of tension has only been demonstrated in yeast, i.e. when the essential SAC factor Aurora B is under control of shugoshin.

5.10. Sgo2 inactivation in meiosis

For Sgo2 inactivation in meiosis II, relocalization from centromere to kinetochore likely constitutes an important step. It has been proposed that by this means Sgo2 is physically separated from Rec8. Only then, Rec8 is phosphorylated and subsequently cleaved by separase. Relocalization of Sgo2 has been attributed to spindle-associated pulling forces occurring at kinetochores. Why then does Sgo2 stay at centromeres throughout meiosis I? There, two homologous chromosomes are tethered by means of chiasmata and arm cohesin forming a so-called bivalent. Within a bivalent, each homolog shows mono-orientation of fused sister kinetochores. In such a "pseudo-syntelic" arrangement, sister centromeres will not experience tension. In contrast, they will come under tension in meiosis II when sister kinetochores biorient as they do in mitosis. Preservation or disappearance of Sgo2 from centromeric cohesin has therefore been attributed to lack or presence of centromeric tension, respectively.

Is tension really necessary and sufficient to redirect Sgo2 from centromeres to kinetochores? In this thesis, mitotic cells were treated with taxol to address this question. Although this results in abrogation of spindle forces, attachment of kinetochores to microtubules is still possible. Surprisingly, relocalization of Sgo2 from centromeres to kinetochores still occurred under these conditions, i.e. in the absence of centromeric tension (Fig. 33). Thus, attachment can already cause relocalization. This raises the next question, namely, why MT-kinetochore interaction does not trigger premature dissociation of Sgo2 from centromeres in meiosis I? This could be explained by a meiosis I specific mechanism that prevents attachment induced relocalization of Sgo2 at this early stage of meiosis. The literature provides some evidence for this hypothesis to be actually correct. Before homologous recombination and the appearance of crossing-overs, mouse homologous chromosomes associate with each other by means of the synaptonemal complex (SC) in prophase of meiosis I. Mice lacking *Scp3*, an SC component, show less crossing-overs (Yuan et al., 2000). In such mice, cells enter meiosis not only with bivalents but instead with some mitosis-like chromosomes

(univalents). Another effect observed in the *scp3* knockout is bipolar attachment of these chromosomes already in meiosis I (Kouznetsova et al., 2007). The resulting meiosis I spindle is therefore partially reminiscent of meiosis II or mitosis. Although sister centromeres of the bioriented chromosomes are necessarily under tension, separation of sister chromatids is not observed in all cases when the corresponding oocytes progress through this abnormal meiosis I (Kouznetsova et al., 2007). It remains to be demonstrated that Sgo2 indeed persists at centromeres in meiosis I of *scp3*^{-/-} mice. Nevertheless, the work of Kouznetsova and colleagues strongly suggests that Sgo2 relocalization is suppressed by an as yet unknown mechanism during meiosis I. Further investigation of this idea could involve creation of a subtractive plasmid library representing transcripts present specifically in meiosis I and not in meiosis II with the subsequent screening of this library for factors artificially inhibiting sister chromatid separation in meiosis II.

In summary, centromeric tension is neither necessary nor sufficient for the redirection of Sgo2 from centromeres to kinetochores.

6. Materials and methods

If not indicated otherwise, companies are situated in Germany.

6.1. Materials

6.1.1. Hard- and software

This work was written on an "Apple MacBook5.2" (Apple Inc., Cupertino, CA, USA) using "Microsoft Word 2008" (Microsoft Corporation, Redmond, WA, USA). "Microsoft Excel 2008" (Microsoft Corporation, Redmond, WA, USA) as well as "OpenOffice" were used for generation of diagrams. Chemiluminescence signals of Western blots as well as Coomassie stained gels were digitized using an "LAS-4000" system (Fuji Film Europe, Düsseldorf). The image analysis software MultiGauge (Fuji Film Europe, Düsseldorf) was used to quantify chemiluminescence signals from immunoblots. X-Ray structure visualization was performed with "MacPyMol" (DeLano Scientific, Palo Alto, CA, USA). Image processing was performed with "Adobe Photoshop CS4" (Adobe Systems Inc., San Jose, CA, USA). Figures were generated using "Adobe Illustrator CS4" (Adobe Systems Inc., San Jose, CA, USA) and "Microsoft Powerpoint 2008" (Microsoft Corporation, Redmond, WA, USA). "DNASTAR Lasergene" (GATC Biotech, Konstanz) was used for analysis of DNA and protein sequences. Literature and database searches were done with electronic online services provided by the "National Center for Biotechnology Information" (<http://www.ncbi.nlm.nih.gov/>). A service of the European Bioinformatics Institute was used for sequence alignments ("EMBOSS Pairwise alignment" algorithm, <http://www.ebi.ac.uk/Tools/emboss/align/index.html>).

6.1.2. Protocols

The methods described in this section are based on standard techniques or follow the manufacturer's instructions. When protocols have been modified, detailed information is provided. For all methods, de-ionized sterile water and – when appropriate – sterile solutions and sterile flasks were used.

6.1.3. Chemicals and reagents

Unless otherwise noticed, chemicals and reagents (pro analysis grade) were purchased from AppliChem (Darmstadt), Biomol (Hamburg), Biorad (München), , Fermentas (St. Leon-Rot), Invitrogen (via Fisher Scientific, Schwerte), Merck/Calbiochem (Darmstadt),

New England Biolabs (NEB, Frankfurt a. M.), GE Healthcare (Munich), Promega (Mannheim), Roche Diagnostics (Mannheim), Roth (Karlsruhe), Serva (Heidelberg), Sigma-Aldrich (Steinheim), Millipore (Schwalbach) and Pierce/Fisher Scientific (Schwerte).

6.1.4. Antibodies

Antibodies and affinity matrices were as follows: sheep polyclonal anti-BubR1 (Kind gift from Steven S. Taylor, Manchester, UK) mouse monoclonal anti-Hec1 (Genetex, Irvine, CA, USA), mouse monoclonal anti-Myc (Clone 4A6, Millipore, Schwalbach), mouse monoclonal anti-Flag M2 (Sigma-Aldrich, Steinheim), rabbit polyclonal anti-Mad2 (Bethyl, Montgomery, TX, USA), mouse monoclonal anti-Mad2 (Santa Cruz Biotechnology, Santa Cruz, CA, USA), rabbit polyclonal anti-MCAK (kind gift from Thomas U. Mayer, Konstanz), rat polyclonal anti-PICH (kind gift from Erich A. Nigg, Basel, Switzerland), rabbit polyclonal anti-Sgo2 (Bethyl, Montgomery, TX, USA), mouse monoclonal anti- β -tubulin (Developmental Studies Hybridoma Bank, clone E7), unspecific rabbit (Bethyl, Montgomery, TX, USA) IgG (Sigma-Aldrich, Steinheim) and IgG sepharose (4 Fast Flow; GE Healthcare, Munich). Polyclonal goat anti-mouse-IgG, anti-sheep-IgG or anti-rabbit-IgG coupled to peroxidase (Sigma-Aldrich, Steinheim) were used as secondary antibodies in immunoblotting. Polyclonal goat anti-mouse-Cy3 and goat anti-rabbit-Alexa488 (Invitrogen/Fisher Scientific, Schwerte) were used for secondary detection in immunofluorescence.

6.1.5. DNA oligonucleotides

Primer	Sequence
5'Fse-hSgo1	5'-AATGGCCGGCCAGGCATGGCCAAGGAAAGATGCCT-3'
hSgo1-3'Asc	5'-TTAGGCGCGCCTCATTGTATTTGTTTCATACTTTTTTTAG-3'
5'Fse-Sgo2	5'-AATGGCCGGCCAGGCATGGAGTGCCAGTGATGGAAAC-3'
hSgo2-3'Asc	5'-TTAGGCGCGCCTCATCTTCTCATCTTGTCTCTGAGGCT-3'
hSgo2-N250-3'Asc	5'-AGATGGCGCGCCTCACATTAGAGAAGTCTTAGAACT-3'
hSgo2-N1066-3'Asc	5'-TACTGGCGCGCCTTACTCTCCTTCTTTTATTCTTCCAC-3'A
5'Fse-xSgo1	5'-ATAGGCCGGCCCGGCATGGTAAAGGAAAGATGCCCAAAGCA-3'
xSgo1-3'Asc	5'-TTAGGCGCGCCTCATCTGCGGCAGCCAACAAATACT-3'
xSgo1-100-3'Asc	5'- TTAGGCGCGCCCCGTAACATAAATAT-3'
xSgo1-101-5'Fse	5'-ATAGGCCGGCCCGGCCGAGGCTGCAGTCA-3'
xSgo1-200-3'Asc	5'- TTAGGCGCGCCTTTGTCTTTGAAATT-3'
xSgo1-201-5'Fse	5'- ATAGGCCGGCCCGGCGTGGTTTTGGAAGCC-3'
xSgo1-300-3'Asc	5'- TTAGGCGCGCCCGTCTGTCTACTTTTC-3'
xSgo1-301-5'Fse	5'- ATAGGCCGGCCCGAGAAATAGACAATGTTGA-3'
xSgo1-400-3'Asc	5'- TTAGGCGCGCCCATGAATTCAGGGAAGA-3'
xSgo1-401-5'Fse	5'- ATAGGCCGGCCCGGCGGAGATGCCTTTGAC-3'
xSgo1-500-3'Asc	5'- TTAGGCGCGCCTCTTGTAATTTTCTT-3'
xSgo1-501-5'Fse	5'- ATAGGCCGGCCCGCAACGGCTTGAAAAGG-3'

Hormad1-5'Fse	5'-AATGGCCGCGCCAATGGCCACTGCCCA-3'
Hormad1-3'Asc	5'-AATGGCGCGCCTTATATATGTTCCCTTGGTTCAC-3'
CK2beta-5'Fse	5'F-AATGGCCGCGCGATGAGCAGCTCAGAGGAGGTGT-3'A
CK2beta-3'Asc	5'F-TATGGCGCGCCTCAGCGAATCGTCTTGACTGGGCT-3'A
PP2A-B'delta-5'Fse	5'F-TAAGGCCGCGCCATGCCCTATAAACTGAAAAAGGAG-3'A
PP2A-B'delta-3'Asc	5'F-TTTGGCGCGCCTCAGAGAGCCTCCTGGCTG-3'A
hSgo2-R153A	5'-AGTGCAAGTTGATGGCTCTCCATTGCAAG-3'
hSgo2-N58I-S	5'-TATCTTTAAAGCACAAACATCAGGGCATTAGCTCA-3'
hSgo2-N58I-A	5'-TGAGCTAATGCCCTGATGTTGTGCTTTAAAGATA-3'
hSgo2-Yen#2res-S	5'-AGAAACTGAATTTTGAAGAATACGTTTCTTCGGCTTAAGCTAAA TAACTTGA-3'
hSgo2-Yen#2res-A	5'-TCAAGTTATTTAGCTTAAGCCGAAGAAACGTATTCTCAAATTC AGTTTCT-3'

6.1.6. Target sequences for dsRNA oligonucleotides

Target mRNA	siRNA target sequence
Sgo1	5'-CAGTAGAACCTGCTCAGAA-3'
Sgo2	5'-GAACACATTTCTTCGCCTATT-3'
Mad1	5'-CCAGCGGCTCAAGGAGTTTT-3'
Mad2	5'-GAGTCGGGACCACAGTTTATT-3'

6.1.7. Plasmids

Plasmid	Insert	Tag	Vector
pBM684	hSgo1	N-Flag ₃ -Tev ₂ -	pCS2
pBM720	hSgo1	N-Flag ₃ -Tev ₂ - - His ₆ FlagHis ₆ Flag-C	pCS2
pBM787	hSgo1	N-Gal4-AD-	pACT
pBM798	hSgo1 ¹⁻⁶⁶	N-Gal4-AD-	pACT
pBM799	hSgo1 ³⁴⁻¹⁰⁰	N-Gal4-AD-	pACT
pBM800	hSgo1 ⁶⁷⁻¹³³	N-Gal4-AD-	pACT
pBM801	hSgo1 ¹⁰¹⁻¹⁶⁶	N-Gal4-AD-	pACT
pBM802	hSgo1 ¹³⁴⁻²⁰⁰	N-Gal4-AD-	pACT
pBM803	hSgo1 ¹⁶⁷⁻²³³	N-Gal4-AD-	pACT
pBM804	hSgo1 ²⁰¹⁻²⁶⁶	N-Gal4-AD-	pACT
pBM805	hSgo1 ²³⁴⁻³⁰⁰	N-Gal4-AD-	pACT
pBM806	hSgo1 ³⁶⁷⁻³³³	N-Gal4-AD-	pACT
pBM807	hSgo1 ³⁰¹⁻³⁶⁶	N-Gal4-AD-	pACT
pBM808	hSgo1 ³³⁴⁻⁴⁰⁰	N-Gal4-AD-	pACT
pBM809	hSgo1 ³⁶⁷⁻⁴³³	N-Gal4-AD-	pACT
pBM810	hSgo1 ⁴⁰¹⁻⁴⁶⁶	N-Gal4-AD-	pACT
pBM811	hSgo1 ⁴³⁴⁻⁵⁰⁰	N-Gal4-AD-	pACT
pBM812	hSgo1 ⁴⁶⁷⁻⁵³³	N-Gal4-AD-	pACT
pBM813	hSgo1 ^{501-end}	N-Gal4-AD-	pACT
pBM815	xSgo1 ¹⁻¹⁰⁰	N-Gal4-AD-	pACT
pBM816	xSgo1 ¹⁰¹⁻²⁰⁰	N-Gal4-AD-	pACT
pBM817	xSgo1 ²⁰¹⁻³⁰⁰	N-Gal4-AD-	pACT
pBM818	xSgo1 ³⁰¹⁻⁴⁰⁰	N-Gal4-AD-	pACT
pBM819	xSgo1 ⁴⁰¹⁻⁵⁰⁰	N-Gal4-AD-	pACT
pBM820	xSgo1 ^{501-end}	N-Gal4-AD-	pACT
pMO937	xSgo1 ¹⁻²⁰⁷	N-MBP-	pMal
pBM794	hMad2 (Mad2L1)	N-Gal4-DBD-	pAS

pBM795	hMad2-D10	N-Gal4-DBD-	pAS
pBM995	hMad2	N-Myc ₆ -	pCS2
pBM1007	hMad2-D10	N-Myc ₆ -	pCS2
pBM940	hMad2-5xD	N-Myc ₆ -	pCS2
pBM942	hMad2-5xA	N-Myc ₆ -	pCS2
pMO1091	hMad2	N-HA3-	pCS2
pAS900	hMad2	N-His ₆ -	pQE80
pMO919	hMad2-D10	N-His ₆ -	pQE80
pAS899	hMad2-5xD	N-His ₆ -	pQE80
pAS902	hMad2-5xA	N-His ₆ -	pQE80
pBM1884	hCdc20 ¹¹¹⁻¹³⁸	N-GST-	pGex
pMO677	hp31	N-Flag ₃ -Tev ₂ -	pCS2
pEB1056	hCK2beta	N-HA ₃ -	pCS2
pEB1060	hCK2beta	N-Gal4-DBD-	pAS
pJH2112	hPP2A-B'delta	N-Flag ₃ -Tev ₂ -	pCS2
pBM911	hPP2A-B'delta	N-Gal4-DBD-	pAS
pMO1067	hSgo2	N-Flag ₃ -Tev ₂ -	pCS2
pBM1172	hSgo2	N-Myc ₆ -	pCS2
pBM1140	hSgo2-R153A	N-Flag ₃ -Tev ₂ -	pCS2
pBM1145	hSgo2-N58I	N-Flag ₃ -Tev ₂ -	pCS2
pBM1153	hSgo2 ¹⁻²⁵⁰	N-Flag ₃ -Tev ₂ -	pCS2
pJH2245	hSgo2 ¹⁻¹⁰⁶⁶ ; Yen#2 siRNA-res	N-Myc ₆ -	pCS2
pEB1134	hSgo2	N-Gal4-AD-	pACT
pAS1157	hSgo2 ¹⁻²⁵⁰	N-Gal4-AD-	pACT
pAS1158	hSgo2 ¹⁻²⁵⁰ -R153A	N-Gal4-AD-	pACT
pBM2222	-	-	pBOS SR-eGFP
pBM2223	hSgo2-wt; Yen#2 siRNA-res	-	pBOS SR-eGFP
pBM2224	hSgo2-R153A; Yen#2 siRNA-res	-	pBOS SR-eGFP
pBM2225	hSgo2-N58I; Yen#2 siRNA-res	-	pBOS SR-eGFP

Source: pBM – this study; others – Stemmann laboratory plasmid collection

6.2. Microbiological techniques

6.2.1. *E. coli* strains

XL-1 blue (Molecular cloning, plasmid production):

E. coli supE44 hsdR17 recA1 gyrA46 thi relA1 lac⁻ F'[proAB⁺ lacI^q Δ(lacZ)M15 Tn10(tet^r)] (Stratagene/Agilent Technologies, Santa Clara, CA, USA)

Rosetta 2 (Protein expression):

E. coli F⁻ ompT hsdSB(rB⁻ mB⁻) gal dcm pRARE2 (CamR) (Novagen/Merck, Darmstadt)

6.2.2. *E. coli* vectors

pGEX4T1 (GE Healthcare, Munich) with modified MCS (FseI/AscI sites inserted)
 pMal (New England Biolabs) with modified MCS (FseI/AscI sites inserted)
 pQE80 (Qiagen, Hilden) with modified MCS (FseI/AscI sites inserted)

6.2.3. *E. coli* media*LB medium*

1% (w/v) Tryptone (Difco, BD Bioscience, Heidelberg)
 0.5% (w/v) yeast extract (Difco, BD Bioscience, Heidelberg)
 1% NaCl (w/v)
 dissolved in ddH₂O and sterilized by autoclaving

LB agar

LB-medium with 1.5% agar (Roth, Karlsruhe)

6.2.4. Cultivation and storage of *E. coli*

E. coli strains were grown in LB medium by shaking at 200 rpm at 37°C, LB agar plates were incubated at 37°C. Antibiotics for selection of transformed bacteria were added to media at 100 µg/ml (ampicillin) and 30 µg/ml (kanamycin) final. Culture densities were determined by measuring the absorbance at a wavelength of 600 nm (OD₆₀₀). Cultures on agar plates were stored at 4°C for up to 30 days. For long term storage, liquid cultures were supplemented with glycerol to 20% final concentration, subsequently snap frozen and stored at -80°C.

6.2.5. Preparation of chemically competent *E. coli**Tbf1 buffer*

30 mM KAc
 50 mM MnCl₂
 100 mM KCl
 15% (v/v) glycerol
 pH adjusted to 5.8

Tbf2 buffer

10 mM MOPS-NaOH
 75 mM CaCl₂
 10 mM KCl
 15% (v/v) glycerol
 pH adjusted to 7.0

SOB medium

0.5% (w/v) NaCl
 0.5% (w/v) yeast extract
 2% (w/v) tryptone
 2.5 mM KCl
 pH 7.0 with NaOH
 dissolved in ddH₂O and sterilized by autoclaving

For preparation of chemically competent bacteria, 300 ml SOB medium was inoculated with 4 ml of an overnight culture derived from a single *E. coli* colony and grown at 37°C to an OD₆₀₀ of 0.5.

After chilling the culture flask on ice for 15 min, cells were harvested by centrifugation (4°C, 3,000 g, 15 min). All following steps were performed with prechilled sterile materials and solutions at 4°C. Sedimented bacteria were carefully resuspended in 90 ml Tbf1 buffer and chilled on ice for 15 min (XL-1 blue) or 45 min (Rosetta 2). After a second centrifugation (4°C, 1500 g, 15 min), bacteria were resuspended in 15 ml Tbf2 buffer and chilled on ice for 5 min. Finally, the suspension of bacteria was aliquoted, snap-frozen and stored at -80°C.

6.2.6. Transformation of plasmid DNA into chemically competent *E. coli*

Chemically competent bacteria were thawed on ice. For chemical transformation, 50 µl of competent bacteria were mixed with 1 µl of plasmid DNA or 5 µl ligation reaction and incubated on ice for 30 min. A heat shock at 42°C was performed for 45 s. Subsequently, the cell suspension was incubated on ice for 2 min and after addition of 1 ml SOB medium without antibiotics incubated on a shaker at 37°C for 45 min. After recovery, transformed cells were selected by streaking out the bacteria suspension on LB agar plates containing the respective antibiotic(s) and incubated overnight at 37°C.

6.2.7. Expression of proteins in *E. coli*

For expression of recombinant proteins, the *E. coli* strain Rosetta 2 (Novagen/Merck, Darmstadt) was used. LB medium was inoculated with a dilution of 1:100 of an overnight culture from a freshly transformed colony. Besides the appropriate selection conditions for the transformed plasmid, chloramphenicol was used to prevent loss of pRARE2 encoding for low abundance tRNAs. In the case of MBP-tagged constructs, glucose was added to a final concentration of 0.2% (w/v) to suppress amylase expression. The culture was grown at 37°C and expression of protein(s) was induced by addition of IPTG (1 mM final concentration) at an OD₆₀₀ of 0.5 - 0.7. After shaking for 2 h at 37°C, cells were cooled on ice and subsequently harvested by centrifugation (4°C, 5,000 g, 10 min). Pellets were either processed directly or stored at -80°C after snap-freezing.

6.2.8. *S. cerevisiae* strain

PJ69-4A: *MATa trp-901 leu2-3,112 ura3-52 his3-200 gal4Δ gal80Δ LYS2::GAL1-HIS3 GAL2-ADE2 met2::Gal7-lacZ* (James et al., 1996)

6.2.9. Yeast media

YPD medium

1% (w/v) yeast extract (Difco, BD Bioscience, Heidelberg)

2% (w/v) Bacto Peptone (Difco, BD Bioscience, Heidelberg)

The solution was autoclaved and subsequently supplemented with sterile filtered glucose solution to a final concentration of 2% (w/v) glucose.

Amino acid supplement

Amino acid supplement was used for the preparation of SC medium. An amino acid mixture was prepared using the following quantities: 2.0 g adenine hemisulfate, 2.0 g arginine-HCl, 2.0 g histidine-HCl, 2.0 g isoleucine, 2.0 g leucine, 2.0 g lysine-HCl, 2.0 g methionine, 3.0 g phenylalanine, 2.0 g serine, 2.0 g threonine, 3.0 g tryptophan, 2.0 g tyrosine, 1.2 g uracil, 9.0 g valine. To ensure homogeneity, the mixture was mechanically inverted over night.

Synthetic complete (SC) medium

0.65% (w/v) yeast nitrogen base

2% (w/v) glucose

0.083% amino acid supplement

The pH was set to 5.6 and the solution subsequently autoclaved. To prepare dropout medium for plasmid selection in auxotrophic yeast strains, the respective amino acids were omitted from the supplement mixture. SC agar plates were made by addition of 2% (w/v) Bacto agar (Difco, BD Bioscience, Heidelberg) before autoclaving. Approx. 25 ml of agar containing SC medium were poured on a 10 cm plastic dish (Greiner Bio-One, Kremsmünster, Austria).

6.2.10. Yeast vectors

pAS, pACT (Clontech, BD Biosciences, Heidelberg) with modified MCS (FseI and AscI site inserted)

6.2.11. Preparation of chemically competent *S. cerevisiae*

SORB solution

0.1 M lithium acetate

10 mM Tris-HCl pH 8.0

1 mM EDTA

1 M sorbitol

(0.2 µm sterile filtered)

50 ml of YPD were inoculated with an overnight culture of the yeast strain PJ69-4A to achieve an OD₆₀₀ of 0.1. The culture was shaken at 30°C until it reached an OD₆₀₀ of 0.5. Cells were harvested by centrifugation at 1,000 g and washed once with 25 ml sterile

ddH₂O. The pellet was resuspended in 1 ml of SORB solution and transferred to a 1.5 ml reaction tube. After centrifugation at 1,000 g for 3 min, the cells were resuspended in 360 µl SORB solution. As a carrier for transformation, 40 µl of salmon sperm DNA (10 mg/ml; Invitrogen/Fisher Scientific, Schwerte) were heated to 95°C for 10 min, quickly cooled on ice and finally mixed with the cell suspension. The now competent yeast cells were stored for up to 2 h on ice.

6.2.12. Plasmid transformation in *S. cerevisiae*

PEG solution

0.1 M lithium acetate
10 mM Tris-HCl pH 8.0
1 mM EDTA
40% (w/v) polyethylene glycol PEG-3350
(0.2 µm sterile filtered)

10 µl of chemically competent yeast cells were mixed with 1 µl plasmid DNA (250 ng/µl) and 65 µl PEG solution in a sterile 1.5 ml reaction tube. The contents were mixed by vortexing at maximum speed for 5 s and incubated at room temperature for 25 min followed by a heat shock at 42°C for 10 min. The cells were centrifuged at 1,000 g 3 times for 1 min. Between centrifugation steps, the tubes were turned 180° in the rotor to facilitate sedimentation of the yeast cells in the viscous liquid. The supernatant was discarded, the pellet resuspended in 100 µl of water and finally plated onto SC dropout agar plates. Leucine and tryptophan auxotrophy were used to select for transformants.

6.2.13. Yeast-2-Hybrid assay

Yeast-2-Hybrid assays were used to study protein-protein interactions. The system exploits the fact that the yeast transcription factor Gal4p can be split into two separate domains, the DNA binding domain (DBD) and the transactivation domain (AD). If the two fragments are brought into close proximity, they reconstitute a functional Gal4 transcription factor. To test protein-protein interaction, the coding sequences of the two candidates were cloned into the vectors pAS (DBD-fusion) and pACT (AD-fusion) and transformed into the yeast strain PJ69-4A. This strain is devoid of the endogenous Gal4 transcription factor. In addition, one of the genes required for histidine biosynthesis is expressed under the control of a GAL promoter. Cells are only able to survive on SC-His medium if they are two plasmids encoding fusion proteins that interact physically. Since certain AD or DBD fusion proteins show Gal4-like activity on their own ("auto-

activation"), control transformations are required. For that reason, the respective fusion construct was tested in combination with the complementary empty vector.

6.2.14. Preparation of denatured cell extracts from *S. cerevisiae*

HU buffer

8 M urea

5% SDS

200 mM Tris-HCl pH 6.8

1 mM EDTA

A few crystals bromophenol blue

100 mM DTT (added immediately before use)

Cells from a yeast culture (equivalent to 1 ml at OD₆₀₀=1) were harvested by centrifugation (1,000 g, 2 min), resuspended in 1 ml cold ddH₂O, and lysed with 150 µl 1.85 M NaOH / 7.5% β-Mercaptoethanol. After incubation for 15' on ice, the proteins were precipitated by addition of 150 µl 55% trichloroacetic acid (TCA) for 10 min, and centrifuged for 10 min at 4°C, 16,000 g. The pellet was resuspended in 100 µl HU-buffer with freshly added DTT (from 1 M stock, 1/10 volume). The samples were heated to 65°C for 10 min before loading on SDS-PAGE gels,.

6.3. Molecular biological methods

6.3.1. Isolation of plasmid DNA from *E. coli*

3ml of LB medium containing the appropriate antibiotic was inoculated with a single *E. coli* colony harboring the DNA plasmid of interest and shaken for 8-14 h at 37°C. Plasmid-DNA was purified via alkaline lysis of the bacteria and subsequent isolation by anion exchange columns according to the manufacturer's instructions (Qiagen (Hilden) Plasmid Purification Handbook, Plasmid Mini Preparation for up to 20 µg DNA). Larger amounts of DNA for transfection of human cells were isolated from a 250 ml overnight culture according to the manufacturer's protocol (Qiagen (Hilden) Plasmid Purification Handbook, Plasmid Maxi Preparation for up to 1 mg DNA).

6.3.2. Determination of DNA/RNA concentration in solution

DNA or RNA concentrations were determined by measuring the absorbance at a wavelength of 260 nm (OD₂₆₀) with a ND-1000 Spectrophotometer (Peqlab, Erlangen). An OD₂₆₀=1 equals a concentration of either 50 µg/ml double-stranded DNA or 40 µg/ml RNA.

6.3.3. Restriction digestion of DNA

Sequence-specific cleavage of DNA with restriction enzymes was performed according to standard protocols (Sambrook and Russell, 2001) and the instructions of the manufacturer (New England Biolabs, NEB, Frankfurt a. M.). Usually, 5-10 units of restriction enzyme were used for digestion of 1 µg DNA. Reaction samples were incubated in appropriate buffer at the recommended temperature for 30 min to 1 h. Restriction digestion was then stopped by addition of DNA loading buffer.

6.3.4. Dephosphorylation of DNA fragments

To avoid religation of linearized vectors, the 5' end of vector DNA was dephosphorylated by adding 0.1 units of shrimp alkaline phosphatase and the appropriate buffer concentrate (Roche, Mannheim) followed by incubation for 1 h at 37°C. Finally, shrimp alkaline phosphatase was heat-inactivated at for 20 min at 72°C.

6.3.5. Separation of DNA fragments by gel electrophoresis

TBE buffer

90 mM Tris base
90 mM Boric acid
2.5 mM EDTA

DNA loading buffer (5x)

0.5% SDS
0.25% Orange G
25% Glycerol
25mM EDTA (pH 8,0)

For analysis or preparative isolation, DNA fragments were electrophoretically separated on agarose gels (0.8-2.0% of agarose in TPE) containing ethidium bromide (0.5 µg/ml final concentration). DNA samples were mixed with DNA loading buffer and separated at 100 V in TBE buffer. DNA fragments could be visualized by intercalation of ethidium bromide into DNA by using a UV transilluminator (324 nm). The size of the fragments was estimated by standard size markers (O'GeneRuler 1 kb or 100 bp DNALadder, Fermentas, St. Leon-Rot).

6.3.6. Isolation of DNA from agarose gels

After gel electrophoresis DNA fragments were isolated by excising the respective piece of agarose using a scalpel. DNA was extracted from the gel slice using QiaExII Gel Extraction kit (Qiagen, Hilden) according to manufacturer's instructions and eluted with 30 µl TE buffer (5 mM Tris-HCl pH 8.0, 1 mM EDTA).

6.3.7. Ligation of DNA fragments

Amounts of isolated DNA fragments ("insert") and linearized vectors were estimated on an ethidium bromide-containing agarose gel. For a ligation reaction an approximate molar ratio of 1:3 of vector to insert was used. The reaction sample with a total volume of 10 µl usually contained 50 ng of vector DNA and 4 U of T4 DNA Ligase (Fermentas, St. Leon-Rot) and was incubated for 1 h at RT in the appropriate reaction buffer (Fermentas, St. Leon-Rot). Following heat inactivation for 10 min at 72°C 5 µl of the ligation reaction were transformed into 50 µl chemically competent XL1-Blue cells.

6.3.8. Sequencing of DNA

Sequencing PCR and sample preparation were performed with the DYEnamic ET Terminator Cycle Sequencing Premix kit according to the manufacturer's instructions (GE Healthcare, Munich). One sample usually contained 1 µg of plasmid DNA and 20 pmol of primer. DNA sequencing was carried out by the core facility of the MPI for biochemistry (Martinsried) with an Abi-Prism 377 sequencer (Perkin Elmer) or by an external commercial provider (SeqLab, Göttingen).

6.3.9. Site-directed mutagenesis of DNA

First approach

Site directed mutagenesis was performed using a fusion PCR based approach using two reverse complementary oligos harboring the desired mutation(s). In two separate PCR reactions each oligo was used to create an upstream and a downstream fragment, respectively. The outer primers were designed to terminate at useful restriction sites. After gel purification the two products were combined and fused in a PCR reaction with the two outer primers. The resulting fragments were restriction cloned into the respective wild-type sequence. Verification was done by sequencing.

Second approach

Specific point mutations in gene sequences were inserted by the GeneEditor *in vitro* site-directed mutagenesis system (Promega, Mannheim) according to the manufacturer's instructions. The underlying principle is the use of two oligonucleotides, one containing the desired point mutation and the other one introducing a mutation into the *AmpR* gene leading to resistance against the "GeneEditor" antibiotic. After denaturation of the plasmid of interest, both oligos were allowed to anneal and the second strand was

completed by PCR. Subsequently, the double stranded plasmid was transformed into bacteria that were then selected on “GeneEditor” antibiotic containing agar plates. Introduced mutations were verified by sequencing.

6.3.10. Polymerase chain reaction (PCR)

PCR reactions were performed in a final volume of 20 µl with 2.5 µl each of forward and reverse oligonucleotide primer (10 µM each), 5 µl deoxyribonucleotide mix (each 10 mM, NEB, Frankfurt a. M.) and 0.3 µl of DNA polymerase (Phusion, Finnzymes, Espoo, Finland) in the corresponding PCR buffer (Phusion HF or GC buffer, Finnzymes). As a template, either 20 ng of plasmid DNA or 2 µl of cDNA library (thymus, testis; BD Bioscience, Heidelberg) were used. Alternatively, self-made first-round cDNA derived by RT-PCR served as PCR template. Amplification was carried out in a TC-512 temperature cycler (Techne, Burlington, NJ, USA). The denaturing step was done at 98°C for 12 s, elongation time was 30 s/kbp and annealing temperature were optimized for the individual primer pairs.

6.3.11. Reverse transcription (RT)-PCRs

Total RNA was isolated from HeLa cells using a spin column kit (Qiagen, Hilden). Reverse transcription was carried out in a total volume of 20 µl by incubation of 50 - 100 ng of total HeLa RNA with 1 µl of M-MuLV Reverse Transcriptase (200 U/µl, Fermentas, St. Leon-Rot), 2 µl Oligo(dT) primer (10 µM), 2 µl of deoxynucleotide mix (10 mM each, NEB, Frankfurt a. M.), 0.5 µl of RNasin (Promega, Mannheim) and in the corresponding M-MuLV buffer (Fermentas, St. Leon-Rot). The reaction mix was incubated for 1 h at 42°C. Subsequently, 2 µl were used as template (instead of plasmid DNA) in a PCR carried out as described above.

6.4. Protein methods

6.4.1. SDS-polyacrylamide gel electrophoresis (SDS-PAGE)

7x Bis-Tris/HCl

2.5 M Bis-Tris

1.5 M HCl

adjusted to pH 6.5

6% gel solution
 42.2 ml H₂O
 13 ml 30% acrylamide; 0.8%
 bisacrylamide
 9.3 ml 7x Bis-Tris/HCl
 163 µl 20% SDS (w/v)
 54.2 µl TEMED
 325 µl 10% APS (w/v)

Sample buffer (4x)
 40% glycerol
 564 mM Tris base
 424 mM HCl
 8% SDS
 2.04 mM EDTA/NaOH
 0.88 mM Coomassie G250
 0.7 mM Phenol red
 2 M beta-mercaptoethanol

15% gel solution
 16.5 ml H₂O
 4.6 ml 2,5 M sucrose
 30 ml 30% acrylamide; 0.8%
 bisacrylamide
 8.6 ml 7x Bis-Tris/HCl
 150 µl 20% SDS
 25 µl TEMED
 300 µl 10% APS

MOPS running buffer
 50 mM MOPS
 1 mM EDTA
 0.1% SDS
 50 mM Tris base

For the separation of proteins under denaturing conditions, SDS-PAGE was performed with the NuPAGE system (Adapted from Invitrogen/Fisher Scientific, Schwerte). 6-15% gradient gels were poured with a gradient mixer using pre-cooled 6% and 15% gel solutions. Prior to loading, protein samples were mixed with sample buffer and denatured at 95°C for 5 min. As a molecular weight standard, PageRuler Prestained Protein Ladder (Fermentas, St. Leon-Rot) was used. Alternatively, commercially available neutral gradient gels (Serva, Heidelberg) were used. Electrophoresis of NuPAGE and Serva gels was carried out at 40 mA in MOPS buffer and at 25 mA Laemmli running buffer, respectively.

6.4.2. Immunoblotting

Blotting buffer
 25 mM Tris
 192 mM Glycine
 15% Methanol
 0.01% SDS

TBS-w
 25 mM Tris, pH 7.5
 137 mM NaCl
 2.6 mM KCl
 0.05% Tween-20 (v/v)

After separation via SDS-PAGE, proteins were transferred electrophoretically to a polyvinylidene fluoride (PVDF) blotting membrane (Immobilon P, Millipore,

Schwalbach). For that purpose a sandwich consisting of gel and membrane covered with blotting paper and sponges on both sides was assembled in a wet blotting apparatus (XCell II, Invitrogen/Fisher Scientific, Schwerte). Sandwich assembly was done submerged in blotting buffer. The hydrophobic PVDF membrane was made accessible for the aqueous blotting buffer by a brief incubation in 100% methanol. Transfer was done at constant voltage of 25 V for 80 min at 10 - 15°C.

The membrane was blocked for unspecific binding with 5% skim milk and 1% BSA in TBS-w for 20 min at RT. This was followed by incubation in primary antibody diluted in RotiBlock (Roth, Karlsruhe) either at RT for 1 h or at 4°C o/n. The membrane was then rinsed twice briefly with TBS-w and washed two times with TBS-w for 10 min each. After incubation with secondary horse radish peroxidase (HRP) coupled antibody the membrane was washed in TBS-w for a total of 45 min with at least 5 exchanges of buffer. Detection was carried out using the chemiluminescence protocol provided with the kit (ECL, GE Healthcare, Munich) and a LAS-4000 camera system (Fuji).

6.4.3. Coomassie staining

Colloidal Coomassie suspension: to prepare the staining solution, 80 g $(\text{NH}_4)_2\text{SO}_4$ were dissolved in 760 ml ddH₂O. Then 18.8 ml 85% phosphoric acid were added. In a second vessel, 800 mg Coomassie Brilliant Blue G-250 were dissolved in 16 ml ddH₂O. Subsequently, the two solutions were combined while stirring with a magnetic stir bar. For Coomassie staining, gels were incubated in freshly mixed 80% (v/v) colloidal Coomassie stain with 20% (v/v) Methanol after SDS-PAGE for either 4 h or over night. To remove unspecific stain, gels were repeatedly washed with deionized water for 1 to 2 days. For long-term storage, Coomassie-stained gels were dried on a whatman paper in a "GD2000" slab gel dryer (Hoefler, Holliston, MA, USA).

6.4.4. Purification of proteins - common buffers and steps

Lysis Buffer

537 mM NaCl
2.7 mM KCl
8 mM Na₂HPO₄
1.4 mM KH₂PO₄ (pH 7.4)

Dialysis Buffer

10 mM Tris-HCl pH 8.0
100 mM NaCl
0.5 mM EDTA
1 mM DTT

Protein expression was done as described in chapter 6.2.7. A bacterial pellet obtained from 1 l of *E. coli* culture was resuspended in 35 ml of ice cold Lysis Buffer. Cells were lysed in a high pressure homogenizer (Avestin, Ottawa, Canada) by cycling the cell

suspension for 10 min. The lysate was cleared from debris by centrifugation in an JA-25.50 rotor (Beckman Coulter, Krefeld) at 25,000 g for 30 min.

6.4.5. Amylose affinity purification of maltose binding protein (MBP)-tagged proteins

Amylose affinity purification was used to purify MBP-tagged protein fusions of N-terminal *X. laevis* Sgo1 fragments (xSgo1¹⁻²⁰⁷; expression plasmid: pMal). Quite similarly, a short fragment of human Cdc20 was expressed with an N-terminal GST-tag (hCdc20¹¹¹⁻¹³⁸; expression plasmid pGEX-4T1). Lysate obtained from 1 l equivalent of expression culture (see chapter 6.4.4) was incubated with 2 ml of amylose resin (MBP-tag, NEB, Frankfurt a. M.) or 1 ml of glutathion sepharose (GST-tag, GE Healthcare, Munich) for 4 h at 4°C on a rocking and rotating mixer. After centrifugation for 5 min at 400 g, the bead pellet was resuspended in 10 ml of lysis buffer. The suspension was transferred to a 20 ml column (Biorad, München). When nearly drained, the resin bed was washed extensively with a total of 100 ml of lysis buffer. Finally, the beads were eluted with 2 ml of lysis buffer supplemented with 50 mM maltose (MBP-tag) or 50 mM Glutathion (GST-tag). The purified protein solution was dialyzed 4 times against dialysis buffer (4°C, 500 ml each, 24 h in total). Aliquots were snap-frozen using liquid nitrogen.

6.4.6. Ni²⁺-NTA affinity purification of 6x-Histidine-tagged proteins

Wash Buffer

50 mM Hepes KOH, pH 7.0
100 mM NaCl
15 mM imidazole
5 mM 2-mercaptoethanol
0.1% Tween-20

Elution Buffer

50 mM Hepes KOH, pH 7.0
100 mM NaCl
200 mM imidazole
5 mM 2-mercaptoethanol
0.1% Tween-20

Ni²⁺-NTA affinity purification was used to isolate recombinant His₆-tagged Mad2 from *E. coli* lysates (prepared as described in chapter 6.4.4). Lysate derived from 1 l of expression culture was incubated with 500 µl of Ni²⁺-NTA resin (Qiagen, Hilden) for 2 h at 4°C with gentle shaking. Beads were washed once with 10 ml of wash buffer and transferred to a 20 ml column (Biorad, München). After extensive washing with 100 ml of wash buffer, bound protein was eluted using 4 times 1 ml of elution buffer. Protein containing fractions were pooled and dialyzed 4 times against 500 ml each of dialysis buffer. Purified protein was aliquoted, snap-frozen using liquid nitrogen and subsequently stored at -80°C.

6.4.7. Coupled *in vitro* transcription/translation

In vitro transcription/translation in reticulocyte lysate supplemented with SP6 RNA polymerase was carried out using "TNT Quick Coupled Transcription/Translation System" (Promega, Mannheim). For a single reaction, 20 µl TNT Quick Master Mix, 1 µl of pCS2 plasmid DNA (500 ng/µl), 1 µl of [³⁵S]methionine and 3 µl of RNase free water were combined and incubated for 90 min at 30°C.

6.4.8. *In vitro* pulldown assay

Buffer DP1

10 mM Tris-HCl pH 8.0
100 mM NaCl
0.5 mM EDTA
0.01% Triton X-100

In order to test direct protein-protein interactions, *in vitro* pulldown assays were performed using recombinant purified proteins. One of the candidates was immobilized via its affinity tag to an appropriate matrix in a final volume of 100 µl DP1 for 1 h at 4°C. Beads were then incubated with the putative binding partner as indicated. Beads devoid of immobilized bait served as negative control. At least 5 washing steps with 1 ml each of DP1 were followed by elution using SDS-PAGE sample buffer. Eluates were subjected to SDS-PAGE and Coomassie staining.

6.4.9. Phosphatase activity assay

Phosphatase assays were performed using a Ser-/Thr-Phosphatase assay kit (Millipore, Schwalbach) essentially following the manufacturers instructions. Briefly, phosphatase activity was measured by dephosphorylation of a phosphopeptide substrate and subsequent detection of liberated inorganic phosphate by the malachite green method.

6.4.10. Lambda phosphatase treatment

This method was used to determine whether differential migration behavior of proteins in SDS-PAGE was caused by phosphorylation. For each sample approx. 10⁵ cells were lysed by repeated pipetting on ice in 75 µl LP2+ (see chapter 6.5.8, omitting NaF and beta-glycerophosphate). MnCl₂ was set to a final concentration of 2 mM. To each sample 400 U Lambda phosphatase (NEB, Frankfurt a. M.) were added and the samples were incubated for 30 min at 30°C. This was followed by addition of 25 µl SDS-PAGE sample buffer, 5 min boiling at 95°C and SDS-PAGE/immunoblotting.

6.5. Cell biological methods

6.5.1. Mammalian cell lines

293T	Human embryonic kidney cell line transformed SV40 and adeno viral sequences (e.g. t antigens)
HeLa	Human cervix epithelial adenocarcinoma
HeLaS3	HeLa cells adapted to culture in suspension

6.5.2. Vectors for cell culture

pCS2	(Turner and Weintraub, 1994) with modified MCS (FseI, AscI sites introduced)
pBOS-SReGFP	the H2B-GFP coding sequence of pBOS-H2B-GFP (BD Bioscience, Heidelberg) was replaced by a linker containing FseI and AscI restriction endonuclease cleavage sites. An additional FseI restriction site had been deleted from the vector. Furthermore, the eGFP open reading frame was placed under the control of a separate pSRalpha promoter present in the vector sequence.

6.5.3. Cultivation of mammalian cells

PBS

137 mM	NaCl
2.7 mM	KCl
8 mM	Na ₂ HPO ₄
1.4 mM	KH ₂ PO ₄ , pH 7.4

HeLa and 293T cells were cultured in Dulbecco's Modified Eagle Medium (DMEM, PAA, Pasching, Austria). Media were supplemented with 10% heat inactivated (56°C, 30 min) fetal bovine serum (Biochrom, Berlin), 100 units/ml penicillin and 0.1 mg/ml streptomycin (PAA, Pasching, Austria). Monolayer cultures were grown in cell culture dishes (Greiner Bio-One, Kremsmünster, Austria) at 37°C in a 5% CO₂ atmosphere and were split at a ratio of 1:4 to 1:8 twice a week. To split cells, medium was removed, cells were washed once with PBS and subsequently incubated with 16 µl/cm² Trypsin/EDTA solution (PAA, Pasching, Austria) at 37°C for 1 min (293T cells) or 5 min (Hela cells). By repeated pipetting in fresh medium, cells were detached from each other as well as from the culture dish. Subsequently, the cell suspension was diluted in medium and distributed on new cell culture dishes. Cell concentrations of suspensions were determined with a Vi-Cell counter (Beckman Coulter, Krefeld).

6.5.4. Storage of mammalian cells

Cells were harvested at 80% confluence by trypsination as described above, resuspended in freezing medium (10% DMSO, 90% fetal bovine serum, Biochrom, Berlin), and

aliquoted in cryovials (Nalgene). The cell suspension was then slowly frozen in a cardboard box at -80°C . For long-term storage cryo vials were transferred to a liquid nitrogen tank.

Cryo-stocks were rapidly thawed in a 37°C water bath. To remove DMSO, tubes were briefly centrifuged (300 g, 2 min). The supernatant was discarded and the cell pellet resuspended in DMEM (PAA, Pasching, Austria) and transferred to an appropriate cell culture dish containing DMEM (PAA, Pasching, Austria).

6.5.5. Transfection of 293T cells

2x HBS (50 ml)

800 mg NaCl

37 mg KCl

10.65 mg Na_2HPO_4

100 mg Glucose

500 mg HEPES

pH 7.05 adjusted with NaOH, sterile filtered (0.2 μm pore size)

293T cells were transfected by the calcium phosphate method. $3 \cdot 10^6$ cells per cell culture dish (\varnothing 10 cm) were spread and grown overnight. Shortly before transfection the next day, chloroquin was added to the medium to a final concentration of 20 μM . For one transfection mix, 5-20 μg (depending on the construct) of plasmid DNA were mixed first with 680 μl water and then with 99.2 μl sterile 2 M CaCl_2 . Then 800 μl of 2x HBS solution were slowly added in small drops while gently vortexing. After incubation for 10 min at RT, the transfection mix was dropped onto the medium of the prepared cells. 12 h later medium was exchanged. 24 h after transfection, nocodazole was added to the medium at a final concentration of 0.2 $\mu\text{g}/\text{ml}$ to arrest cells in mitosis (unless interphase samples were prepared). 36 h after transfection, cells were harvested by rinsing the plate with the used cell culture medium. Following centrifugation (300 g, 3 min) cell pellets were washed once with PBS. Cell pellets were subsequently either lysed directly or snap frozen in liquid nitrogen and stored at -80°C for further use.

6.5.6. Transfection of HeLa cells

HeLa cells were transfected based on nucleic acid packaging into liposomes formed by cationic lipids. Commercial transfection reagents were Lipofectamine 2000 (Invitrogen/Fisher Scientific, Schwerte) for plasmid DNA and Lipofectamine RNAi-Max or Oligofectamine (Invitrogen/Fisher Scientific, Schwerte) for transfection of double stranded RNA (siRNAs). Transfections were carried out according to the manufacturers

instructions. In the case of Lipofectamine 2000 a 1:2 ratio for DNA(μ g):Lipofectamine(μ l) was used.

6.5.7. Synchronization of mammalian cells

Synchronization at the G1/S boundary: thymidine was used to interfere with the cellular nucleotide metabolism and to block DNA replication. 2 mM Thymidine (Sigma-Aldrich, Steinheim) was added to the culture medium for 16 h. Cells were then released from the block by washing twice with medium followed by a 30 min incubation in the cell culture incubator and another medium change. In the case of a double thymidine block, 2 mM thymidine was readded 7 h after the release. 16 h later cells were released as described above.

Synchronization in prometaphase: nocodazole was used to disrupt the microtubule cytoskeleton. 0.2 ng/ml nocodazole were added either to an asynchronous cell population for 12-16 h or 6 h after release from thymidine block for another 8 h.

6.5.8. Co-Immuno-Precipitation (Co-I.P.) experiments from transfected 293T cells

LP2

20 mM Tris-HCl, pH7.6
100 mM NaCl
10 mM NaF
20 mM beta-glycerophosphate
5 mM MgCl₂
0.1% Triton X-100
5% glycerol

LP2+

supplemented with 1x protease inhibitor cocktail (Roche, Mannheim) and 1 mM PMSF

Cells were harvested by scraping from a 10 cm cell culture dish. After centrifugation for 2 min at 400 g at RT, cells were washed once with 1x PBS (see chapter 6.5.3) and centrifuged again. From here on all steps were carried out either on ice or in at 4°C. The cell pellets were resuspended in 500 μ l LP2+ and lysed with 14 strokes with a "tight" pestle in a glass dounce homogenizer (Wheaton, Millville, NJ, USA). Lysates were centrifuged at 16,000 g for 25 min and the supernatant was transferred to a new tube. An input sample of 20 μ l was mixed with 40 μ l 2x SDS-PAGE sample buffer. Subsequently 10 μ l of the appropriate affinity matrix were washed twice with 1 ml LP2 and combined with the lysates. The suspensions were incubated on a turning wheel for 2 h. Next the samples were centrifuged briefly in a tabletop micro-centrifuge and the pelleted beads

were washed 6 times with 1 ml LP2. Subsequently, the pellet was resuspended in 250 μ l LP2 and transferred to a Mobicol microcolumn (Mobitec, Göttingen). The column was allowed to drain, capped at the bottom and proteins bound to the beads were eluted by gentle shaking with 35 μ l of 2x SDS-PAGE sample buffer (without beta-mercaptoethanol) at 85°C for 5 min. The bottom plug was removed and the eluate centrifuged into a 1.5 ml reaction tube at 200 g for 1 min. Samples were mixed with 0.2 μ l beta-mercaptoethanol and finally incubated for 5 min at 95°C.

6.5.9. Co-I.P. experiments of endogenous proteins

Co-I.P.s of endogenous proteins were carried out essentially as for overexpressed proteins. Approximately 2 μ g of specific antibodies were coupled to 10 μ l of Protein G Sepharose (GE Healthcare, Munich) beads in 50 μ l PBS (see chapter 6.5.3). For that purpose, the bead suspension was incubated at 4°C over night with gentle agitation. Cells from confluent 150-750 cm² of culture dishes were lysed in 1-5 ml LP2 and cleared by centrifugation. The supernatant was incubated with the prepared antibody beads for 4 h at 4°C. Protein G Sepharose coupled non-specific IgG served as negative controls. After washing 6 times with LP2, bound proteins were eluted with 35 μ l 2x SDS-PAGE sample buffer (with beta-mercaptoethanol).

6.5.10. Competitive elution

TBS

50 mM Tris-HCl pH 7.5

137 mM NaCl

2.7 mM KCl

A competitive approach was used for elution of native Flag-tagged proteins bound to anti-Flag agarose. Beads from an I.P. experiment as described in 6.5.8 were washed with TBS. Elution buffer was prepared by dissolving 15 μ g of Flag₃ peptide (Sigma-Aldrich, Steinheim) in 100 μ l of TBS. Beads were mixed with 30 μ l of elution buffer and incubated for 45 min at 4°C with gentle agitation. The supernatant was either used directly or aliquoted and snapfrozen using liquid nitrogen. Samples were then stored in a -80°C freezer.

6.5.11. Elution by TEV protease cleavage

TEV protease cleavage was used for native elution of proteins carrying a Flag₃-Tev₂ tag from anti-Flag agarose beads. At the same time, the untagged proteins could be obtained.

Beads derived from an I.P. experiment (6.5.8) were washed twice with TBS (see 6.5.10). TEV-Elution buffer was prepared by mixing 1 part of His₆-tagged TEV protease (12,000 U/ml, Core facility, MPI Martinsried) with 5 parts of TBS. Beads carrying Flag₃-Tev₂-tagged proteins were incubated with 20 µl of TEV-elution buffer for 1 h at 18°C with gentle agitation. The supernatant was then used for further experiments (for example phosphatase assay, see chapter 6.4.9).

6.5.12. Plasmid transfection of HeLa cells

Plasmid DNA was transfected using the commercial cationic lipid reagent Lipofectamine 2000 (Invitrogen/Fisher Scientific, Schwerte). The amounts given here refer to the transfection of one well of a 12-well plate. On the day prior to transfection cells were seeded at a density of $3.5 \cdot 10^5$ cells/ml in DMEM (PAA, Pasching, Austria) with fetal bovine serum (Biochrom, Berlin) but without antibiotics. 1 ml of cell suspension was plated per well. Transfection mixes were prepared in two steps. First, 1.6 µg of DNA was diluted in 100 µl OptiMEM (Invitrogen/Fisher Scientific, Schwerte). In a separate tube, 3.2 µl of Lipofectamine 2000 were mixed well with 100 µl of OptiMEM by flicking the tube 20 times. After a 10 min incubation, the DNA solution was pipetted to the Lipofectamine solution and mixed well. Following another incubation for 20 min, the transfection mix was added to the cells. To limit cytotoxicity, medium had to be changed after 6 h, again using antibiotics-free medium.

6.5.13. siRNA transfection of HeLa cells

Transfection of dsRNAs for RNAi experiments was done with Lipofectamine RNAiMax (Invitrogen/Fisher Scientific, Schwerte). Amounts are given for transfection of one well of a 12-well plate. First, two tubes were prepared containing 100 µl of OptiMEM (Invitrogen/Fisher Scientific, Schwerte) each. 50 pmol of dsRNA were added to the first tube. In the second tube, 2 µl of transfection reagent were added and mixed by flicking the tube 20 times. Then, immediately the two solutions were combined, mixed well and incubated for 15 min. The transfection complexes were then added to the cells.

6.5.14. siRNA rescue experiment

In order to study mutant constructs of Sgo2 in a loss of function background, a combination of siRNA and plasmid transfection was used. HeLa cells were plated at a density of $1.6 \cdot 10^5$ cells/ml in DMEM (PAA, Pasching, Austria) with serum but without antibiotics. On the next day, Sgo2 siRNA transfection was performed. One day later,

medium was changed and Sgo2 rescue plasmids were transfected as described using Lipofectamine 2000. These constructs were mutated at 4 wobble positions leading to resistance to the siRNA oligo without changing the amino acid sequence. The modified pBOS vector used in rescue experiments carried in addition the gene for soluble eGFP thus allowing for selection of transfected cells in microscopic downstream analysis.

6.5.15. Immunofluorescence staining and microscopy

PBS: see chapter 6.5.3

Fixation Solution (FS): 3.7% Formaldehyde in PBS
(+0.3% Triton X-100 for anti-Mad2 staining)

Quenching Solution (QS): 100 mM glycine in PBS

Washing Solution (WS): 0.1% Triton X-100 in PBS

Permeabilization Solution (PS): 0.5% Triton X-100 in PBS

Blocking Solution (BS): 1% BSA in PBS

Mounting medium: 0,233 g DABCO (Diaza-bicyclo(2.2.2)octane), dissolved in 800 µl ddH₂O+ 200 µl 1 M Tris-HCl pH 8.0 + 9 ml 87% glycerol

For immunofluorescence stainings, cells grown on coverslips were washed once with PBS in a 24-well culture plate. The samples were then fixed for 10 min in FS followed by 2 washes with QS and 1 wash with PBS. Cells were permeabilized by incubation in PS for 5 min. After washing once with PBS samples were incubated in BS for 20 min to overnight. Coverslips were transferred onto Parafilm and placed in a wet chamber. Staining was done by incubation with a dilution of primary antibodies in BS for 1h followed by 4 washes with WS. After incubation with a dilution of fluorescently labeled secondary antibodies for 40 min, samples were washed once with WS, once with 1 µg/ml Hoechst 33342 in WS and again 4 times with WS. Coverslips were finally mounted on a small drop of Mounting Medium placed on a glass slide. Images were acquired using an Axiovert upright microscope equipped with a Plan-APOCHROMAT 100x/0.4 objective (Carl Zeiss MicroImaging, Jena).

6.5.16. Determination of the mitotic index by flow cytometry

Buffers see *Immunofluorescence*

Cells were harvested by trypsination and the resuspended cells were pooled with the material derived from culture supernatant and PBS wash. Cells were fixed by addition of

1/10 volume of 16% formaldehyde in PBS for 15 min. Cells were washed twice with QS and then permeabilized with methanol precooled at -20°C for 15 min on ice. Following 2 washing steps with PBS, cells were blocked for 30 min with BS and then incubated for 1 h with anti-phospho Histone H3 antibodies (1:100 in BS, Sigma-Aldrich, Steinheim). The cell pellet was washed again twice with PBS and subsequently stained with a secondary antibody labeled with the fluorescent dye Cy3 (1:100 in BS; Millipore, Schwalbach). Following two PBS washing steps, the cell suspension was analyzed in a "Cytomics FC-500" flow cytometer (Beckman Coulter, Krefeld) using the FL-2 channel.

6.5.17. Live cell imaging

Live cell imaging was carried out on a DMI 6000 inverted microscope stand (Leica Microsystems, Wetzlar) equipped with a digital camera (Leica Microsystems, Wetzlar) and with an HCX PL FLUOTAR L 20x/0.4 objective (Leica Microsystems, Wetzlar). Cell culture conditions were provided by a temperature controlled chamber maintained at 37°C and a small lid covering the sample for application of a humidified 5% CO₂ atmosphere (Pecon, Erbach). Cells were seeded at least 10 h prior to imaging on standard multi-well cell culture plates (Ibidi, Planegg-Martinsried). A typical movie was acquired with the phase contrast method at a frame rate of 5 min. Live cell imaging was used to determine the duration of mitosis. The time point of mitotic entry was defined as a marked rounding of the cell and end of mitosis was identified by the first signs of cleavage furrow ingression and/or separation of the DNA masses.

6.5.18. Chromosome spreads

Hypotonic buffer I:

30 mM Tris-HCl pH 8.2
50 mM sucrose
17 mM sodium citrate
400 ng/ml nocodazole

Hypotonic buffer II:

100 mM sucrose
400 ng/ml nocodazole

Fixative:

1% Formaldehyde
5 mM sodium borate pH 9.2
0.15% (v/v) Triton X-100

Hela cells were synchronized via a thymidine nocodazole protocol and mitotic cells were harvested by shake-off. $5 \cdot 10^5$ cells were resuspended in 250 μ l hypotonic buffer I. Then the cell suspension was mixed with another 250 μ l, and in a third round mixed with 2 ml

hypotonic buffer I Following incubation for 7 min at room temperature, cells were spun down (400 g, 2 min) and resuspended in 100 - 250 μ l hypotonic buffer II. A small volume of the cell suspension (approx. 10 μ l) was dropped onto a slide glass that had been dipped in fixative and dispersed on the slide by continuous tilting. After drying in partially opened wet chamber, coverslips were washed with PBS (see 6.5.3) and blocked in 2% BSA in PBS for 20 min. Samples were then treated as described in the section "Immunofluorescence". Anti-Hec1 staining (kinetochores) and DNA staining with the dye Hoesct-33342 were performed and the chromosome spreads were counted by fluorescence microscopy (as described for immunofluorescence) for the degree of sister chromatid separation.

6.5.19. Preparation of *Xenopus laevis* egg extract

All glasware used for buffers or extract preparation was rinsed twice with ddH₂O prior to use to remove especially contaminating calcium ions.

<i>25x MMR (pH 7.8 with NaOH)</i>	<i>20x XB salts</i>	<i>Dejelling solution</i>
2.5 M NaCl	2 M KCl	2% (w/v) Cysteine in
50 mM KCl	2 mM CaCl ₂	0.5x XB salts
25 mM MgCl ₂	20 mM MgCl ₂	pH 7.8 (set with KOH)
50 mM CaCl ₂		
2.5 mM EDTA-NaOH pH8.0		
125 mM HEPES-NaOH pH7.8		
<i>CSF-XB (pH 7.7 with KOH)</i>	<i>SD buffer</i>	<i>25x CaCl₂</i>
100 mM KCl	1 mM MgCl ₂	15 mM CaCl ₂
0.1 mM CaCl ₂	100 mM KCl	in SD buffer
2 mM MgCl ₂	150 mM sucrose	
10 mM Hepes-KOH pH 7.7	5 mM Hepes-KOH pH	
50 mM sucrose	7.7	
5 mM EGTA-KOH pH 8.0		

Cytochalasin B

10 mg/ml in DMSO

To induce egg laying, female frogs were injected with human chorionic gonadotropin (hCG, 200 U/ml in ddH₂O, Sigma-Aldrich, Steinheim). Depending on the size of the frog, about 0.7-1.0 ml of hCG solution were injected into the dorsal lymph sac using a 27-gauge needle. 6-8 h later, frogs were transferred to single vessels containing 2 l of 1x MMR each. About 22 h after injection, the frogs were put back to their tanks, MMR was discarded and the eggs were transferred to flat-bottomed glass dishes. Eggs with undesired

morphology were removed at this stage. After two washes with CSF-XB, the supernatant was completely removed in preparation for the dejellying procedure. Then eggs were briefly rinsed with and then incubated in dejellying solution with gentle agitation. Removal of the jelly coat took about 5-10 min and resulted in dense packaging of the eggs. The procedure was terminated by 5 washes in CSF-XB. Only eggs with appropriate morphology (white and brown hemispheres) were used in further steps. All aspects of egg extract preparation were performed by centrifugation (packaging of eggs, crushing and separation). Towards this end, 1 ml CSF-XB and 10 μ l Cytochalasin were added to a thin-walled 12 ml centrifuge tubes (Beckman Coulter, Krefeld). Then eggs were transferred to the tube using a disposable 5 ml plastic pipet which had been cut at the tip to increase its opening diameter. After removal of excess liquid, the tubes were subjected to the following centrifugation steps: first, eggs were packed by a 1 min spin at 200 g and a 1 min spin at 600 g. Again, buffer that had accumulated on top of the packed eggs was removed. Next, eggs were crushed and fractionated in a single centrifugation step for 10 min at 13,000 g. Egg lysate was thereby separated into three distinct layers: a lipid phase (white) on top, then in the middle the cytoplasmic layer ("egg extract") and cellular debris on the bottom of the tube. The tube was poked with a 18-gauge syringe needle at the lower end of the middle layer and egg extract was allowed to drop into a fresh 2 ml reaction tube by gravity flow.

6.5.20. Purification of active recombinant human separase

293T cells were cotransfected with separase (Protein A tag) and securin expression plasmids (Stemmann et al., 2001). Nocodazole arrested cells were lysed in LP2+ (see chapter 6.5.8) and separase was isolated using IgG sepharose. After washing with LP2 and XB (Murray, 1991), the immobilized separase/securin complexes were incubated with *X. laevis* anaphase egg extract for degradation of securin (1 h, 18°C, 100 ng/ml of His-tagged human cyclin B1 Δ 90 isolated from baculovirus-infected insect cells, Calcium chloride from 25x stock; recombinant cyclin B1 Δ 90 was a kind gift from Olaf Stemmann). After washing the beads with LP2 and XB, separase was eluted by cleaving off the Protein A tag with Tev-protease (1 h, 18°C).

6.5.21. Isolation of Metaphase Chromosomes

Metaphase chromosomes were isolated according to (Gasser and Laemmli, 1987) with modifications. At a density of $2 \cdot 10^5$ cells/ml, HeLaS3 cells grown in suspension (0.5 liter culture) were synchronized by a thymidine-nocodazole protocol (Stemmann et al., 2001).

Because metaphase-arrested cells could not be stored, they were immediately swollen for 5 min in 50 ml 1x PME (5 mM Pipes/NaOH pH 7.2, 5 mM NaCl, 5 mM MgCl₂, 1 mM EGTA). This step was repeated once. Cells were pelleted at 1,000 g for 5 min and the supernatant was removed. All following steps were carried out at 4°C. The cells were lysed in 25 ml lysis buffer 4 (1x PME, 1% thiodiethylene glycol, protease inhibitors without EDTA (Roche, Mannheim) 2.5 mM microcystin-LR, 1 mM okadaic acid, 1 mM ATP, 0.2% digitonin) using a dounce homogenizer with loose pestle. The lysate was put on top of sucrose step gradients, each consisting of 2 ml HSS (1x PME, 1% thiodiethylene glycol, protease inhibitors without EDTA, 1 mM microcystin-LR, 1 mM ATP, 1.8 M sucrose) at the bottom and 28 ml LSS (1x PME, 1% thiodiethylene glycol, protease inhibitors without EDTA, 1 mM microcystin-LR, 1 mM ATP, 0.9 M sucrose, 0.02% digitonin) at the top. After centrifugation in a SW28 rotor (Beckman Coulter, Krefeld) for 30 min at 4,000 rpm, the cytosol and the LSS layer were aspirated off for all but 2 ml. Chromosomes were resuspended in the remaining liquid and combined with wash solution (1x PME, 0.25% thiodiethylene glycol, complete protease inhibitor cocktail without EDTA (Roche, Mannheim), 1 mM microcystin-LR, 1 mM ATP), 1.6 ml 0.2 M spermidine, and 0.8 ml 0.2 M spermine (in the given order) to produce a total volume of 49 ml. After incubation for 5 min, 31 ml percoll (GE Healthcare, Munich) was added. The mixture was dounced and then centrifuged in a 70 Ti rotor (Beckman Coulter, Krefeld) for 30 min at 21,000 rpm. Chromosomes were recovered from a diffuse band 1 cm above the bottom of the tubes, passed through a 70 µm cell strainer (BD Biosciences, Heidelberg) and mixed with 35 ml wash solution in a conical tube. After putting 0.3 ml of storage solution (1x PME, 70% glycerol) at the bottom of the tube, the tube was spun in a RC3C centrifuge (Sorvall, Thermo Fisher Scientific,) for 30 min at 3300 rpm. Chromosomes were recovered from the bottom of the tube, washed once more and finally resuspended in 0.3 ml storage solution.

6.5.22. Metaphase chromosome separation assay

Metaphase chromosome separation was performed in separate cleavage buffer containing 30 mM HEPES/KOH pH 7.7, 30% glycerol, 25 mM KCl, 5 mM MgCl₂, 1.5 mM ATP, 100 µg/ml BSA and 1 mM EGTA. In a total reaction volume of 10 µl, 0.4 µl metaphase chromosomes, 1 µl of active or protease-dead separase, and 50 µM ICRF-193 were used as indicated. The reaction was carried out at 30°C for 1 h, while shaking the samples at 300 rpm to prevent chromosome aggregation. To determine the extent of

chromosome separation, 5 μ l of 4% formaldehyde was added into 5 μ l of chromosomes, before samples were incubated for 5 min, spotted onto glass slides and air-dried. The slides were rinsed twice with PBS-T (PBS see chapter 6.5.3, +0.1% Tween 20), and subjected to immunostaining. The rest of the metaphase chromosomes were incubated with an equal volume of sample loading buffer, boiled for 5 min and cohesin cleavage was determined by immunoblotting.

7. Abbreviations

a.a.	amino acid(s)
AD	transactivation domain (<i>S. cerevisiae</i> Gal4)
amp	ampicillin
APS	ammonium peroxodisulfate
ATP	adenosine 5'-triphosphate
bp	base pairs
BSA	bovine serum albumin
Bub	budding uninhibited by benzimidazole
CAK	cdk-activating kinase
Cdk	cyclin-dependent kinase
CHX	cycloheximide
co-I.P.	analysis of protein-protein interactions in an immuno-precipitation experiment
CSF	cytostatic factor
C-terminal	carboxy-terminal
C-terminus	carboxy-terminus
DBD	DNA binding domain (<i>S. cerevisiae</i> Gal4)
<i>D. melanogaster</i>	<i>Drosophila melanogaster</i>
DMSO	dimethylsulfoxide
DNA	deoxyribonucleic acid
dNTP	deoxynucleotide 5'-triphosphate
DTT	dithiothreitol
<i>E. coli</i>	<i>Escherichia coli</i>
EDTA	ethylenediamine tetraacetic acid
EGTA	ethylen glycol tetraacetic acid
f.l.	full length
Fig.	figure
g	gram or gravitational constant (9.81 m/s ²)
GST	glutathione S transferase
h	hour or human
HA	hemagglutinin
HAc	acetic acid
HEAT	helical repeat protein domain (<u>H</u> untingtin, <u>e</u> longation factor 3, PP2A- <u>A</u> , <u>T</u> or1)
HECT	<u>h</u> omologous to <u>E</u> 6AP <u>C</u> -terminus
HEPES	4-(2-hydroxyethyl)-1piperazineethansulfonic acid
<i>H.s.</i>	<i>Homo sapiens</i>
Ig	immunoglobulin
I.P.	immunoprecipitate
IPTG	isopropyl- β -D-thiogalactopyranoside
IVT	coupled <i>in vitro</i> transcription/translation in reticulocyte lysate, the product thereof
k	kilo
kb	kilo base pairs
kDa	kilo dalton
LB	Luria-Bertani
m	milli

μ	micro
M	molar
Mad	mitotic arrest deficient
MCS	multiple cloning site
min	minute(s)
MMR	Marc's modified Ringer
MOPS	N-morpholinopropane sulfonic acid
MT	microtubule
mRNA	messenger RNA
n	nano
NEM	N-ethylmaleimide
NHS	N-hydroxysuccinimid
NTA	nitriolo tetra acetate
N-terminal	amino-terminal
N-terminus	amino-terminus
OD	optical density
ORF	open reading frame
p.a.	<i>pro analysi</i>
PAGE	polyacrylamide gel electrophoresis
PBS	phosphate buffered saline
PCR	polymerase chain reaction
PEG	polyethylene glycol
PP2A	protein phosphatase 2A
PPase	phosphatase
PVDF	polyvinylidene fluoride
RING	really interesting new gene
RNA	ribonucleic acid
RNase	ribonuclease
rpm	revolutions per minute
RT	room temperature
SAC	spindle assembly checkpoint
<i>S. cerevisiae</i>	<i>Saccharomyces cerevisiae</i> (baker's yeast)
SDS	sodium dodecylsulfate
s	seconds
hSgo	human shugoshin
<i>S. pombe</i>	<i>Schizosaccharomyces pombe</i> (fission yeast)
Suppl. fig.	supplementary figure
TBS	Tris buffered saline
TEMED	N,N,N',N'-tetramethylethylenediamine
Tev	tobacco etch virus
Tris	tris(hydroxymethyl)aminomethane
U	unit
Ub	ubiquitin
V	volt
v/v	volume per volume
w/v	weight per volume
W.B.	Western Blot
wt	wild-type
xErp1	<i>X. laevis</i> Erp1
xSgo1	<i>X. laevis</i> shugoshin 1
<i>X. laevis/X.l.</i>	<i>Xenopus laevis</i>

8. References

- Ackerman, P., Glover, C.V., and Osheroff, N. (1985). Phosphorylation of DNA topoisomerase II by casein kinase II: modulation of eukaryotic topoisomerase II activity in vitro. *Proc Natl Acad Sci U S A* 82, 3164-3168.
- Alberts, B., Wilson, J.H., and Hunt, T. (2008). *Molecular biology of the cell*, 5th edn (New York, Garland Science).
- Alexandru, G., Uhlmann, F., Mechtler, K., Poupart, M.A., and Nasmyth, K. (2001). Phosphorylation of the cohesin subunit Scc1 by Polo/Cdc5 kinase regulates sister chromatid separation in yeast. *Cell* 105, 459-472.
- Andrews, P.D., Ovechkina, Y., Morrice, N., Wagenbach, M., Duncan, K., Wordeman, L., and Swedlow, J.R. (2004). Aurora B regulates MCAK at the mitotic centromere. *Dev Cell* 6, 253-268.
- Aravind, L., and Koonin, E.V. (1998). The HORMA domain: a common structural denominator in mitotic checkpoints, chromosome synapsis and DNA repair. *Trends Biochem Sci* 23, 284-286.
- Arumugam, P., Gruber, S., Tanaka, K., Haering, C.H., Mechtler, K., and Nasmyth, K. (2003). ATP hydrolysis is required for cohesin's association with chromosomes. *Curr Biol* 13, 1941-1953.
- Baumann, C., Korner, R., Hofmann, K., and Nigg, E.A. (2007). PICH, a centromere-associated SNF2 family ATPase, is regulated by Plk1 and required for the spindle checkpoint. *Cell* 128, 101-114.
- Biggins, S., and Murray, A.W. (2001). The budding yeast protein kinase Ipl1/Aurora allows the absence of tension to activate the spindle checkpoint. *Genes Dev* 15, 3118-3129.
- Blangy, A., Lane, H.A., d'Herin, P., Harper, M., Kress, M., and Nigg, E.A. (1995). Phosphorylation by p34cdc2 regulates spindle association of human Eg5, a kinesin-related motor essential for bipolar spindle formation in vivo. *Cell* 83, 1159-1169.
- Boyarchuk, Y., Salic, A., Dasso, M., and Arnaoutov, A. (2007). Bub1 is essential for assembly of the functional inner centromere. *J Cell Biol* 176, 919-928.
- Brar, G.A., Kiburz, B.M., Zhang, Y., Kim, J.E., White, F., and Amon, A. (2006). Rec8 phosphorylation and recombination promote the step-wise loss of cohesins in meiosis. *Nature* 441, 532-536.
- Brito, D.A., and Rieder, C.L. (2006). Mitotic checkpoint slippage in humans occurs via cyclin B destruction in the presence of an active checkpoint. *Curr Biol* 16, 1194-1200.
- Buffin, E., Emre, D., and Karess, R.E. (2007). Flies without a spindle checkpoint. *Nat Cell Biol* 9, 565-572.
- Buonomo, S.B., Clyne, R.K., Fuchs, J., Loidl, J., Uhlmann, F., and Nasmyth, K. (2000). Disjunction of homologous chromosomes in meiosis I depends on proteolytic cleavage of the meiotic cohesin Rec8 by separin. *Cell* 103, 387-398.

- Chan, K.L., North, P.S., and Hickson, I.D. (2007). BLM is required for faithful chromosome segregation and its localization defines a class of ultrafine anaphase bridges. *EMBO J* 26, 3397-3409.
- Charles, J.F., Jaspersen, S.L., Tinker-Kulberg, R.L., Hwang, L., Szidon, A., and Morgan, D.O. (1998). The Polo-related kinase Cdc5 activates and is destroyed by the mitotic cyclin destruction machinery in *S. cerevisiae*. *Curr Biol* 8, 497-507.
- Cheeseman, I.M., Chappie, J.S., Wilson-Kubalek, E.M., and Desai, A. (2006). The conserved KMN network constitutes the core microtubule-binding site of the kinetochore. *Cell* 127, 983-997.
- Chen, R.H., Brady, D.M., Smith, D., Murray, A.W., and Hardwick, K.G. (1999). The spindle checkpoint of budding yeast depends on a tight complex between the Mad1 and Mad2 proteins. *Mol Biol Cell* 10, 2607-2618.
- Ciferri, C., Pasqualato, S., Screpanti, E., Varetto, G., Santaguida, S., Dos Reis, G., Maiolica, A., Polka, J., De Luca, J.G., De Wulf, P., *et al.* (2008). Implications for kinetochore-microtubule attachment from the structure of an engineered Ndc80 complex. *Cell* 133, 427-439.
- Cimini, D. (2008). Merotelic kinetochore orientation, aneuploidy, and cancer. *Biochim Biophys Acta* 1786, 32-40.
- Cimini, D., and Degrassi, F. (2005). Aneuploidy: a matter of bad connections. *Trends Cell Biol* 15, 442-451.
- Ciosk, R., Shirayama, M., Shevchenko, A., Tanaka, T., Toth, A., and Nasmyth, K. (2000). Cohesin's binding to chromosomes depends on a separate complex consisting of Scc2 and Scc4 proteins. *Mol Cell* 5, 243-254.
- Cleveland, D.W., Mao, Y., and Sullivan, K.F. (2003). Centromeres and kinetochores: from epigenetics to mitotic checkpoint signaling. *Cell* 112, 407-421.
- Cohen-Fix, O., Peters, J.M., Kirschner, M.W., and Koshland, D. (1996). Anaphase initiation in *Saccharomyces cerevisiae* is controlled by the APC-dependent degradation of the anaphase inhibitor Pds1p. *Genes Dev* 10, 3081-3093.
- Conn, C.W., Lewellyn, A.L., and Maller, J.L. (2004). The DNA damage checkpoint in embryonic cell cycles is dependent on the DNA-to-cytoplasmic ratio. *Dev Cell* 7, 275-281.
- Darwiche, N., Freeman, L.A., and Strunnikov, A. (1999). Characterization of the components of the putative mammalian sister chromatid cohesion complex. *Gene* 233, 39-47.
- De Antoni, A., Pearson, C.G., Cimini, D., Canman, J.C., Sala, V., Nezi, L., Mapelli, M., Sironi, L., Faretta, M., Salmon, E.D., *et al.* (2005). The Mad1/Mad2 complex as a template for Mad2 activation in the spindle assembly checkpoint. *Curr Biol* 15, 214-225.
- Desai, A., Verma, S., Mitchison, T.J., and Walczak, C.E. (1999). Kin I kinesins are microtubule-destabilizing enzymes. *Cell* 96, 69-78.

- Ditchfield, C., Johnson, V.L., Tighe, A., Ellston, R., Haworth, C., Johnson, T., Mortlock, A., Keen, N., and Taylor, S.S. (2003). Aurora B couples chromosome alignment with anaphase by targeting BubR1, Mad2, and Cenp-E to kinetochores. *J Cell Biol* *161*, 267-280.
- Elder, K., and Dale, B. (2000). *In vitro fertilization*, 2nd edn (Cambridge ; New York, Cambridge University Press).
- Fang, G., Yu, H., and Kirschner, M.W. (1998). The checkpoint protein MAD2 and the mitotic regulator CDC20 form a ternary complex with the anaphase-promoting complex to control anaphase initiation. *Genes Dev* *12*, 1871-1883.
- Fukuda, T., Daniel, K., Wojtasz, L., Toth, A., and Hoog, C. (2009). A novel mammalian HORMA domain-containing protein, HORMAD1, preferentially associates with unsynapsed meiotic chromosomes. *Exp Cell Res*.
- Gandhi, R., Gillespie, P.J., and Hirano, T. (2006). Human Wapl is a cohesin-binding protein that promotes sister-chromatid resolution in mitotic prophase. *Curr Biol* *16*, 2406-2417.
- Ganem, N.J., Godinho, S.A., and Pellman, D. (2009). A mechanism linking extra centrosomes to chromosomal instability. *Nature* *460*, 278-282.
- Gascoigne, K.E., and Taylor, S.S. (2008). Cancer cells display profound intra- and interline variation following prolonged exposure to antimetabolic drugs. *Cancer Cell* *14*, 111-122.
- Gasser, S.M., and Laemmli, U.K. (1987). Improved methods for the isolation of individual and clustered mitotic chromosomes. *Exp Cell Res* *173*, 85-98.
- Ge, S., Skaar, J.R., and Pagano, M. (2009). APC/C- and Mad2-mediated degradation of Cdc20 during spindle checkpoint activation. *Cell Cycle* *8*, 167-171.
- Giet, R., and Glover, D.M. (2001). *Drosophila* aurora B kinase is required for histone H3 phosphorylation and condensin recruitment during chromosome condensation and to organize the central spindle during cytokinesis. *J Cell Biol* *152*, 669-682.
- Glotzer, M., Murray, A.W., and Kirschner, M.W. (1991). Cyclin is degraded by the ubiquitin pathway. *Nature* *349*, 132-138.
- Gomez, R., Valdeolillos, A., Parra, M.T., Viera, A., Carreiro, C., Roncal, F., Rufas, J.S., Barbero, J.L., and Suja, J.A. (2007). Mammalian SGO2 appears at the inner centromere domain and redistributes depending on tension across centromeres during meiosis II and mitosis. *EMBO Rep* *8*, 173-180.
- Gorr, I.H., Boos, D., and Stemmann, O. (2005). Mutual inhibition of separase and Cdk1 by two-step complex formation. *Mol Cell* *19*, 135-141.
- Gruber, S., Arumugam, P., Katou, Y., Kuglitsch, D., Helmhart, W., Shirahige, K., and Nasmyth, K. (2006). Evidence that loading of cohesin onto chromosomes involves opening of its SMC hinge. *Cell* *127*, 523-537.
- Gruber, S., Haering, C.H., and Nasmyth, K. (2003). Chromosomal cohesin forms a ring. *Cell* *112*, 765-777.

- Guacci, V., Koshland, D., and Strunnikov, A. (1997). A direct link between sister chromatid cohesion and chromosome condensation revealed through the analysis of MCD1 in *S. cerevisiae*. *Cell* *91*, 47-57.
- Haccard, O., Sarcevic, B., Lewellyn, A., Hartley, R., Roy, L., Izumi, T., Erikson, E., and Maller, J.L. (1993). Induction of metaphase arrest in cleaving *Xenopus* embryos by MAP kinase. *Science* *262*, 1262-1265.
- Haering, C.H., Farcas, A.M., Arumugam, P., Metson, J., and Nasmyth, K. (2008). The cohesin ring concatenates sister DNA molecules. *Nature* *454*, 297-301.
- Hauf, S., Cole, R.W., LaTerra, S., Zimmer, C., Schnapp, G., Walter, R., Heckel, A., van Meel, J., Rieder, C.L., and Peters, J.M. (2003). The small molecule Hesperadin reveals a role for Aurora B in correcting kinetochore-microtubule attachment and in maintaining the spindle assembly checkpoint. *J Cell Biol* *161*, 281-294.
- Hauf, S., Roitinger, E., Koch, B., Dittrich, C.M., Mechtler, K., and Peters, J.M. (2005). Dissociation of cohesin from chromosome arms and loss of arm cohesion during early mitosis depends on phosphorylation of SA2. *PLoS Biol* *3*, e69.
- Hauf, S., Waizenegger, I.C., and Peters, J.M. (2001). Cohesin cleavage by separase required for anaphase and cytokinesis in human cells. *Science* *293*, 1320-1323.
- Heald, R., and McKeon, F. (1990). Mutations of phosphorylation sites in lamin A that prevent nuclear lamina disassembly in mitosis. *Cell* *61*, 579-589.
- Hershko, A., and Ciechanover, A. (1992). The ubiquitin system for protein degradation. *Annu Rev Biochem* *61*, 761-807.
- Holland, A.J., Bottger, F., Stemmann, O., and Taylor, S.S. (2007). Protein phosphatase 2A and separase form a complex regulated by separase autocleavage. *J Biol Chem* *282*, 24623-24632.
- Homer, H.A., McDougall, A., Levasseur, M., Yallop, K., Murdoch, A.P., and Herbert, M. (2005). Mad2 prevents aneuploidy and premature proteolysis of cyclin B and securin during meiosis I in mouse oocytes. *Genes Dev* *19*, 202-207.
- Hornig, N.C., and Uhlmann, F. (2004). Preferential cleavage of chromatin-bound cohesin after targeted phosphorylation by Polo-like kinase. *EMBO J* *23*, 3144-3153.
- Howell, B.J., McEwen, B.F., Canman, J.C., Hoffman, D.B., Farrar, E.M., Rieder, C.L., and Salmon, E.D. (2001). Cytoplasmic dynein/dynactin drives kinetochore protein transport to the spindle poles and has a role in mitotic spindle checkpoint inactivation. *J Cell Biol* *155*, 1159-1172.
- Hoyt, M.A., Totis, L., and Roberts, B.T. (1991). *S. cerevisiae* genes required for cell cycle arrest in response to loss of microtubule function. *Cell* *66*, 507-517.
- Huang, H., Feng, J., Famulski, J., Rattner, J.B., Liu, S.T., Kao, G.D., Muschel, R., Chan, G.K., and Yen, T.J. (2007). Tripin/hSgo2 recruits MCAK to the inner centromere to correct defective kinetochore attachments. *J Cell Biol* *177*, 413-424.
- Huang, X., Hatcher, R., York, J.P., and Zhang, P. (2005). Securin and separase phosphorylation act redundantly to maintain sister chromatid cohesion in mammalian cells. *Mol Biol Cell* *16*, 4725-4732.

- Hunt, P., LeMaire, R., Embury, P., Sheean, L., and Mroz, K. (1995). Analysis of chromosome behavior in intact mammalian oocytes: monitoring the segregation of a univalent chromosome during female meiosis. *Hum Mol Genet* 4, 2007-2012.
- Hunter, A.W., Caplow, M., Coy, D.L., Hancock, W.O., Diez, S., Wordeman, L., and Howard, J. (2003). The kinesin-related protein MCAK is a microtubule depolymerase that forms an ATP-hydrolyzing complex at microtubule ends. *Mol Cell* 11, 445-457.
- Hwang, L.H., Lau, L.F., Smith, D.L., Mistrot, C.A., Hardwick, K.G., Hwang, E.S., Amon, A., and Murray, A.W. (1998). Budding yeast Cdc20: a target of the spindle checkpoint. *Science* 279, 1041-1044.
- Indjeian, V.B., and Murray, A.W. (2007). Budding yeast mitotic chromosomes have an intrinsic bias to biorient on the spindle. *Curr Biol* 17, 1837-1846.
- Indjeian, V.B., Stern, B.M., and Murray, A.W. (2005). The centromeric protein Sgo1 is required to sense lack of tension on mitotic chromosomes. *Science* 307, 130-133.
- Irniger, S., Piatti, S., Michaelis, C., and Nasmyth, K. (1995). Genes involved in sister chromatid separation are needed for B-type cyclin proteolysis in budding yeast. *Cell* 81, 269-278.
- Ivanov, D., and Nasmyth, K. (2005). A topological interaction between cohesin rings and a circular minichromosome. *Cell* 122, 849-860.
- Ivanov, D., and Nasmyth, K. (2007). A physical assay for sister chromatid cohesion in vitro. *Mol Cell* 27, 300-310.
- Iwaizumi, M., Shinmura, K., Mori, H., Yamada, H., Suzuki, M., Kitayama, Y., Igarashi, H., Nakamura, T., Suzuki, H., Watanabe, Y., *et al.* (2009). Human Sgo1 downregulation leads to chromosomal instability in colorectal cancer. *Gut* 58, 249-260.
- James, P., Halladay, J., and Craig, E.A. (1996). Genomic libraries and a host strain designed for highly efficient two-hybrid selection in yeast. *Genetics* 144, 1425-1436.
- Jaspersen, S.L., Charles, J.F., and Morgan, D.O. (1999). Inhibitory phosphorylation of the APC regulator Hct1 is controlled by the kinase Cdc28 and the phosphatase Cdc14. *Curr Biol* 9, 227-236.
- Katis, V.L., Galova, M., Rabitsch, K.P., Gregan, J., and Nasmyth, K. (2004). Maintenance of cohesin at centromeres after meiosis I in budding yeast requires a kinetochore-associated protein related to MEI-S332. *Curr Biol* 14, 560-572.
- Kawashima, S.A., Tsukahara, T., Langeegger, M., Hauf, S., Kitajima, T.S., and Watanabe, Y. (2007). Shugoshin enables tension-generating attachment of kinetochores by loading Aurora to centromeres. *Genes Dev* 21, 420-435.
- Keeney, S., Giroux, C.N., and Kleckner, N. (1997). Meiosis-specific DNA double-strand breaks are catalyzed by Spo11, a member of a widely conserved protein family. *Cell* 88, 375-384.
- Kerrebrock, A.W., Miyazaki, W.Y., Birnby, D., and Orr-Weaver, T.L. (1992). The *Drosophila* mei-S332 gene promotes sister-chromatid cohesion in meiosis following kinetochore differentiation. *Genetics* 130, 827-841.

- Kerrebrock, A.W., Moore, D.P., Wu, J.S., and Orr-Weaver, T.L. (1995). Mei-S332, a *Drosophila* protein required for sister-chromatid cohesion, can localize to meiotic centromere regions. *Cell* *83*, 247-256.
- Kimata, Y., Baxter, J.E., Fry, A.M., and Yamano, H. (2008). A role for the Fizzy/Cdc20 family of proteins in activation of the APC/C distinct from substrate recruitment. *Mol Cell* *32*, 576-583.
- Kimura, K., and Hirano, T. (1997). ATP-dependent positive supercoiling of DNA by 13S condensin: a biochemical implication for chromosome condensation. *Cell* *90*, 625-634.
- King, R.W., Peters, J.M., Tugendreich, S., Rolfe, M., Hieter, P., and Kirschner, M.W. (1995). A 20S complex containing CDC27 and CDC16 catalyzes the mitosis-specific conjugation of ubiquitin to cyclin B. *Cell* *81*, 279-288.
- Kirschner, M.W., and Mitchison, T. (1986). Microtubule dynamics. *Nature* *324*, 621.
- Kitajima, T.S., Kawashima, S.A., and Watanabe, Y. (2004). The conserved kinetochore protein shugoshin protects centromeric cohesion during meiosis. *Nature* *427*, 510-517.
- Kitajima, T.S., Sakuno, T., Ishiguro, K., Iemura, S., Natsume, T., Kawashima, S.A., and Watanabe, Y. (2006). Shugoshin collaborates with protein phosphatase 2A to protect cohesin. *Nature* *441*, 46-52.
- Kline-Smith, S.L., Khodjakov, A., Hergert, P., and Walczak, C.E. (2004). Depletion of centromeric MCAK leads to chromosome congression and segregation defects due to improper kinetochore attachments. *Mol Biol Cell* *15*, 1146-1159.
- Knowlton, A.L., Lan, W., and Stukenberg, P.T. (2006). Aurora B is enriched at merotelic attachment sites, where it regulates MCAK. *Curr Biol* *16*, 1705-1710.
- Koshland, D., and Hartwell, L.H. (1987). The structure of sister minichromosome DNA before anaphase in *Saccharomyces cerevisiae*. *Science* *238*, 1713-1716.
- Kouznetsova, A., Lister, L., Nordenskjold, M., Herbert, M., and Hoog, C. (2007). Bi-orientation of achiasmatic chromosomes in meiosis I oocytes contributes to aneuploidy in mice. *Nat Genet* *39*, 966-968.
- Kraft, C., Vodermaier, H.C., Maurer-Stroh, S., Eisenhaber, F., and Peters, J.M. (2005). The WD40 propeller domain of Cdh1 functions as a destruction box receptor for APC/C substrates. *Mol Cell* *18*, 543-553.
- Kudo, N.R., Anger, M., Peters, A.H., Stemmann, O., Theussl, H.C., Helmhart, W., Kudo, H., Heyting, C., and Nasmyth, K. (2009). Role of cleavage by separase of the Rec8 kleisin subunit of cohesin during mammalian meiosis I. *J Cell Sci* *122*, 2686-2698.
- Kueng, S., Hegemann, B., Peters, B.H., Lipp, J.J., Schleiffer, A., Mechtler, K., and Peters, J.M. (2006). Wapl controls the dynamic association of cohesin with chromatin. *Cell* *127*, 955-967.
- Kulukian, A., Han, J.S., and Cleveland, D.W. (2009). Unattached kinetochores catalyze production of an anaphase inhibitor that requires a Mad2 template to prime Cdc20 for BubR1 binding. *Dev Cell* *16*, 105-117.

- Lai, J.S., and Herr, W. (1992). Ethidium bromide provides a simple tool for identifying genuine DNA-independent protein associations. *Proc Natl Acad Sci U S A* *89*, 6958-6962.
- Lan, W., Zhang, X., Kline-Smith, S.L., Rosasco, S.E., Barrett-Wilt, G.A., Shabanowitz, J., Hunt, D.F., Walczak, C.E., and Stukenberg, P.T. (2004). Aurora B phosphorylates centromeric MCAK and regulates its localization and microtubule depolymerization activity. *Curr Biol* *14*, 273-286.
- Lee, J., Kitajima, T.S., Tanno, Y., Yoshida, K., Morita, T., Miyano, T., Miyake, M., and Watanabe, Y. (2008). Unified mode of centromeric protection by shugoshin in mammalian oocytes and somatic cells. *Nat Cell Biol* *10*, 42-52.
- LeMaire-Adkins, R., Radke, K., and Hunt, P.A. (1997). Lack of checkpoint control at the metaphase/anaphase transition: a mechanism of meiotic nondisjunction in mammalian females. *J Cell Biol* *139*, 1611-1619.
- Lengronne, A., Katou, Y., Mori, S., Yokobayashi, S., Kelly, G.P., Itoh, T., Watanabe, Y., Shirahige, K., and Uhlmann, F. (2004). Cohesin relocation from sites of chromosomal loading to places of convergent transcription. *Nature* *430*, 573-578.
- Lengronne, A., McIntyre, J., Katou, Y., Kanoh, Y., Hopfner, K.P., Shirahige, K., and Uhlmann, F. (2006). Establishment of sister chromatid cohesion at the *S. cerevisiae* replication fork. *Mol Cell* *23*, 787-799.
- Li, M., Li, S., Yuan, J., Wang, Z.B., Sun, S.C., Schatten, H., and Sun, Q.Y. (2009). Bub3 is a spindle assembly checkpoint protein regulating chromosome segregation during mouse oocyte meiosis. *PLoS One* *4*, e7701.
- Li, R., and Murray, A.W. (1991). Feedback control of mitosis in budding yeast. *Cell* *66*, 519-531.
- Li, Y., Gorbea, C., Mahaffey, D., Rechsteiner, M., and Benezra, R. (1997). MAD2 associates with the cyclosome/anaphase-promoting complex and inhibits its activity. *Proc Natl Acad Sci U S A* *94*, 12431-12436.
- Liu, D., Ding, X., Du, J., Cai, X., Huang, Y., Ward, T., Shaw, A., Yang, Y., Hu, R., Jin, C., *et al.* (2007). Human NUF2 interacts with centromere-associated protein E and is essential for a stable spindle microtubule-kinetochore attachment. *J Biol Chem* *282*, 21415-21424.
- Liu, D., Vader, G., Vromans, M.J., Lampson, M.A., and Lens, S.M. (2009). Sensing chromosome bi-orientation by spatial separation of aurora B kinase from kinetochore substrates. *Science* *323*, 1350-1353.
- Llano, E., Gomez, R., Gutierrez-Caballero, C., Herran, Y., Sanchez-Martin, M., Vazquez-Quinones, L., Hernandez, T., de Alava, E., Cuadrado, A., Barbero, J.L., *et al.* (2008). Shugoshin-2 is essential for the completion of meiosis but not for mitotic cell division in mice. *Genes Dev* *22*, 2400-2413.
- Luo, X., Fang, G., Coldiron, M., Lin, Y., Yu, H., Kirschner, M.W., and Wagner, G. (2000). Structure of the Mad2 spindle assembly checkpoint protein and its interaction with Cdc20. *Nat Struct Biol* *7*, 224-229.

- Luo, X., Tang, Z., Rizo, J., and Yu, H. (2002). The Mad2 spindle checkpoint protein undergoes similar major conformational changes upon binding to either Mad1 or Cdc20. *Mol Cell* *9*, 59-71.
- Luo, X., Tang, Z., Xia, G., Wassmann, K., Matsumoto, T., Rizo, J., and Yu, H. (2004). The Mad2 spindle checkpoint protein has two distinct natively folded states. *Nat Struct Mol Biol* *11*, 338-345.
- Mailhes, J.B., Hilliard, C., Fuseler, J.W., and London, S.N. (2003). Okadaic acid, an inhibitor of protein phosphatase 1 and 2A, induces premature separation of sister chromatids during meiosis I and aneuploidy in mouse oocytes in vitro. *Chromosome Res* *11*, 619-631.
- Mapelli, M., Massimiliano, L., Santaguida, S., and Musacchio, A. (2007). The Mad2 conformational dimer: structure and implications for the spindle assembly checkpoint. *Cell* *131*, 730-743.
- Maresca, T.J., and Salmon, E.D. (2009). Intrakinetochore stretch is associated with changes in kinetochore phosphorylation and spindle assembly checkpoint activity. *J Cell Biol* *184*, 373-381.
- Martin-Castellanos, C., Blanco, M., Rozalen, A.E., Perez-Hidalgo, L., Garcia, A.I., Conde, F., Mata, J., Ellermeier, C., Davis, L., San-Segundo, P., *et al.* (2005). A large-scale screen in *S. pombe* identifies seven novel genes required for critical meiotic events. *Curr Biol* *15*, 2056-2062.
- Masui, Y., and Markert, C.L. (1971). Cytoplasmic control of nuclear behavior during meiotic maturation of frog oocytes. *J Exp Zool* *177*, 129-145.
- Mc Intyre, J., Muller, E.G., Weitzer, S., Snyderman, B.E., Davis, T.N., and Uhlmann, F. (2007). In vivo analysis of cohesin architecture using FRET in the budding yeast *Saccharomyces cerevisiae*. *EMBO J* *26*, 3783-3793.
- McEwen, B.F., Chan, G.K., Zubrowski, B., Savoian, M.S., Sauer, M.T., and Yen, T.J. (2001). CENP-E is essential for reliable bioriented spindle attachment, but chromosome alignment can be achieved via redundant mechanisms in mammalian cells. *Mol Biol Cell* *12*, 2776-2789.
- McGuinness, B.E., Anger, M., Kouznetsova, A., Gil-Bernabe, A.M., Helmhart, W., Kudo, N.R., Wuensche, A., Taylor, S., Hoog, C., Novak, B., *et al.* (2009). Regulation of APC/C activity in oocytes by a Bub1-dependent spindle assembly checkpoint. *Curr Biol* *19*, 369-380.
- McGuinness, B.E., Hirota, T., Kudo, N.R., Peters, J.M., and Nasmyth, K. (2005). Shugoshin prevents dissociation of cohesin from centromeres during mitosis in vertebrate cells. *PLoS Biol* *3*, e86.
- Melby, T.E., Ciampaglio, C.N., Briscoe, G., and Erickson, H.P. (1998). The symmetrical structure of structural maintenance of chromosomes (SMC) and MukB proteins: long, antiparallel coiled coils, folded at a flexible hinge. *J Cell Biol* *142*, 1595-1604.
- Michaelis, C., Ciosk, R., and Nasmyth, K. (1997). Cohesins: chromosomal proteins that prevent premature separation of sister chromatids. *Cell* *91*, 35-45.

- Minshull, J., Straight, A., Rudner, A.D., Dernburg, A.F., Belmont, A., and Murray, A.W. (1996). Protein phosphatase 2A regulates MPF activity and sister chromatid cohesion in budding yeast. *Curr Biol* 6, 1609-1620.
- Morrison, C., Henzing, A.J., Jensen, O.N., Osheroff, N., Dodson, H., Kandels-Lewis, S.E., Adams, R.R., and Earnshaw, W.C. (2002). Proteomic analysis of human metaphase chromosomes reveals topoisomerase II alpha as an Aurora B substrate. *Nucleic Acids Res* 30, 5318-5327.
- Murray, A.W. (1991). Cell cycle extracts. *Methods Cell Biol* 36, 581-605.
- Murray, A.W., and Szostak, J.W. (1985). Chromosome segregation in mitosis and meiosis. *Annu Rev Cell Biol* 1, 289-315.
- Nasmyth, K. (2005). How do so few control so many? *Cell* 120, 739-746.
- Nasmyth, K., and Haering, C.H. (2005). The structure and function of SMC and kleisin complexes. *Annu Rev Biochem* 74, 595-648.
- Neumann, E., Garcia-Saez, I., DeBonis, S., Wade, R.H., Kozielski, F., and Conway, J.F. (2006). Human kinetochore-associated kinesin CENP-E visualized at 17 Å resolution bound to microtubules. *J Mol Biol* 362, 203-211.
- Nilsson, J., Yekezare, M., Minshull, J., and Pines, J. (2008). The APC/C maintains the spindle assembly checkpoint by targeting Cdc20 for destruction. *Nat Cell Biol* 10, 1411-1420.
- Orth, J.D., Tang, Y., Shi, J., Loy, C.T., Amendt, C., Wilm, C., Zenke, F.T., and Mitchison, T.J. (2008). Quantitative live imaging of cancer and normal cells treated with Kinesin-5 inhibitors indicates significant differences in phenotypic responses and cell fate. *Mol Cancer Ther* 7, 3480-3489.
- Panizza, S., Tanaka, T., Hochwagen, A., Eisenhaber, F., and Nasmyth, K. (2000). Pds5 cooperates with cohesin in maintaining sister chromatid cohesion. *Curr Biol* 10, 1557-1564.
- Peters, J.M., Tedeschi, A., and Schmitz, J. (2008). The cohesin complex and its roles in chromosome biology. *Genes Dev* 22, 3089-3114.
- Pfleghaar, K., Heubes, S., Cox, J., Stemmann, O., and Speicher, M.R. (2005). Securin is not required for chromosomal stability in human cells. *PLoS Biol* 3, e416.
- Pickart, C.M. (1997). Targeting of substrates to the 26S proteasome. *FASEB J* 11, 1055-1066.
- Pinsky, B.A., Kung, C., Shokat, K.M., and Biggins, S. (2006). The Ipl1-Aurora protein kinase activates the spindle checkpoint by creating unattached kinetochores. *Nat Cell Biol* 8, 78-83.
- Porter, A.C., and Farr, C.J. (2004). Topoisomerase II: untangling its contribution at the centromere. *Chromosome Res* 12, 569-583.
- Potapova, T.A., Daum, J.R., Pittman, B.D., Hudson, J.R., Jones, T.N., Satinover, D.L., Stukenberg, P.T., and Gorbsky, G.J. (2006). The reversibility of mitotic exit in vertebrate cells. *Nature* 440, 954-958.

- Rabitsch, K.P., Gregan, J., Schleiffer, A., Javerzat, J.P., Eisenhaber, F., and Nasmyth, K. (2004). Two fission yeast homologs of *Drosophila* Mei-S332 are required for chromosome segregation during meiosis I and II. *Curr Biol* *14*, 287-301.
- Rauh, N.R., Schmidt, A., Bormann, J., Nigg, E.A., and Mayer, T.U. (2005). Calcium triggers exit from meiosis II by targeting the APC/C inhibitor XErp1 for degradation. *Nature* *437*, 1048-1052.
- Reddy, S.K., Rape, M., Margansky, W.A., and Kirschner, M.W. (2007). Ubiquitination by the anaphase-promoting complex drives spindle checkpoint inactivation. *Nature* *446*, 921-925.
- Riedel, C.G., Katis, V.L., Katou, Y., Mori, S., Itoh, T., Helmhart, W., Galova, M., Petronczki, M., Gregan, J., Cetin, B., *et al.* (2006). Protein phosphatase 2A protects centromeric sister chromatid cohesion during meiosis I. *Nature* *441*, 53-61.
- Rieder, C.L., Cole, R.W., Khodjakov, A., and Sluder, G. (1995). The checkpoint delaying anaphase in response to chromosome monoorientation is mediated by an inhibitory signal produced by unattached kinetochores. *J Cell Biol* *130*, 941-948.
- Rieder, C.L., Schultz, A., Cole, R., and Sluder, G. (1994). Anaphase onset in vertebrate somatic cells is controlled by a checkpoint that monitors sister kinetochore attachment to the spindle. *J Cell Biol* *127*, 1301-1310.
- Sakuno, T., Tada, K., and Watanabe, Y. (2009). Kinetochore geometry defined by cohesion within the centromere. *Nature* *458*, 852-858.
- Sakuno, T., and Watanabe, Y. (2009). Studies of meiosis disclose distinct roles of cohesion in the core centromere and pericentromeric regions. *Chromosome Res* *17*, 239-249.
- Sambrook, J., and Russell, D.W. (2001). *Molecular cloning : a laboratory manual*, 3rd edn (Cold Spring Harbor, N.Y., Cold Spring Harbor Laboratory Press).
- Sandall, S., Severin, F., McLeod, I.X., Yates, J.R., 3rd, Oegema, K., Hyman, A., and Desai, A. (2006). A Bir1-Sli15 complex connects centromeres to microtubules and is required to sense kinetochore tension. *Cell* *127*, 1179-1191.
- Sandler, L., Lindsley, D.L., Nicoletti, B., and Trippa, G. (1968). Mutants affecting meiosis in natural populations of *Drosophila melanogaster*. *Genetics* *60*, 525-558.
- Santaguida, S., and Musacchio, A. (2009). The life and miracles of kinetochores. *EMBO J* *28*, 2511-2531.
- Scanlan, M.J., Gout, I., Gordon, C.M., Williamson, B., Stockert, E., Gure, A.O., Jager, D., Chen, Y.T., Mackay, A., O'Hare, M.J., *et al.* (2001). Humoral immunity to human breast cancer: antigen definition and quantitative analysis of mRNA expression. *Cancer Immun* *1*, 4.
- Schmidt, A., Duncan, P.I., Rauh, N.R., Sauer, G., Fry, A.M., Nigg, E.A., and Mayer, T.U. (2005). *Xenopus* polo-like kinase Plx1 regulates XErp1, a novel inhibitor of APC/C activity. *Genes Dev* *19*, 502-513.

- Sigrist, S., Jacobs, H., Stratmann, R., and Lehner, C.F. (1995). Exit from mitosis is regulated by *Drosophila* fizzy and the sequential destruction of cyclins A, B and B3. *EMBO J* 14, 4827-4838.
- Sigrist, S.J., and Lehner, C.F. (1997). *Drosophila* fizzy-related down-regulates mitotic cyclins and is required for cell proliferation arrest and entry into endocycles. *Cell* 90, 671-681.
- Sironi, L., Mapelli, M., Knapp, S., De Antoni, A., Jeang, K.T., and Musacchio, A. (2002). Crystal structure of the tetrameric Mad1-Mad2 core complex: implications of a 'safety belt' binding mechanism for the spindle checkpoint. *EMBO J* 21, 2496-2506.
- Sironi, L., Melixetian, M., Faretta, M., Prosperini, E., Helin, K., and Musacchio, A. (2001). Mad2 binding to Mad1 and Cdc20, rather than oligomerization, is required for the spindle checkpoint. *EMBO J* 20, 6371-6382.
- Skoufias, D.A., Andreassen, P.R., Lacroix, F.B., Wilson, L., and Margolis, R.L. (2001). Mammalian mad2 and bub1/bubR1 recognize distinct spindle-attachment and kinetochore-tension checkpoints. *Proc Natl Acad Sci U S A* 98, 4492-4497.
- Sonoda, E., Matsusaka, T., Morrison, C., Vagnarelli, P., Hoshi, O., Ushiki, T., Nojima, K., Fukagawa, T., Waizenegger, I.C., Peters, J.M., *et al.* (2001). Scc1/Rad21/Mcd1 is required for sister chromatid cohesion and kinetochore function in vertebrate cells. *Dev Cell* 1, 759-770.
- Stegmeier, F., Rape, M., Draviam, V.M., Nalepa, G., Sowa, M.E., Ang, X.L., McDonald, E.R., 3rd, Li, M.Z., Hannon, G.J., Sorger, P.K., *et al.* (2007). Anaphase initiation is regulated by antagonistic ubiquitination and deubiquitination activities. *Nature* 446, 876-881.
- Stemmann, O., Zou, H., Gerber, S.A., Gygi, S.P., and Kirschner, M.W. (2001). Dual inhibition of sister chromatid separation at metaphase. *Cell* 107, 715-726.
- Stern, B.M., and Murray, A.W. (2001). Lack of tension at kinetochores activates the spindle checkpoint in budding yeast. *Curr Biol* 11, 1462-1467.
- Sudakin, V., Chan, G.K., and Yen, T.J. (2001). Checkpoint inhibition of the APC/C in HeLa cells is mediated by a complex of BUBR1, BUB3, CDC20, and MAD2. *J Cell Biol* 154, 925-936.
- Sudakin, V., Ganoth, D., Dahan, A., Heller, H., Hershko, J., Luca, F.C., Ruderman, J.V., and Hershko, A. (1995). The cyclosome, a large complex containing cyclin-selective ubiquitin ligase activity, targets cyclins for destruction at the end of mitosis. *Mol Biol Cell* 6, 185-197.
- Sumara, I., Vorlaufer, E., Gieffers, C., Peters, B.H., and Peters, J.M. (2000). Characterization of vertebrate cohesin complexes and their regulation in prophase. *J Cell Biol* 151, 749-762.
- Sumara, I., Vorlaufer, E., Stukenberg, P.T., Kelm, O., Redemann, N., Nigg, E.A., and Peters, J.M. (2002). The dissociation of cohesin from chromosomes in prophase is regulated by Polo-like kinase. *Mol Cell* 9, 515-525.
- Sundin, O., and Varshavsky, A. (1980). Terminal stages of SV40 DNA replication proceed via multiply intertwined catenated dimers. *Cell* 21, 103-114.

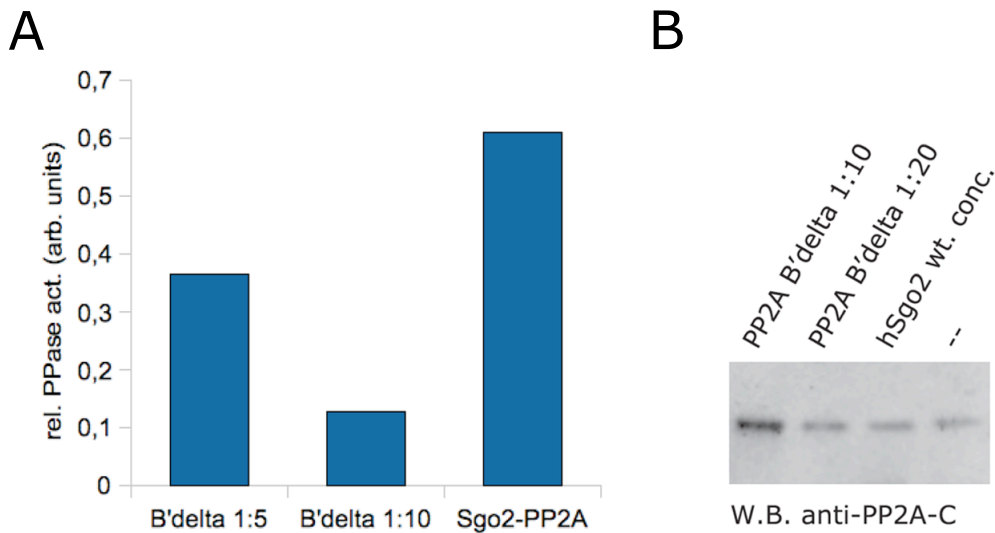
- Taagepera, S., Rao, P.N., Drake, F.H., and Gorbsky, G.J. (1993). DNA topoisomerase II alpha is the major chromosome protein recognized by the mitotic phosphoprotein antibody MPM-2. *Proc Natl Acad Sci U S A* *90*, 8407-8411.
- Tanaka, T.U., Rachidi, N., Janke, C., Pereira, G., Galova, M., Schiebel, E., Stark, M.J., and Nasmyth, K. (2002). Evidence that the Ipl1-Sli15 (Aurora kinase-INCENP) complex promotes chromosome bi-orientation by altering kinetochore-spindle pole connections. *Cell* *108*, 317-329.
- Tang, T.T., Bickel, S.E., Young, L.M., and Orr-Weaver, T.L. (1998). Maintenance of sister-chromatid cohesion at the centromere by the Drosophila MEI-S332 protein. *Genes Dev* *12*, 3843-3856.
- Tang, Z., Bharadwaj, R., Li, B., and Yu, H. (2001). Mad2-Independent inhibition of APCCdc20 by the mitotic checkpoint protein BubR1. *Dev Cell* *1*, 227-237.
- Tang, Z., Shu, H., Qi, W., Mahmood, N.A., Mumby, M.C., and Yu, H. (2006). PP2A is required for centromeric localization of Sgo1 and proper chromosome segregation. *Dev Cell* *10*, 575-585.
- Tao, W., South, V.J., Zhang, Y., Davide, J.P., Farrell, L., Kohl, N.E., Sepp-Lorenzino, L., and Lobell, R.B. (2005). Induction of apoptosis by an inhibitor of the mitotic kinesin KSP requires both activation of the spindle assembly checkpoint and mitotic slippage. *Cancer Cell* *8*, 49-59.
- Thornton, B.R., and Toczyski, D.P. (2003). Securin and B-cyclin/CDK are the only essential targets of the APC. *Nat Cell Biol* *5*, 1090-1094.
- Toth, A., Ciosk, R., Uhlmann, F., Galova, M., Schleiffer, A., and Nasmyth, K. (1999). Yeast cohesin complex requires a conserved protein, Eco1p(Ctf7), to establish cohesion between sister chromatids during DNA replication. *Genes Dev* *13*, 320-333.
- Toth, A., Rabitsch, K.P., Galova, M., Schleiffer, A., Buonomo, S.B., and Nasmyth, K. (2000). Functional genomics identifies monopolin: a kinetochore protein required for segregation of homologs during meiosis I. *Cell* *103*, 1155-1168.
- Trinkle-Mulcahy, L., Andrews, P.D., Wickramasinghe, S., Sleeman, J., Prescott, A., Lam, Y.W., Lyon, C., Swedlow, J.R., and Lamond, A.I. (2003). Time-lapse imaging reveals dynamic relocalization of PP1gamma throughout the mammalian cell cycle. *Mol Biol Cell* *14*, 107-117.
- Trinkle-Mulcahy, L., and Lamond, A.I. (2006). Mitotic phosphatases: no longer silent partners. *Curr Opin Cell Biol* *18*, 623-631.
- Tsurumi, C., Hoffmann, S., Geley, S., Graeser, R., and Polanski, Z. (2004). The spindle assembly checkpoint is not essential for CSF arrest of mouse oocytes. *J Cell Biol* *167*, 1037-1050.
- Turner, D.L., and Weintraub, H. (1994). Expression of achaete-scute homolog 3 in *Xenopus* embryos converts ectodermal cells to a neural fate. *Genes Dev* *8*, 1434-1447.
- Uchida, K.S., Takagaki, K., Kumada, K., Hirayama, Y., Noda, T., and Hirota, T. (2009). Kinetochore stretching inactivates the spindle assembly checkpoint. *J Cell Biol* *184*, 383-390.

- Uhlmann, F., Lottspeich, F., and Nasmyth, K. (1999). Sister-chromatid separation at anaphase onset is promoted by cleavage of the cohesin subunit Scc1. *Nature* *400*, 37-42.
- Uhlmann, F., Wernic, D., Poupart, M.A., Koonin, E.V., and Nasmyth, K. (2000). Cleavage of cohesin by the CD clan protease separin triggers anaphase in yeast. *Cell* *103*, 375-386.
- Vader, G., Cruijssen, C.W., van Harn, T., Vromans, M.J., Medema, R.H., and Lens, S.M. (2007). The chromosomal passenger complex controls spindle checkpoint function independent from its role in correcting microtubule kinetochore interactions. *Mol Biol Cell* *18*, 4553-4564.
- Vagnarelli, P., and Earnshaw, W.C. (2004). Chromosomal passengers: the four-dimensional regulation of mitotic events. *Chromosoma* *113*, 211-222.
- Vanoosthuysse, V., Prykhozhij, S., and Hardwick, K.G. (2007). Shugoshin 2 regulates localization of the chromosomal passenger proteins in fission yeast mitosis. *Mol Biol Cell* *18*, 1657-1669.
- Vega, H., Waisfisz, Q., Gordillo, M., Sakai, N., Yanagihara, I., Yamada, M., van Gosliga, D., Kayserili, H., Xu, C., Ozono, K., *et al.* (2005). Roberts syndrome is caused by mutations in ESCO2, a human homolog of yeast ECO1 that is essential for the establishment of sister chromatid cohesion. *Nat Genet* *37*, 468-470.
- Verde, F., Labbe, J.C., Doree, M., and Karsenti, E. (1990). Regulation of microtubule dynamics by cdc2 protein kinase in cell-free extracts of *Xenopus* eggs. *Nature* *343*, 233-238.
- Vink, M., Simonetta, M., Transidico, P., Ferrari, K., Mapelli, M., De Antoni, A., Massimiliano, L., Ciliberto, A., Faretta, M., Salmon, E.D., *et al.* (2006). In vitro FRAP identifies the minimal requirements for Mad2 kinetochore dynamics. *Curr Biol* *16*, 755-766.
- Visintin, R., Prinz, S., and Amon, A. (1997). CDC20 and CDH1: a family of substrate-specific activators of APC-dependent proteolysis. *Science* *278*, 460-463.
- Vodermaier, H.C. (2004). APC/C and SCF: controlling each other and the cell cycle. *Curr Biol* *14*, R787-796.
- Vodermaier, H.C., Gieffers, C., Maurer-Stroh, S., Eisenhaber, F., and Peters, J.M. (2003). TPR subunits of the anaphase-promoting complex mediate binding to the activator protein CDH1. *Curr Biol* *13*, 1459-1468.
- Waizenegger, I.C., Hauf, S., Meinke, A., and Peters, J.M. (2000). Two distinct pathways remove mammalian cohesin from chromosome arms in prophase and from centromeres in anaphase. *Cell* *103*, 399-410.
- Wang, L.H., Schwarzbraun, T., Speicher, M.R., and Nigg, E.A. (2008). Persistence of DNA threads in human anaphase cells suggests late completion of sister chromatid decatenation. *Chromosoma* *117*, 123-135.
- Wang, Z., Moro, E., Kovacs, K., Yu, R., and Melmed, S. (2003). Pituitary tumor transforming gene-null male mice exhibit impaired pancreatic beta cell proliferation and diabetes. *Proc Natl Acad Sci U S A* *100*, 3428-3432.

- Wassmann, K., and Benezra, R. (1998). Mad2 transiently associates with an APC/p55Cdc complex during mitosis. *Proc Natl Acad Sci U S A* 95, 11193-11198.
- Wassmann, K., Liberal, V., and Benezra, R. (2003a). Mad2 phosphorylation regulates its association with Mad1 and the APC/C. *EMBO J* 22, 797-806.
- Wassmann, K., Niaux, T., and Maro, B. (2003b). Metaphase I arrest upon activation of the Mad2-dependent spindle checkpoint in mouse oocytes. *Curr Biol* 13, 1596-1608.
- Watanabe, Y., Yokobayashi, S., Yamamoto, M., and Nurse, P. (2001). Pre-meiotic S phase is linked to reductional chromosome segregation and recombination. *Nature* 409, 359-363.
- Weaver, B.A., and Cleveland, D.W. (2005). Decoding the links between mitosis, cancer, and chemotherapy: The mitotic checkpoint, adaptation, and cell death. *Cancer Cell* 8, 7-12.
- Weaver, B.A., and Cleveland, D.W. (2006). Does aneuploidy cause cancer? *Curr Opin Cell Biol* 18, 658-667.
- Whyte, J., Bader, J.R., Tauhata, S.B., Raycroft, M., Hornick, J., Pfister, K.K., Lane, W.S., Chan, G.K., Hinchcliffe, E.H., Vaughan, P.S., *et al.* (2008). Phosphorylation regulates targeting of cytoplasmic dynein to kinetochores during mitosis. *J Cell Biol* 183, 819-834.
- Wojtasz, L., Daniel, K., Roig, I., Bolcun-Filas, E., Xu, H., Boonsanay, V., Eckmann, C.R., Cooke, H.J., Jasin, M., Keeney, S., *et al.* (2009). Mouse HORMAD1 and HORMAD2, two conserved meiotic chromosomal proteins, are depleted from synapsed chromosome axes with the help of TRIP13 AAA-ATPase. *PLoS Genet* 5, e1000702.
- Woods, L.M., Hodges, C.A., Baart, E., Baker, S.M., Liskay, M., and Hunt, P.A. (1999). Chromosomal influence on meiotic spindle assembly: abnormal meiosis I in female Mlh1 mutant mice. *J Cell Biol* 145, 1395-1406.
- Xia, G., Luo, X., Habu, T., Rizo, J., Matsumoto, T., and Yu, H. (2004). Conformation-specific binding of p31(comet) antagonizes the function of Mad2 in the spindle checkpoint. *EMBO J* 23, 3133-3143.
- Xu, Z., Cetin, B., Anger, M., Cho, U.S., Helmhart, W., Nasmyth, K., and Xu, W. (2009). Structure and function of the PP2A-shugoshin interaction. *Mol Cell* 35, 426-441.
- Yamagishi, Y., Sakuno, T., Shimura, M., and Watanabe, Y. (2008). Heterochromatin links to centromeric protection by recruiting shugoshin. *Nature* 455, 251-255.
- Yamamoto, A., Guacci, V., and Koshland, D. (1996). Pds1p, an inhibitor of anaphase in budding yeast, plays a critical role in the APC and checkpoint pathway(s). *J Cell Biol* 133, 99-110.
- Yang, M., Li, B., Tomchick, D.R., Machius, M., Rizo, J., Yu, H., and Luo, X. (2007). p31comet blocks Mad2 activation through structural mimicry. *Cell* 131, 744-755.
- Yang, Z., Kenny, A.E., Brito, D.A., and Rieder, C.L. (2009). Cells satisfy the mitotic checkpoint in Taxol, and do so faster in concentrations that stabilize syntelic attachments. *J Cell Biol* 186, 675-684.

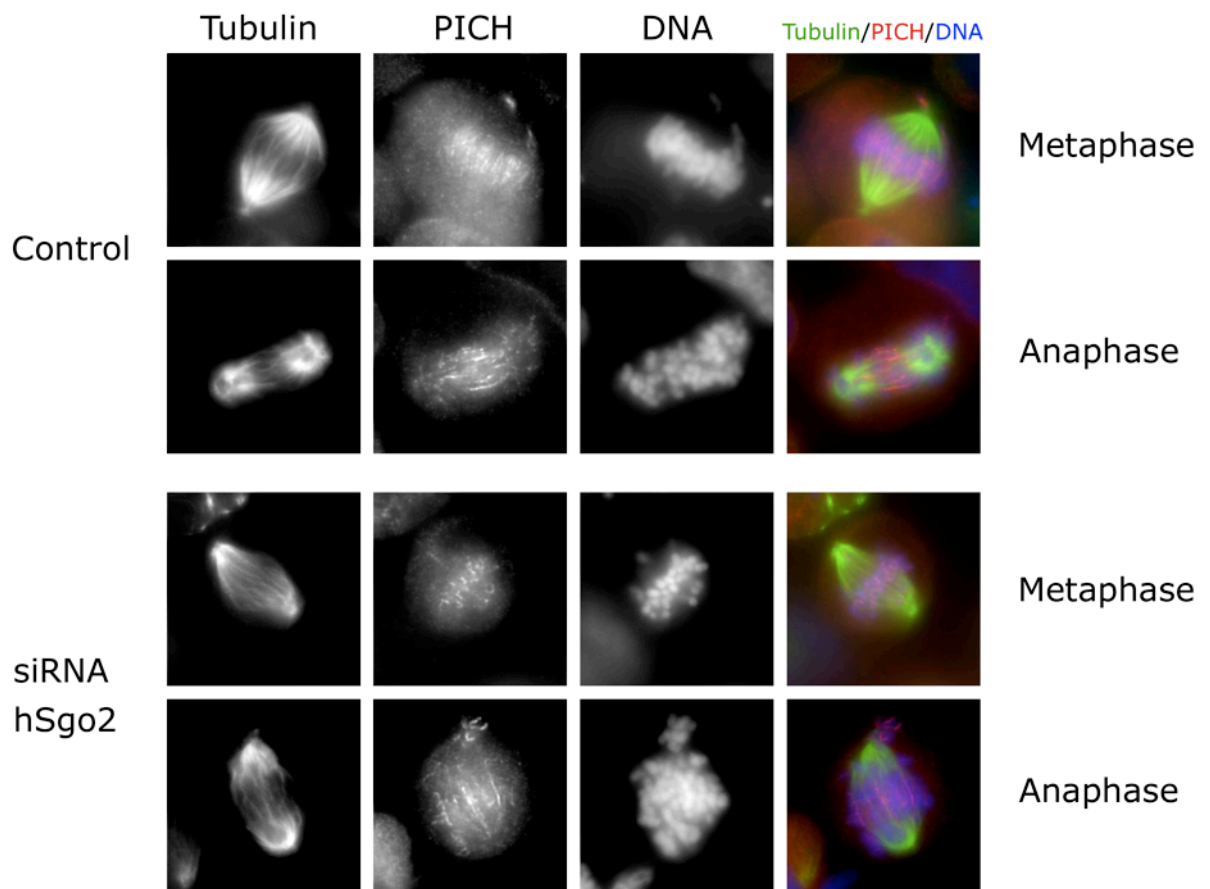
- Yin, S., Wang, Q., Liu, J.H., Ai, J.S., Liang, C.G., Hou, Y., Chen, D.Y., Schatten, H., and Sun, Q.Y. (2006). Bub1 prevents chromosome misalignment and precocious anaphase during mouse oocyte meiosis. *Cell Cycle* 5, 2130-2137.
- Yokobayashi, S., and Watanabe, Y. (2005). The kinetochore protein Moa1 enables cohesion-mediated monopolar attachment at meiosis I. *Cell* 123, 803-817.
- Yuan, L., Liu, J.G., Zhao, J., Brundell, E., Daneholt, B., and Hoog, C. (2000). The murine SCP3 gene is required for synaptonemal complex assembly, chromosome synapsis, and male fertility. *Mol Cell* 5, 73-83.
- Zachariae, W., Schwab, M., Nasmyth, K., and Seufert, W. (1998). Control of cyclin ubiquitination by CDK-regulated binding of Hct1 to the anaphase promoting complex. *Science* 282, 1721-1724.
- Zhang, D., Li, M., Ma, W., Hou, Y., Li, Y.H., Li, S.W., Sun, Q.Y., and Wang, W.H. (2005). Localization of mitotic arrest deficient 1 (MAD1) in mouse oocytes during the first meiosis and its functions as a spindle checkpoint protein. *Biol Reprod* 72, 58-68.
- Zhang, D., Ma, W., Li, Y.H., Hou, Y., Li, S.W., Meng, X.Q., Sun, X.F., Sun, Q.Y., and Wang, W.H. (2004). Intra-oocyte localization of MAD2 and its relationship with kinetochores, microtubules, and chromosomes in rat oocytes during meiosis. *Biol Reprod* 71, 740-748.
- Zhang, X., Lan, W., Ems-McClung, S.C., Stukenberg, P.T., and Walczak, C.E. (2007). Aurora B phosphorylates multiple sites on mitotic centromere-associated kinesin to spatially and temporally regulate its function. *Mol Biol Cell* 18, 3264-3276.

9. Supplementary figures



Suppl. Fig. 1: Sgo2 mediated stimulation of PP2A also occurs when affinity tags have been removed by TEV protease cleavage. (A) Flag-TEV-tagged Sgo2 or PP2A-B'delta were expressed in 293T cells and purified via anti-Flag agarose beads. Elution was performed by cleavage of the tag using TEV protease. Different dilutions were tested in a malachite green phosphatase assay. (B) Immunoblotting of PP2A-B' and Sgo2 preparations using an antibody against PP2A-C to judge the amounts of PP2A catalytic subunit equivalents applied for the assay in (A).

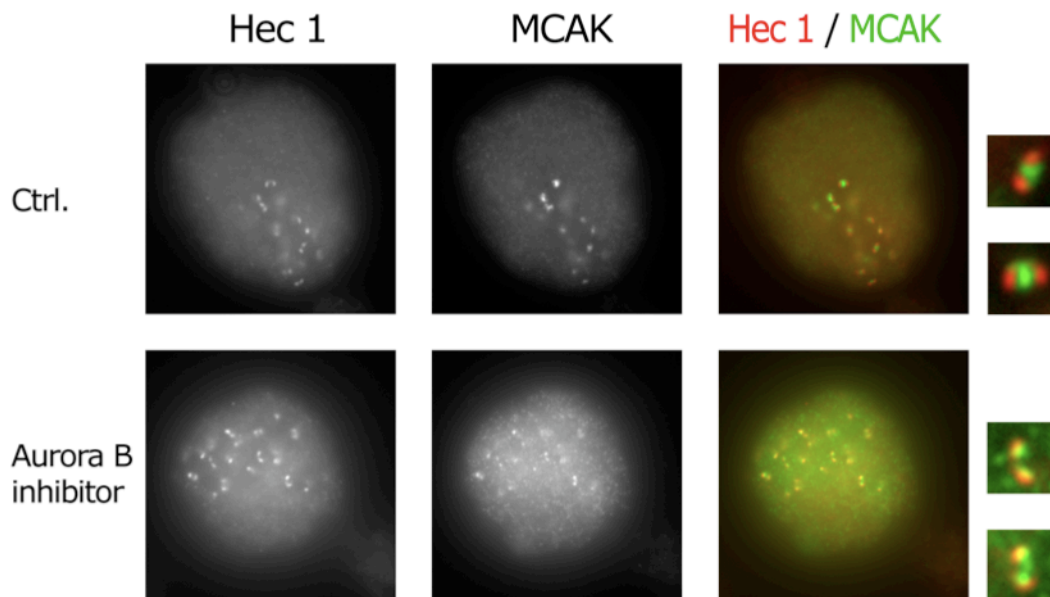
Even when twice the amount of free PP2A equivalent was assayed (B' delta 1:10), Sgo2 bound PP2A showed a much higher phosphatase activity. Importantly, a twofold difference of phosphatase input was appropriately reflected in the assay read (compare B' delta 1:5 and 1:10 dilution) confirming linearity of the measurements.



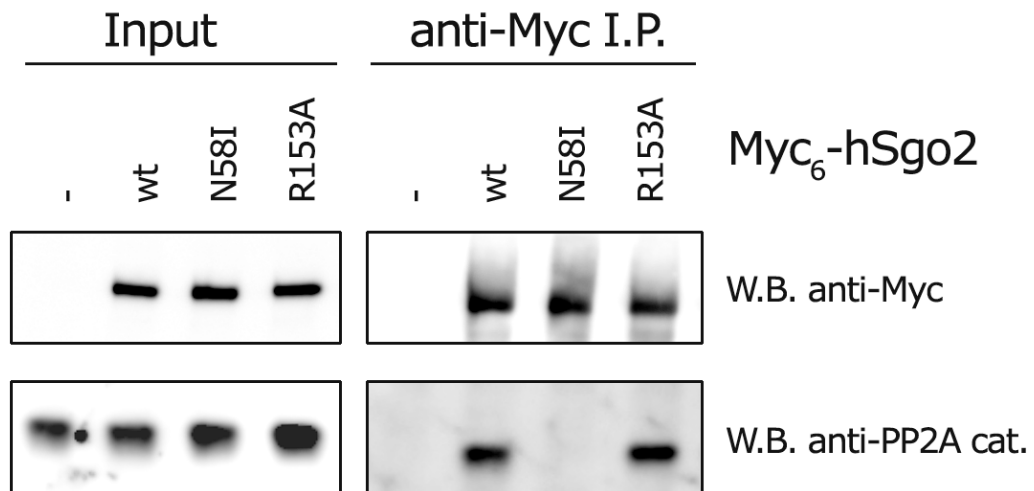
Suppl. Fig. 2: Sgo2 does not protect centromeric DNA catenation. HeLa cells were transfected with dsRNAs directed against the Sgo2 mRNA or with treated with transfection mix only as control (total time of RNAi: 50 h). Cells were synchronized using a single thymidine block/release. 2 h after the release, cells were trypsinized and seeded on glass coverslips. 12 h from the release, cells were fixed and stained for immunofluorescence microscopy using antibodies against tubulin and PICH (red). Hoechst 33342 was used to label DNA (blue).



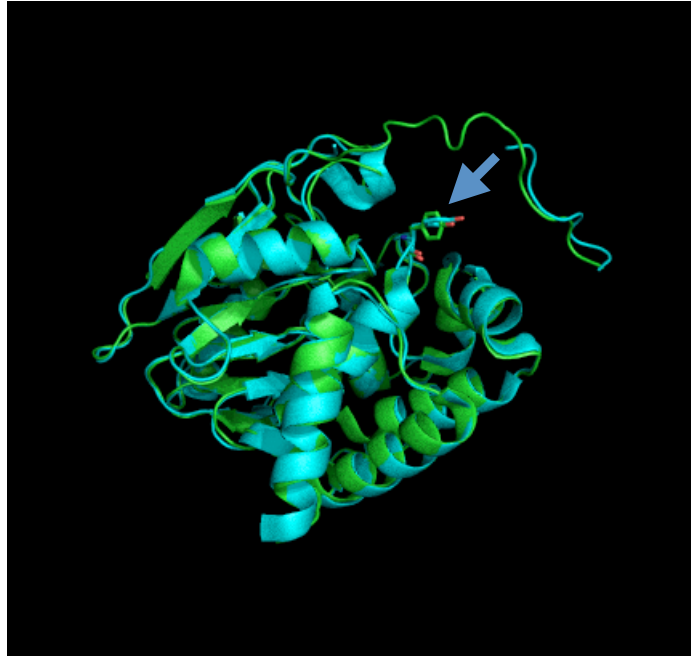
Suppl. Fig. 3: The interaction between Sgo2 and Mad2 is not bridged by chromatin. An I.P. experiment for endogenous Sgo2 was performed as described in with the exception that 200 µg/ml ethidium bromide was included in the lysis buffer. This ensured dissociation of proteins from chromatin. A specific interaction of Sgo2 with Mad2 was observed also in the presence of ethidium bromide. Binding of PP2A was used as a positive control.



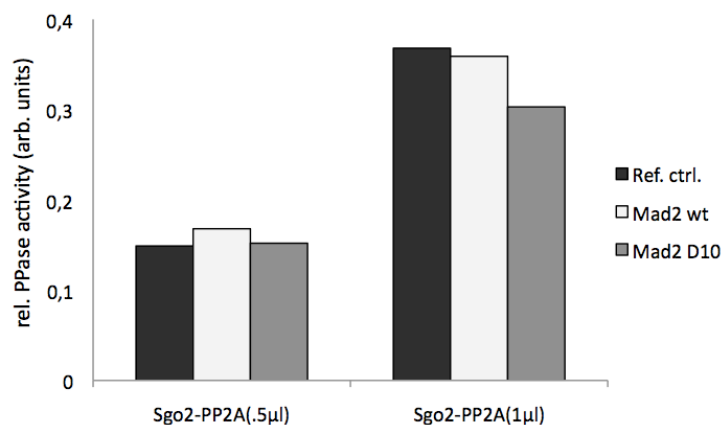
Suppl. Fig. 4: Aurora B catalytic activity is required for keeping MCAK at centromeres. HeLa cells were treated with nocodazole for 6 h. Then, mitotic cells were collected by shake-off. The cells were centrifuged on coverslips (2 min, 300 g) and treated either with the Aurora B inhibitor ZM447439 or the solvent DMSO for 30 min. Then cells were fixed and stained for immunofluorescence microscopy using antibodies against MCAK (green) and Hec1 (red, kinetochore marker). DNA was counterstained with Hoechst 33342. While in the control Sgo2 localized to centromeres, it could be frequently observed at kinetochores upon Aurora B inhibition.



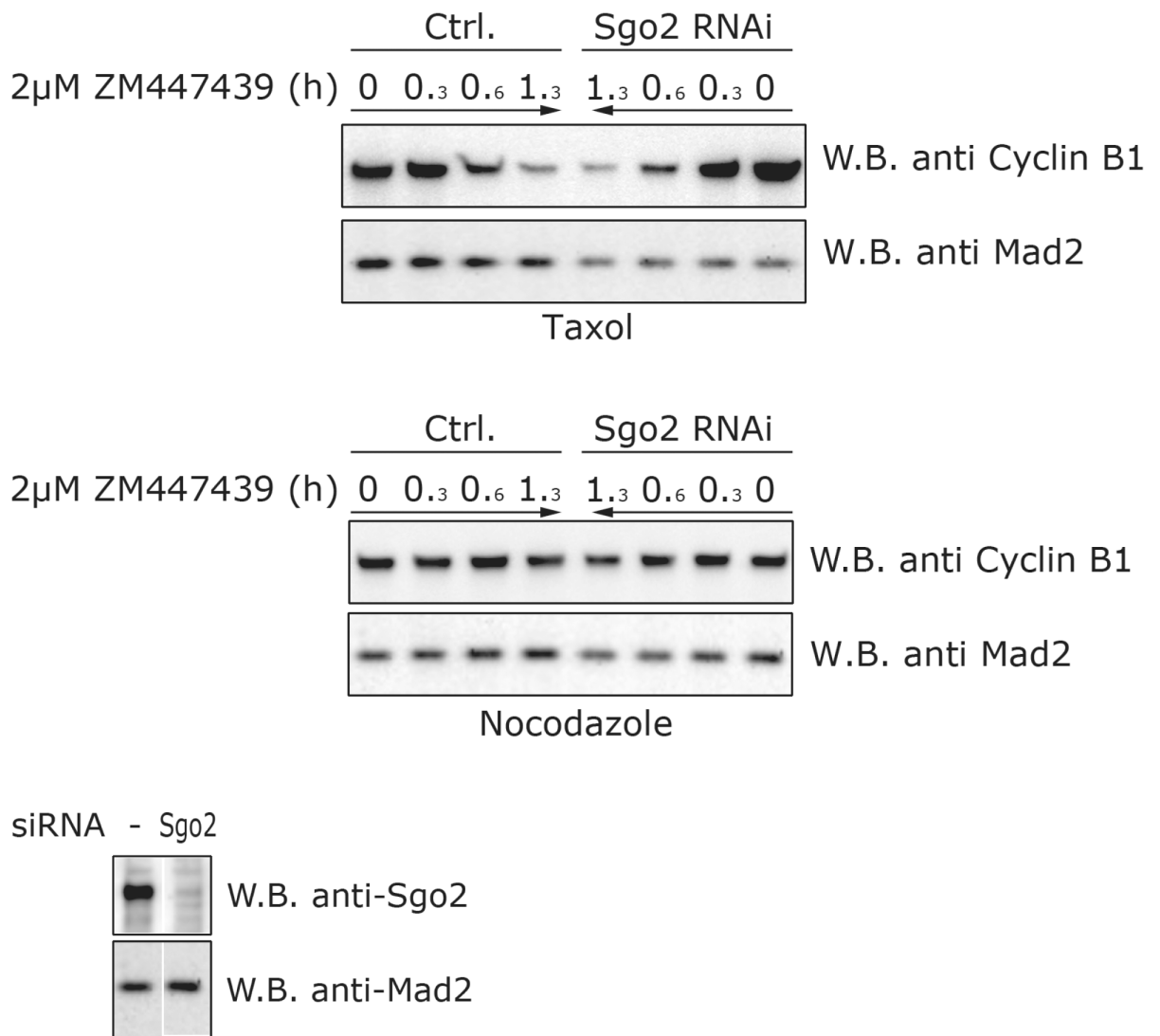
Suppl. Fig. 5: The Mad2 binding deficient Sgo2 mutant R153A is not compromised in PP2A binding. 293T cells were transfected with plasmids coding for the indicated tagged versions of hSgo2 or mock transfected ("-"), neg. control). Cell lysates were prepared using LP2+ with a total NaCl concentration of 350 mM. Myc-tagged Sgo2 was isolated using an anti-Myc affinity matrix. Following 6 washes with lysis buffer, bead associated proteins were analyzed by SDS-PAGE and immunoblotting using antibodies directed against the Myc-tag (Sgo2) and the PP2A C subunit. All three Sgo2 constructs were expressed and immunoprecipitated with similar efficiency. Both wild-type Sgo2 and Mad2 binding deficient Sgo2-R153A interacted with PP2A equally well. The PP2A binding deficient Sgo2-N58I was used as an additional negative control.



Suppl. Fig. 6: Sgo1 binding does not induce major structural changes in the PP2A catalytic C subunit. Overlay of crystal structures of the PP2A C subunit (free (green) or in complex with Sgo1 (cyan)). Most structural elements align neatly in both structures. The arrow indicates a tyrosine residue (Y90) which is the residue with the strongest deviation between the two structures. The catalytic cleft is located on the back side of the molecules in this view (Structure data 2IAE and 3FGA were derived from Protein Data Bank (<http://www.rcsb.org/pdb/home/home.do>), visualization and alignment: MacPyMol.



Suppl. Fig. 7: Mad2 does not change the activity of Sgo2 bound PP2A. A malachite green based peptide dephosphorylation assay was performed (as described in the methods section). Different amounts (0.5 μ l or 1 μ l) of Sgo2-PP2A complex purified from 293T cells were tested. Increase of the amount of PP2A in the assay is appropriately reflected by an increased activity measured. Either reference buffer or purified recombinant wild-type Mad2 or Mad2-D10 (neg. control) were added. Similar phosphatase activities were measured in all three cases.



Suppl. Fig. 8: The specific tension SAC signal pathway branches downstream of Aurora B and upstream of Sgo2. HeLa cells were either transfected with Sgo2 specific siRNA or treated with a control transfection mix (total time of RNAi: 50 h). Cells were presynchronized with thymidine and 6 h from release, either 200 ng/ml taxol (A) or 200 ng/ml nocodazole (B) were added. 12 h from release, mitotic cells were enriched by mitotic shake-off and ZM447439 (2 μ M) was added. The cells were then incubated in the continued presence of either taxol or nocodazole for the indicated periods of time. The "0 h" time point in fact a sample incubated for 1.3 h without addition of ZM447439. The samples were then analyzed by SDS-PAGE and immunoblotting for levels of Cyclin B1 and Mad2 (input control). Sgo2 is not required for both mitotic arrests (unchanged 0 h Cyclin B1 levels upon Sgo2 depletion). A nocodazole arrest (B) is maintained upon ZM447439 treatment while cells exit from a taxol arrest (A) when treated with ZM447439. Also in the absence of Sgo2, an override of the taxol arrest is possible (A). (C) Efficiency of Sgo2 RNAi was determined by immunoblotting using antibodies directed against Sgo2 and Mad2 (control).

10. Publikationsliste

Im Rahmen dieser Arbeit sind folgende Veröffentlichungen entstanden:

Wang L.H.C., Mayer B., Stemmann O., Nigg E.A. (2010) "Centromere DNA decatenation depends on cohesin removal and is required for mammalian cell division". *J Cell Sci* 123, 806-813.

Orth M.*¹, Mayer B.*^{1*2}, Hoffman K., Holak T., Stemmann O. Sgo2 is a Mad1/Cdc20 like interaction partner of Mad2. Manuscript in preparation.

*1: equal contribution, *2 corresponding author

Hiermit versichere ich, die vorliegende Arbeit selbständig angefertigt und keine anderen als die angegebenen Quellen und Hilfsmittel verwendet zu haben.
Ferner erkläre ich, dass ich nicht anderweitig mit oder ohne Erfolg versucht habe, diese Dissertation einzureichen. Ich habe keine gleichartige Doktorprüfung an einer anderen Hochschule endgültig nicht bestanden.

Bayreuth, den 13. Januar 2010

Bernd Mayer

11. Danksagung

Diese Arbeit entstand zwischen Oktober 2005 und Januar 2010 in der Abteilung für molekulare Zellbiologie am Max-Planck-Institut für Biochemie in Martinsried sowie am Lehrstuhl für Genetik der Universität Bayreuth.

Herrn Prof. Dr. Olaf Stemmann danke ich für die Möglichkeit, in einem bestens ausgestatteten Labor zu arbeiten sowie für die Bereitstellung des interessanten Forschungsthemas. Außerdem möchte ich mich für seine große Diskussionsbereitschaft bedanken, sowie dafür, dass er immer ein offenes Ohr für meine Anliegen hatte.

Außerdem bedanke ich mich bei Herrn Prof. Dr. Stefan Jentsch für seine vielfältige Unterstützung während meiner Zeit in Martinsried.

Mein Dank gilt auch allen Mitgliedern der Prüfungskommission, deren Zusammensetzung zum Zeitpunkt des Drucks noch nicht bekannt war.

Dr. Stefan Heidmann danke ich für seine wertvolle Hilfe bei Computerproblemen sowie seiner gesamten Arbeitsgruppe für die freundliche Aufnahme in Bayreuth.

Vielen Dank an Jutta Hübner, für ihre exzellente Unterstützung bei der Herstellung zahlreicher Plasmide und Proteine während des letzten Jahres meiner Doktorarbeit. Petra Helies sei an dieser Stelle dafür gedankt, dass sie immer gute Laune verbreitet hat und dafür, dass ich immer alle möglichen Gefäße sauber und steril einfach aus dem Schrank nehmen konnte.

Allen Angehörigen des Lehrstuhls für Genetik an der Uni Bayreuth danke ich für Diskussionen, den Austausch von Reagenzien und vor allem für die sehr angenehme Atmosphäre im Labor. Ein Extra-Dank geht an meine Mit-DoktorandInnen Franziska Böttger, Andreas Brown, Laura Gebert und Michael Orth, die mir nicht nur durch unsere gemeinsamen Irish-Pub-Besuche die Eingewöhnung in Bayreuth wesentlich erleichtert haben.

Ein ganz herzliches Danke für das Korrekturlesen dieser Arbeit gebührt Franziska, Johannes Buheitl, Andreas und Laura.

Michael danke ich für die gute Zusammenarbeit auf dem Shugoshin-Feld, ohne die diese Arbeit nicht möglich gewesen wäre.

Meinen ehemaligen Kollegen Dominik Boos, Ingo Gorr und Simone Heubes möchte ich für ihre Hilfe beim Start in Martinsried danken. Dominik hat mich außerdem von den Vorzügen des Fußballteams unserer Abteilung überzeugt. An dieser Stelle sei auch Alexander Strasser für technische Assistenz in Martinsried gedankt.

Mit Lily Hui-Ching Wang aus dem Labor von E. A. Nigg verband mich eine hervorragende Kollaboration, die stets durch gegenseitigen Austausch und Diskussion geprägt war. Tad Holak (MPI Martinsried) danke ich für NMR-Analysen und Kay Hoffman (Miltenyi Biotech, Köln) für die Zusammenarbeit bei bioinformatischen Fragestellungen.

Benjamin Sünkel und Anna Karlson im Rahmen von Bachelor-Arbeiten sowie Eva Bartoskova, die ein Praktikum im Labor durchführte, haben zu Teilen meiner Arbeit einen wichtigen Beitrag geleistet. Ihnen danke ich für ihren Einsatz und die gute Zusammenarbeit.

Mirijam Elisabeth Zeller danke ich dafür, dass sie während eines grossen Teils dieser Arbeit für mich da war.

Ein besonderer Dank geht an meine Eltern für ihre Unterstützung auch bei eher aussergewöhnlichen Aktivitäten. Ohne Euch hätte ich diesen Weg nicht gehen können.